Assessment of Seismic Response of Vertically Irregular RC Moment Resisting Frame Structures

Md. Abdullah

MASTER OF SCIENCE IN CIVIL ENGINEERING (STRUCTURAL)

DEPARTMENT OF CIVIL ENGINEERING

BANGLADESH UNIVERSITY OF ENGINEERING AND TECHNOLOGY

DHAKA-1000, BANGLADESH

September, 2020

Assessment of Seismic Response of Vertically Irregular RC Moment Resisting Frame Structures

Md. Abdullah

A thesis submitted to the Department of Civil Engineering,

Bangladesh University of Engineering and Technology (BUET), Dhaka

in partial fulfillment of the requirement for the degree

of

MASTER OF SCIENCE IN CIVIL ENGINEERING (STRUCTURAL)

DEPARTMENT OF CIVIL ENGINEERING

BANGLADESH UNIVERSITY OF ENGINEERING AND TECHNOLOGY

September, 2020

The Thesis Titled "ASSESSMENT OF SEISMIC RESPONSE OF VERTICALLY IRREGULAR RC MOMENT RESISTING FRAME STRUCTURES" Submitted by Md. Abdullah, Roll No: 1015042360P, Session: October/2015; has been accepted as satisfactory in partial fulfillment of the requirement for the degree of Master of Science in Civil Engineering (Structural) on 30th September, 2020.

BOARD OF EXAMINERS

Dr. Mohammad Al Amin Siddique Professor Department of Civil Engineering, BUET, Dhaka-1000.	Chairman (Supervisor)
Dr. Md. Habibur Rahman Professor and Head Department of Civil Engineering BUET, Dhaka-1000.	Member (Ex-Officio)
Dr. Md. Shafiul Bari Professor Department of Civil Engineering BUET, Dhaka-1000.	Member
Dr. Sharmin Reza Chowdhury Professor Department of Civil Engineering AUST, Dhaka-1208.	Member (External)

DECLARATION

It is hereby declared that no part of this thesis has been submitted to any other university or educational institute for the award of any degree or diploma.

Signature of the Candidate

Md. Abdullah

Md. Abdullah

Roll: 1015042360P

ACKNOWLEDGMENT

First of all, I must express gratitude and homage to the Almighty Allah for providing me the knowledge and capability to successfully complete the thesis.

Then I would like to acknowledge my gratefulness and reverence to Dr. Mohammad Al Amin Siddique, Professor, Department of Civil Engineering, BUET, Dhaka, for his continuous guidance, invaluable suggestions and affectionate encouragement at every stage of this thesis work.

A very special debt of deep gratitude is offered to my parents, wife and daughter for their continuous encouragement and cooperation during this study

ABSTRACT

Now-a-days many structures are designed with vertical irregularity due to functional, aesthetic or economic reasons. However, damage or failure of a building may be triggered at the point of weakness induced by the vertical irregularity. In this thesis, a comprehensive numerical studies have been conducted to assess the seismic behavior of the structures with vertical irregularity. Stiffness, mass and geometric–three types of the vertical irregularities have been considered in this study. Stiffness irregularity cases have been considered due to sudden absence of masonry infill walls at open ground floor for parking facility. Bare, fully infilled and open ground floor (OGF) frames have been considered to assess the stiffness irregularity. Mass irregularity cases have been considered by applying a special superimposed dead load at mid storey level. Geometric irregularity cases have been considered due to presence of setback at top floor and mid floor level. 4, 6 and 10-storied reinforced concrete (RC) moment resisting frame buildings located at seismic zone 2 according to draft BNBC 2017 have been considered. All the frames were designed as an Intermediate Moment Resisting frame considering the response reduction factor (R) value of 5 as per draft BNBC 2017. Seismic analysis methods such as equivalent static, response spectrum, time history and nonlinear static or pushover analysis have been conducted.

Open ground floor buildings were not always found with soft storey action as it depends on limits of storey stiffness ratio sets by the Code. Only 4 and 6-storied buildings with the open ground floor resulted extreme soft storey action. R values of 4, 6 and 10-storied bare frames and fully infilled frames were satisfied with the considered R = 5, whereas 4, 6 and 10-storied open ground floor (OGF) frames resulted R values of 3.01, 3.94 and 3.42, respectively were much lower than the considered R = 5. A decrease in R value in OGF frames was observed due to the stiffness irregularity caused by sudden absence of infill wall at the ground floor. Ratios of R values of 4, 6 and 10-storied bare frames to open ground floor (OGF) frames were found 1.71, 1.44 and 1.55, respectively. Therefore, special provision as per draft BNBC 2017 seems reasonably good agreement with the obtained results for the open ground floor buildings. Storey drifts of 4, 6 and 10-storied mass irregular frames were found 3.7%, 4.4% and 8.1%, respectively higher than those of the allowable drift limit. R value of 4, 6 and 10-storied mass irregular frames were found 2.31, 4.55 and 4.64, respectively lower than those of the regular one. R values of

4, 6 and 10-storied buildings with geometric irregular frames also provided lower values than those of the regular one. However, building with the setback at the top floor results higher reduction of R value than that of the mid floor level. A reduction of R value was obtained 39% for the 4-storied geometric irregular building with the setback at the top floor level.

TABLE OF CONTENTS

LIST OF FIGURES

LIST OF TABLES

Chapter 1

INTRODUCTION

1.1 General

Earthquake is one of the most deadly forms of natural hazards. Bangladesh is located at seismically active region. It is situated at the juncture of several active tectonic plate/fault boundaries which have produced many earthquakes in the recent times. Historically, the country had been experienced many earthquakes in the magnitude of 4 to 6 in Richter scale. Global seismic hazard maps indicate that Bangladesh is located in moderate to high seismic hazard zone with a maximum peak ground acceleration of 0.25g with 10% probability of exceedance in 50 years (Giardini et. al. 1999). Over last few decades, reinforced concrete (RC) building construction has rapidly increased especially in the urban areas replacing the old masonry buildings. Therefore, performance assessment of RC buildings during earthquakes has become very essential. Moreover, construction of number of irregular buildings are also increasing day by day for architectural, economic and many other purposes. Behavior of irregular buildings are more complex than those of the regular buildings. Draft BNBC 2017 provides special design consideration for irregular buildings considering the safety issues during earthquakes.

1.2 Background of the study

Uniformity of structural components along the height of the building is very important, since it eliminates the tendency of the occurrence of sensitive zones and prevents the concentrations of stress or large ductility demands which might cause damage or collapse of the structures. Otherwise, non-uniformity may weaken the structure in resisting the seismic force during earthquake and seismic demand on this type of structure may be higher than that of the regular one. During an earthquake, failure of a building may be triggered at the point of weakness occurred by irregularity of the structure. Modern seismic design codes like draft BNBC 2017 distinguish this irregularity in two categories - plan irregularity and vertical irregularity. Vertical irregularity may occur due to sudden changes in stiffness, mass or strength between adjacent stories. Such irregularity may also occur due to sudden variation in the frame geometry along the height.

Vertical irregularities in a building are usually found due to functional, architectural or economic reasons. Over the few years, construction of RC buildings especially in the Dhaka city have been increased very rapidly. Space for parking area surrounding the building has also been narrowed day by day. Consequently, using the ground floor as parking area has become a common trend recently specially in the residential, commercial buildings etc. Therefore, ground floors of those buildings have to keep open and free from any partition infill walls. This sudden absence of masonry infill wall at the ground floor may result in sudden change of stiffness and strength of that floor and can affect the seismic behavior of the whole structure. Another type of vertical irregularity in buildings arises due to presence of setback, i.e. the presence of abrupt reduction of the lateral dimension of the building at the specific levels of the elevation. This building category is known as setback building. This type of building is also becoming popular because of its functional and aesthetic architecture. This setback provides adequate daylight and ventilation for closed spaced building especially at urban localities.

Many researches and investigations have been performed to understand the behavior of vertically irregular structures to ascertain method of improving their performance. Recent seismic codes also provide special design consideration for vertically irregular structures. This study is aimed to assess the seismic behavior of vertically irregular RC moment resisting frame structures following the guidance of upcoming draft BNBC 2017.

1.3 Objectives of the research

The objective of the study is to assess the seismic behavior of vertically irregular RC moment resisting frame structures following different static and dynamic analyses methods. The objectives of this study, more specifically, are as follows:

i) To conduct seismic analysis of vertically irregular RC moment resisting frame structures following draft BNBC 2017 considering equivalent static, response spectrum and time history analyses.

ii) To produce pushover curves of different buildings from nonlinear static analyses.

iii) To investigate the effect of irregularity on natural period (T), base shear capacity, overstrength factor, ductility factor, response reduction factor and storey drift of the considered building frames.

iv) To make a comparison among the obtained results from static and dynamic analyses.

v) To evaluate the applicability of special provision for the soft storey action provided in draft BNBC 2017.

1.4 Outline of methodology

a) 4, 6 and 10-storied RC moment resisting frame structures located at seismic zone 2 according to draft BNBC 2017 have been considered in this study. All frames were designed as intermediate moment resisting frame (IMRF) according to draft BNBC 2017. Modeling, structural analysis and design have been performed using the commercially available finite element software ETABS v16.2.1.

b) Stiffness irregularity, mass irregularity and geometric irregularity – theses three types of vertical irregularity have been considered in this study. Stiffness irregularity cases have been considered due to sudden absence of masonry infill walls at open ground floor for parking facilities. Mass irregularity cases have been considered by applying a special superimposed dead load at mid storey level. Geometric irregularity have been considered due to presence of setback at upper and mid storey levels. Effect of these irregularities in natural period (T), top lateral displacement, storey drift and base shear capacity have been studied.

c) Masonry infill walls have been simulated by equivalent diagonal strut method. Strut width in equivalent diagonal strut method has been determined considering the equations provided by different researchers and codes. A comparative study among the strut widths by those equations have been performed. Strut width determined following FEMA 356 guidelines have been considered in this study.

d) Equivalent static analysis, response spectrum analysis and time history analysis have been conducted in this thesis. Equivalent static analysis has been performed considering design base shear according to draft BNBC 2017. Response spectrum analysis has been performed using the normalized design acceleration response spectrum for soil type SC according to draft BNBC 2017. Time history analysis has been performed for three specific ground motions. All ground motions have been matched with the normalized design acceleration response spectrum as per the code.

e) Nonlinear static pushover (NSP) analyses have been conducted to produce pushover or capacity curves considering the nonlinear parameters provided in ASCE 41-13. Seismic performance of different frames in terms of overstrength factor, ductility factor and response reduction factor have been conducted.

f) Evaluation of special provision of draft BNBC 2017 for application of seismic force magnification factor (2.5) in case of soft storey buildings have been computed. The obtained factors from analyses are compared with the code provisions for the considered buildings.

1.5 Scope of the work

In this study, seismic behavior of vertically irregular RC moment resisting frame structures have been assessed. Three types of vertical irregularities have been considered such as stiffness, mass and geometric irregularities. Stiffness irregularity due to open ground floor, mass irregularity due to application of special superimposed dead load at certain floor levels and geometric irregularity due to presence of setback at certain floor levels have been considered. Although different number of stories and different vertical irregularities are considered, the bay width and storey height are kept the same for all buildings 5m and 3m, respectively. Seismic analyses have been performed by equivalent static, response spectrum and time history analyses. Nonlinear static pushover analysis has been performed to assess the base shear capacity of the structures. Special provision of draft BNBC 2017 for the application of seismic force magnification factor (2.5) using the equivalent static force analysis method for the case of open ground floor buildings have been evaluated.

1.6 Layout of the thesis

The thesis paper is organized into total seven chapters. Apart from chapter one, the following chapters are organized as follows:

Chapter 2: This chapter named "Literature Review", describes vertically irregular structures, criteria for vertical irregularity by national and international codes like draft BNBC 2017, ASCE 7-10, Eurocode 8. Effects of vertical irregularities on the buildings in past earthquakes and review on previous research works related to vertical irregularities in the structures are also provided in this chapter.

Chapter 3: This chapter named "Masonry Infill Wall" describes different methods of simulation of masonry infill walls, equivalent strut method and strut width determination by different researchers and codes. A comparative study among the strut widths by different equations developed by different researchers and codes have been performed in this chapter.

Chapter 4: This chapter named "Response Reduction Factor" describes the definition and formulation of response reduction factor, ductility factor and overstrength factor. A brief discussion on previous research works on these factors are also been provided in this chapter.

Chapter 5: This chapter named "Structural Modeling and Analysis" describes the geometric configurations of considered frames, sizes and thickness of structural elements, material properties, loading and load combinations. Seismic analysis methods such as equivalent static force, response spectrum, time history analyses and nonlinear static pushover analysis have been discussed in this chapter.

Chapter 6: This chapter named "Results and Discussions" focuses on effect of the vertical irregularity in the RC moment resisting frames in terms of natural period (T), storey displacement and storey drift have been assessed. Comparisons of shear force distribution along the height of the building by different seismic analysis methods have been presented. Seismic performance in terms of overstrength factor, ductility factor and response reduction factor have been assessed. Evaluation of applicability of draft BNBC 2017 recommended seismic force magnification factor (2.5) in special case of open ground floor buildings has also been investigated in this chapter.

Chapter 7: This chapter named "Conclusions and Recommendations" presents conclusions derived from the present study and recommendation for future research.

Chapter 2
LITERATURE REVIEW

2.1 General

There are many natural hazards in the world but earthquake is one of the most destructive hazards that can result in severe social and economic impacts. The devastating potential of an earthquake can have major consequences on infrastructures and lifelines. Therefore, the researchers have been reassessing the design procedures, in the wake of devastating earthquakes which have caused extensive damages, loss of life and properties. The structural irregularity in a building now a day is very common due to the architectural design and service requirements. This chapter highlights the effects of vertical irregularities on the structures in terms of seismic behavior.

2.2 Vertical irregularity in structures

The structural irregularity is mainly classified to two categories: (i) plan and (ii) vertical irregularity. The plan irregularity occurs as a result of several reasons such as when the structure is significantly influenced by torsion or a discontinuity in lateral load resisting systems along its horizontal plane. The vertical irregularity could be occurred when there are significant changes in the stiffness, strength, mass, dimensions, or a discontinuity in the in lateral load resisting systems along its height of the building. Five types of vertical irregularities can be found in a structure. These are as follows:

1. Stiffness irregularity
2. Vertical geometric irregularity
3. Mass irregularity
4. Vertical in-plane discontinuity in vertical elements resisting lateral force
5. Strength irregularity (weak storey irregularity)

In the current study, the effect of vertical irregularities on the seismic response of reinforced concrete (RC) moment resisting frame structure has been assessed. The definitions and criterion of different types of vertical irregularities according to modern seismic design codes are reviewed in the subsequent sections.

2.3 Vertical irregularity criteria in different seismic codes

Criterion of vertical irregularity is not the same in all seismic codes. Different seismic codes set different criteria for different vertical irregularities. A brief description of criterion sets for different vertical irregularities has been given in the following sections.

2.3.1 ASCE 7-10

According to the American design guidelines ASCE 7-10, a building exhibits soft story irregularity when a story lateral stiffness (K_i) is less than 60% of the stiffness of the story above (K_{i+1}), or less than 70% of the average stiffness of the three stories above, as explained in Figure 2.1. The mass irregularity occurs when the mass of a story (M_i) is more than 150% of the mass of adjacent story (M_{i+1} or M_{i-1}), as shown in Figure 2.1. The vertical geometric irregularity exists when the horizontal dimension of the lateral force resisting system (LFRS) in any story (L_i) is more than 130% of that in an adjacent story (L_{i+1}), as shown in Figure 2.1.

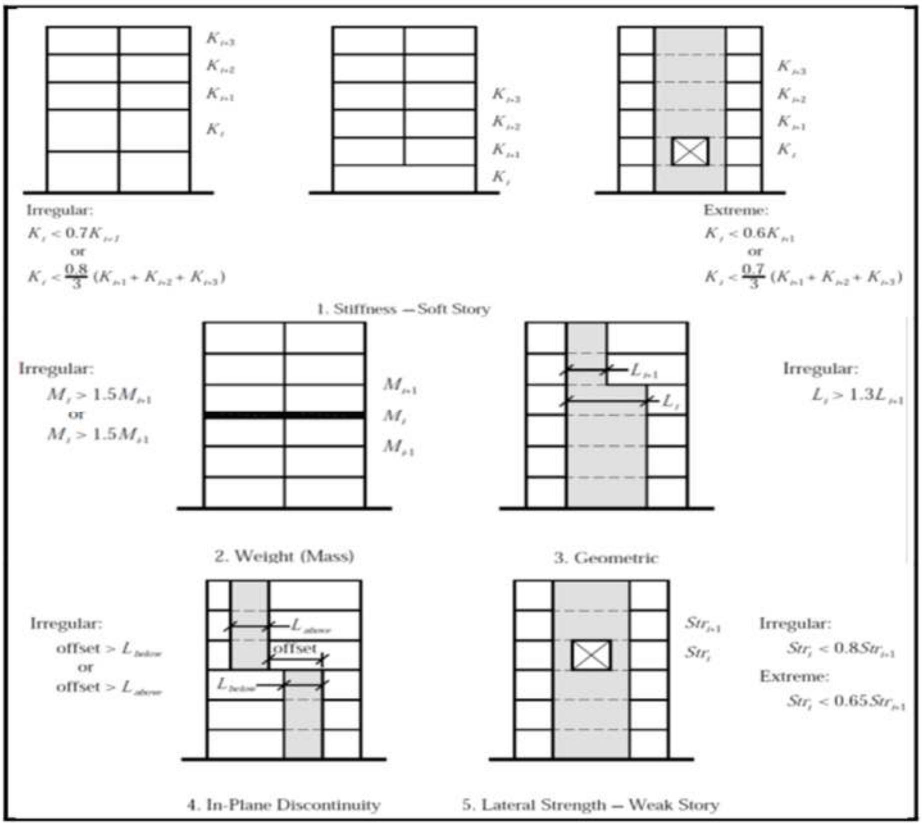

Figure 2.1: Definition of vertical irregularity according to ASCE 7-10

In-plane discontinuity exists when an in-plane offset of a vertical seismic force resisting element of more than the dimension of the seismic force resisting element below (L_{below}) or above (L_{above}) is introduced as shown in Figure 2.1. The weak story irregularity is identified when a story lateral strength (Str_i) is less than 80% of the lateral strength for the story above (Str_{i+1}), as shown in Figure 2.1.

2.3.2 Eurocode 8

Eurocode 8 design guidelines provide criteria for classification of vertically regular and irregular structures, where a structure is defined as being "irregular" when the ratio of one of the quantities (such as masses or strength) between adjacent stories exceeds a minimum prescribed value. For a building to be categorized as being regular in elevation, it shall satisfy the following:

a) All lateral load resisting systems, such as cores, structural walls, or frames, shall run without interruption from their foundations to the top of the building or, if setbacks at different heights are present, to the top of the relevant zone of the building.

b) Both the lateral stiffness and the mass of the individual storey shall remain constant or reduce gradually, without abrupt changes, from the base to the top of a particular building.

c) In framed buildings, the ratio of the actual storey resistance to the resistance required by the analysis should not vary disproportionately between the adjacent storeys.

When setbacks are present, the following additional conditions apply:

a) For gradual setbacks preserving axial symmetry, the setback at any floor shall be not greater than 20 % of the previous plan dimension in the direction of the setback as shown in Figures 2.2 (a) and (b).

b) For a single setback within the lower 15% of the total height of the main structural system, the setback shall be not greater than 50% of the previous plan dimension as illustrated in Figure 2.2(c). In this case, the structure of the base zone within the vertically projected perimeter of the upper stories should be designed to resist at least 75% of the horizontal shear forces that would develop in that zone in a similar building without the base enlargement.

c) If the setbacks do not preserve symmetry, in each face the sum of the setbacks at all storeys shall be not greater than 30% of the plan dimension at the ground floor above the foundation or above the top of a rigid basement, and the individual setbacks shall be not greater than 10% of the previous plan dimension as illustrated in Figure 2.2(d).

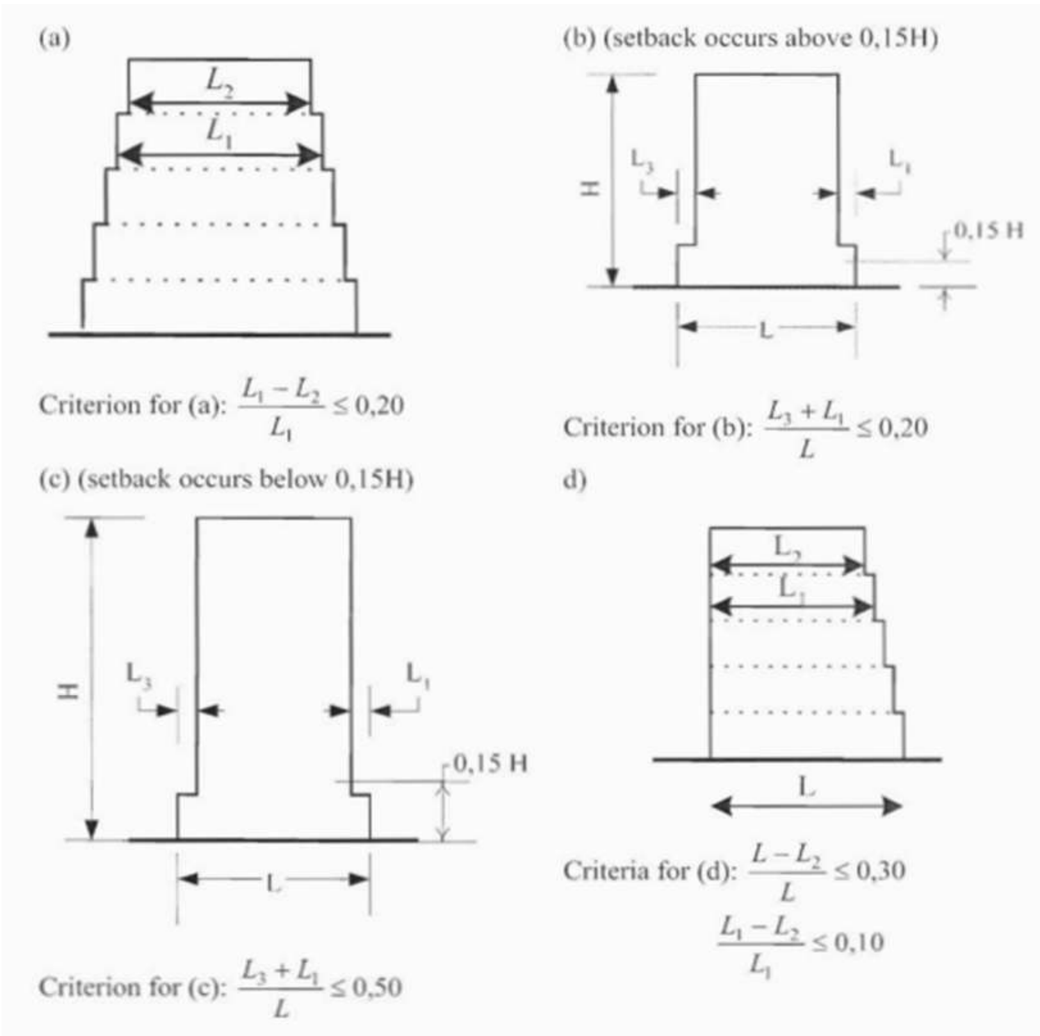

Figure 2.2: Vertical irregularities according to Eurocode 8

2.3.3 Draft BNBC 2017

According to draft BNBC 2017, sec-2.5.5.3.2, following are different types irregularities that may exist along vertical elevations of a building.

(i) Stiffness irregularity - soft storey

A soft storey is one in which the lateral stiffness is less than 70% of that in the storey above or less than 80% of the average lateral stiffness of the three storeys above irregularity as shown in Figure 2.3. An extreme soft storey is defined where its lateral stiffness is less than 60% of that in the storey above or less than 70% of the average lateral stiffness of the three storeys above.

(ii) Mass irregularity

The seismic weight of any storey is more than twice of that of its adjacent storeys as shown in Figure 2.3. This irregularity need not be considered in case of roofs.

(iii) Vertical geometric irregularity

This irregularity exists for buildings with setbacks with dimensions given in Figure 2.4.

(iv) Vertical in-plane discontinuity in vertical elements resisting lateral force

An in-plane offset of the lateral force resisting elements greater than the length of those elements as shown in Figure 2.4.

(v) Discontinuity in Capacity - weak storey

A weak storey is one in which the storey lateral strength is less than 80% of that in the storey above. The storey lateral strength is the total strength of all seismic force resisting elements sharing the storey shear in the considered direction as shown in Figure 2.4. An extreme weak storey is one where the storey lateral strength is less than 65% of that in the storey above.

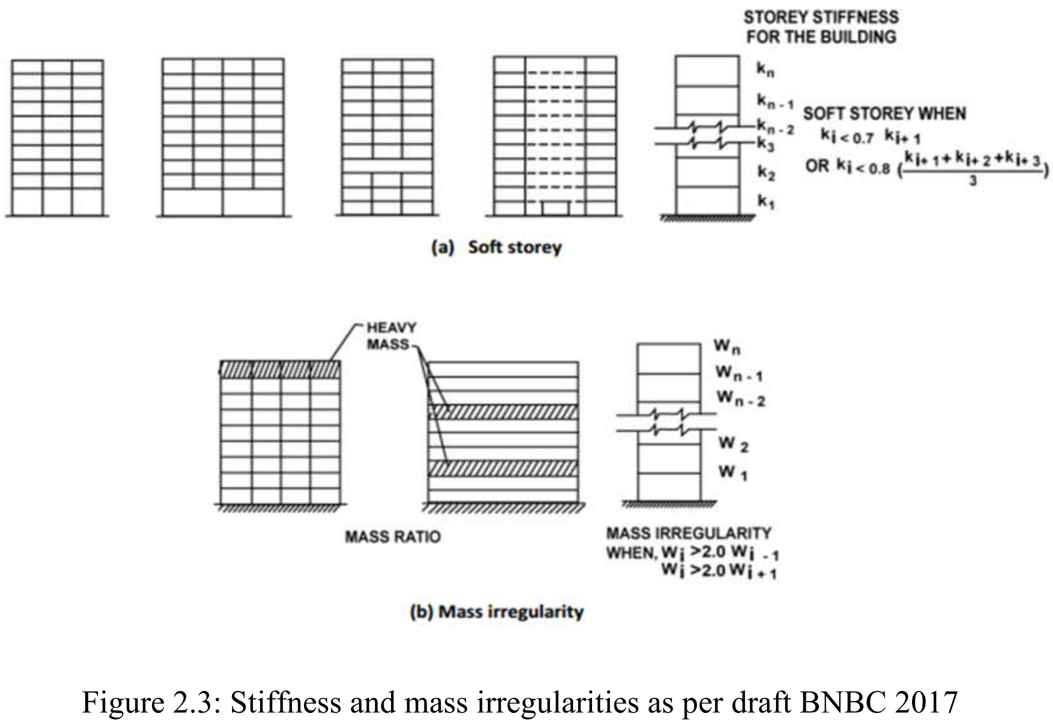

Figure 2.3: Stiffness and mass irregularities as per draft BNBC 2017

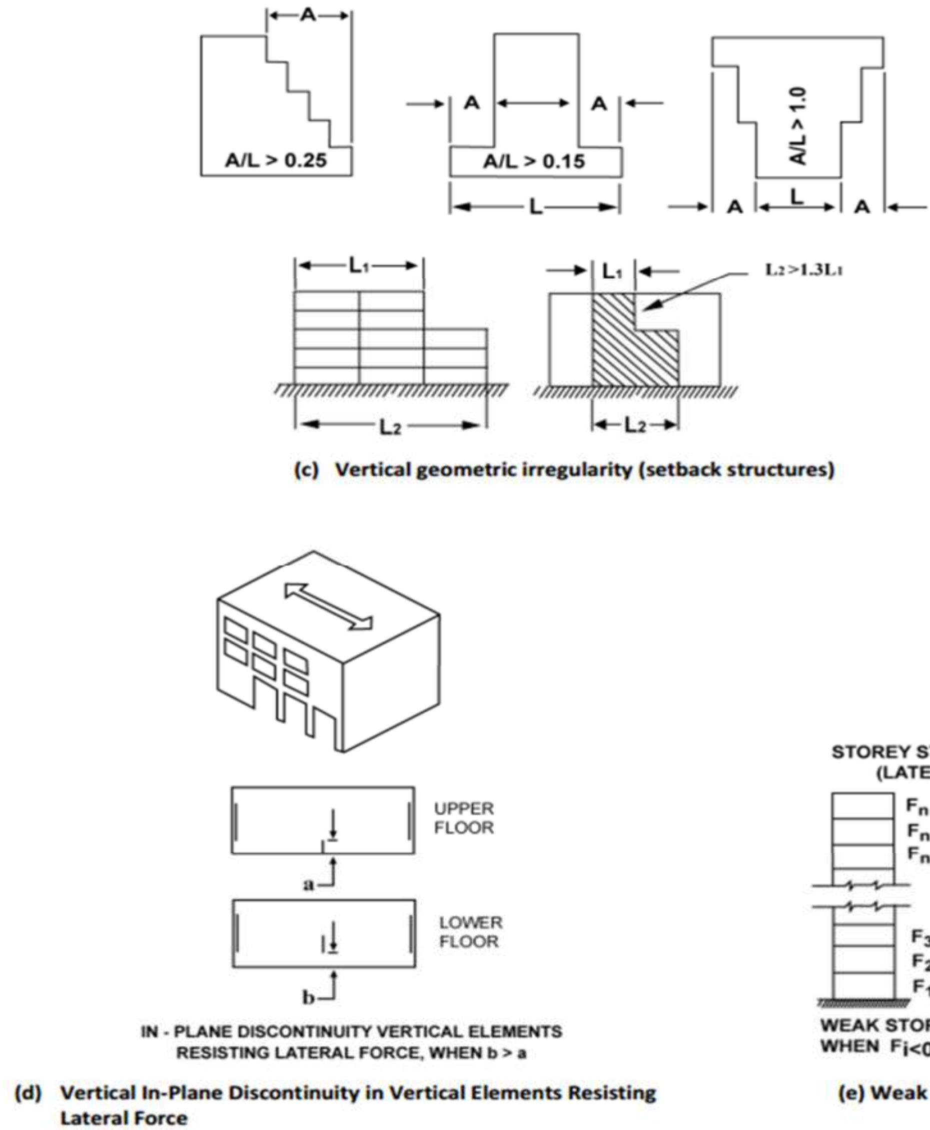

Figure 2.4: Geometric, vertical in-plane discontinuity and weak storey irregularity as per draft BNBC 2017

2.4 Effect of vertical irregularity on RC buildings in previous earthquakes

Reinforced concrete moment resisting frame structures with vertical irregularity behave poorly during past earthquakes. For example, during Kocaeli earthquake in Turkey, 1999), according to an official estimate, more than 20,000 moment resisting frame buildings collapsed and many more suffered minor to severe damage. Many of the collapses were attributed to the formation of soft first storey due to vertical irregularity that formed as a result of differences in framing and infill wall geometry between the first and upper stories. Figure 2.5 shows a moment resisting building which was damaged in Kocaeli earthquake (Turkey, 1999). The ground floor of the building was open and masonry infill was absent. At the upper floor, masonry infill walls were in regular format. So, the lateral stiffness was considerably larger at upper floors than that of the ground floor. Deformations are concentrated at the ground floor and the columns of the ground floor were severely damaged.

Figure 2.5: Formation of soft storey, Kocaeli earthquake, Turkey, 1999

Same pattern of the building soft storey collapse were experienced in Bhuj earthquake, India, 2001. Figure 2.6 shows two collapsed moment resisting buildings in which ground floor was opened for parking facility or any other purpose.

Figure 2.6: Formation of soft storey, Bhuj earthquake, India, 2001

2.5 Previous studies on vertically irregular structures

Researchers from 1960 to till now are working particularly with the seismic behavior and safety issues concerned with the vertical irregular structures.

An experimental study was conducted for a six storied two bay by two bay building having a 50% setback at mid-height moment resisting frame structure by Shahrooz and Moehle (1990). The issues they addressed in their study were: (1) the influence of setbacks on the dynamic response; (2) the adequacy of current equivalent static and dynamic design requirements for the setback buildings; and (3) design methods to improve the seismic response of setback buildings. Only two-dimensional response parallel to the set-back was considered. The acceleration histories of the 1940 El Centro record were used to simulate the earthquake shaking. They found that the conventional dynamic and conventional static design methods were found to be inadequate to prevent concentration of damage in members near the setback for certain configurations. The main conclusions of their study were as follows:

i) The dynamic characteristics of the tested irregular structure were similar to those expected for a regular structure except the torsion. However, a concentration of inelastic behavior was found at the setback level.

ii) There were no major differences between the seismic performances of the frames that were designed using equivalent static or modal spectral design methods.

iii) The fundamental mode dominates the response in the direction parallel to the setback and using equivalent static analysis should be sufficient to predict the seismic response of setback structures without the need to perform dynamic analysis.

Wong and Tsu (1994) studied the elastic response of setback structures by response spectrum analysis and found that the modal weights of higher order modes for setback structures are large. The seismic load distribution by response spectrum analysis was different from that of the static code procedures. They also found that for the setback structures, the first mode dominates the displacement response.

Valmundsson and Nau (1997) evaluated the Uniform Building Code (UBC) limits for mass, strength and stiffness for irregular buildings as shown in Figure 2.7. Three frames buildings with five, ten and twenty stories were considered in their study. The response of these three buildings was assessed under four earthquake records. The study concluded that the mass and stiffness vertical irregularities had a minor impact on the ductility demand compared to the strength vertical irregularity.

Al-Ali and Krawinkler (1998) investigated the effects of vertical irregularities by considering height-wise variations of seismic demands. They used a 10 storied building model. An ensemble of 15 strong ground motions, recorded on rock or firm soil during Western U.S. earthquakes after 1983, were used for the parametric study. The effects of vertical irregularities due to mass, stiffness and strength were considered both in separately and in combinations. The seismic response of irregular structures considering these irregularities was assessed by elastic and inelastic dynamic analyses. The study found that the effect of mass irregularity in seismic response of the structure is the smallest, the effect of strength irregularity is larger than the effect of stiffness irregularity. The effect of combined stiffness and strength irregularity was found the largest.

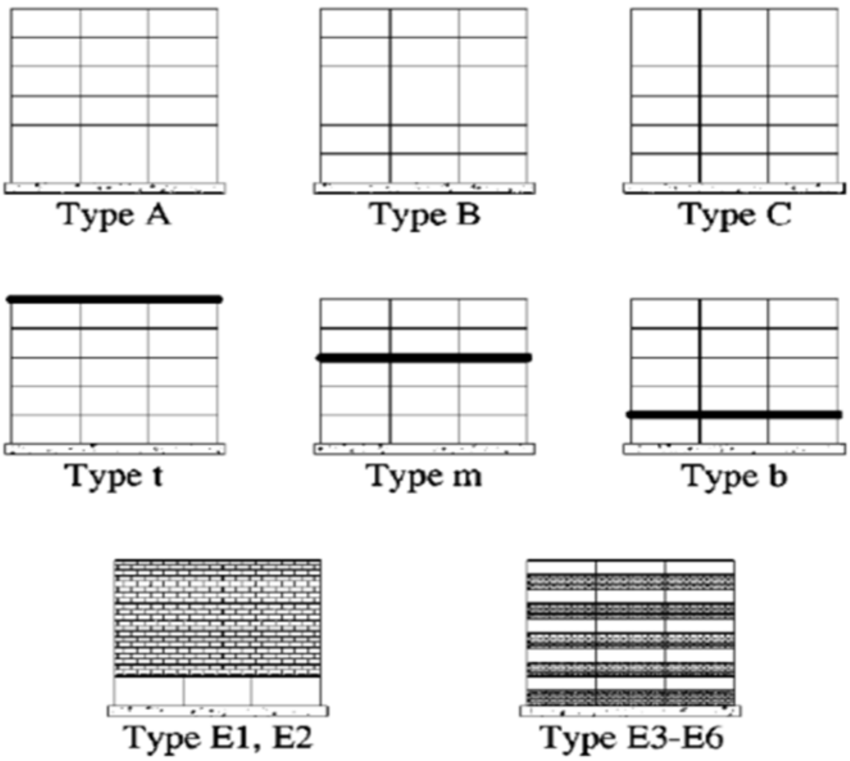

Figure 2.7: Irregular building models studied by Valmundsson and Nau (1997)

Das and Nau (2003) investigated the definition of irregular structures for different vertical irregularities: stiffness, strength, mass, and that due to the presence of nonstructural masonry infills as per uniform building code. They considered ensemble of 78 buildings with various inter-storey stiffness, strength, and mass ratios for detailed parametric study. Special moment-resisting frames was considered as lateral force-resisting systems. They concluded that the restrictions on the applicability of the equivalent lateral force procedure are unnecessarily conservative for certain types of vertical irregularities considered.

Athanassiadou (2008) conducted an assessment for two ten-storied two-dimensional plane frames with two and four large setbacks in the upper floors respectively and a third one which was regular in elevation as per Figure 2.8. Each reference irregular building had different setback configurations. The reference structures were designed for the high and medium ductility classes according to Eurocode 8. The analytical assessment was conducted using the nonlinear static pushover and nonlinear dynamic time history analyses. Eight earthquake records representing the short distance earthquake event were considered. The considered setback irregularity was considered in higher stories and the irregularity in lower stories was not considered, as this is a common scenario in buildings with geometric irregularity.

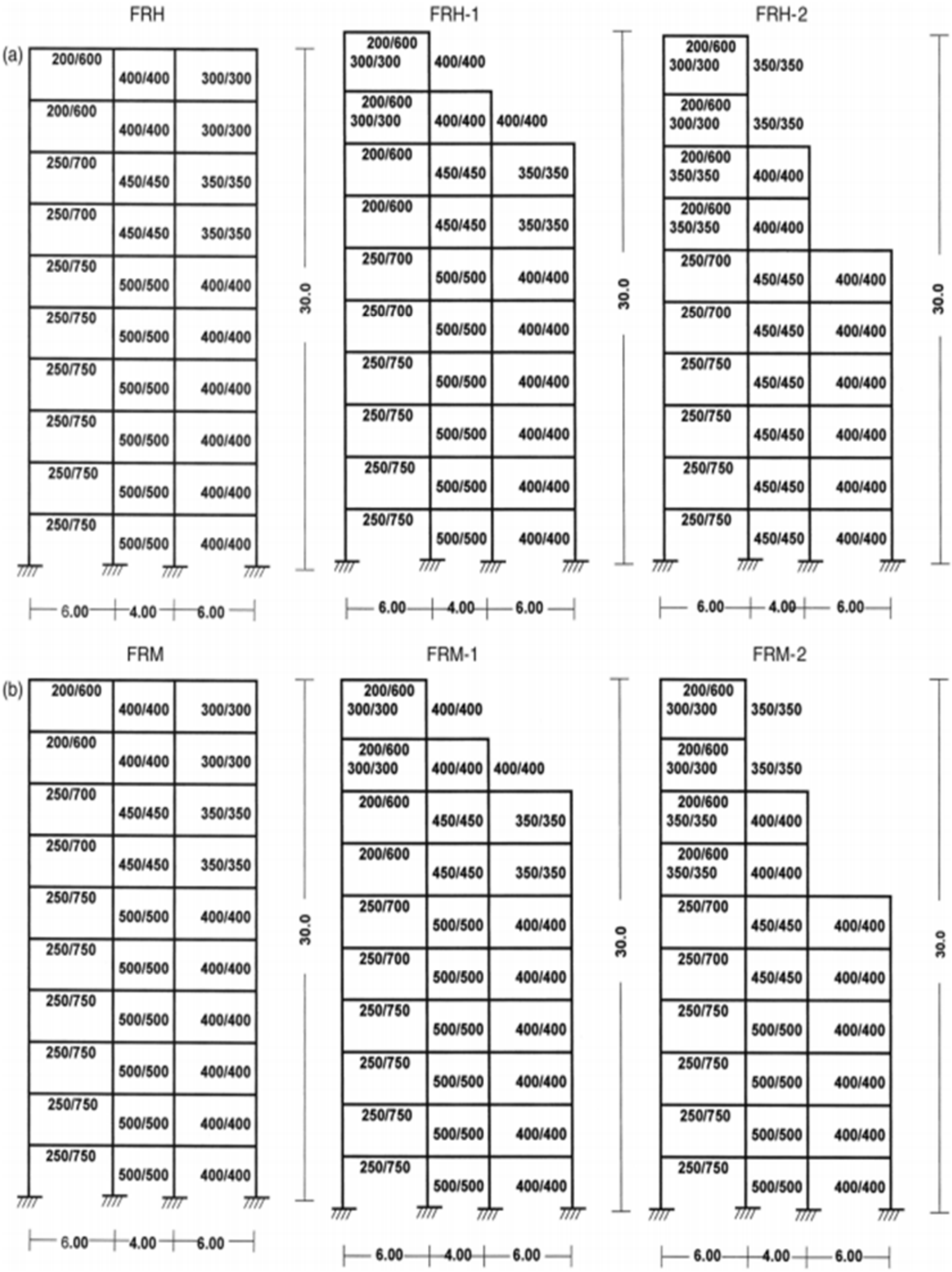

Figure 2.8: Irregular frame models studied by Athanassiadou (2008)

The study concluded that the seismic response of geometrically irregular structures was satisfactory. Most plastic hinges in the irregular frames were generated in beams at the design earthquake, which was consistent with the strong columns – weak beams design code approach. The over strength of the irregular building was similar to that of regular structures. It was concluded that the effect of the ductility class on the cost of buildings is negligible, while the seismic performance of all irregular frames appears to be equally satisfactory. The study also concluded that the inelastic static pushover analysis procedure is not recommended for the seismic assessment of high-rise buildings particularly those with vertical irregularity.

Varadharajan et al. (2013) examined the behavior of irregular buildings (Fig. 2.9) subjected to seismic excitation. A total of 195 frames with different geometrical arrangements of setbacks were considered. They used 27 natural earthquake records to generate 21,060 nos. nonlinear dynamic analysis results. Incremental dynamic analyses (IDAs) were performed to evaluate the impact of the set-back irregularity on the dynamic characteristic of irregular buildings.

The study concluded that the fundamental period and inter-story drift ratio were affected by the setback irregularity configuration. Finally, they proposed equations that can estimate realistic periods of setback frames incorporating the cracking effects. The equations were validated for two dimensional and three dimensional building models. Finally, applicability of the proposed equations in performance based and displacement-based designs were briefly discussed.

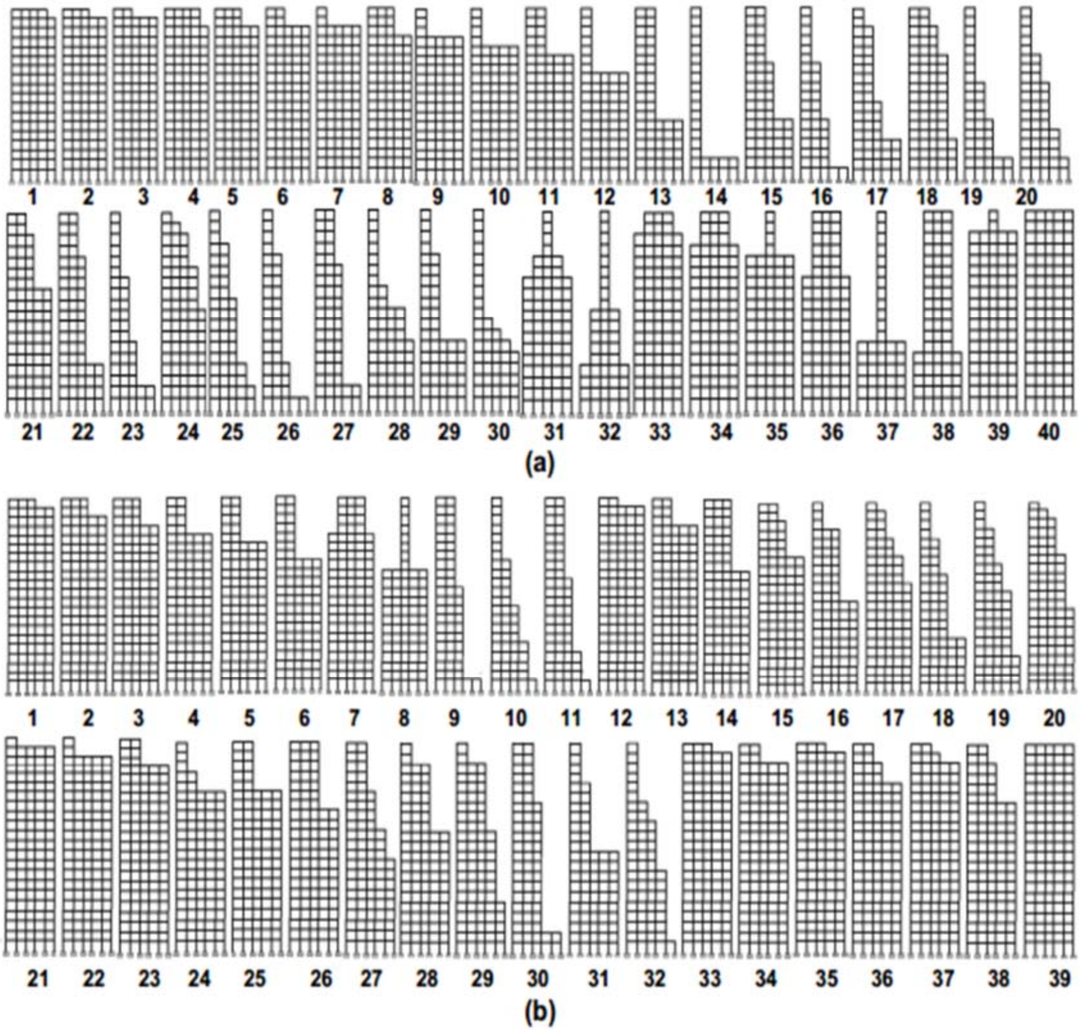

Figure 2.9: Irregular frame models studied by Varadharajan et al. (2013)

Summary of the studies related to vertically irregular structures discussed in section 2.5 can be stated as follows:

a) Shahrooz and Moehle (1990) found a concentration of inelastic behavior at the setback level. The dynamic characteristics of the tested irregular structure were similar to the regular structure except the torsion.

b) Wong and Tsu (1994) found that the modal weights of higher order modes for setback structures are large and seismic load distribution that is different from static code procedures. They also found that for the setback structures the first mode dominates the displacement response.

c) Valmundsson and Nau (1997) concluded that the mass and stiffness vertical irregularities had a minor impact on the ductility demand compared to the strength vertical irregularity.

d) Al-Ali and Krawinkler (1998) found the effect of mass irregularity in seismic response of the structure as the smallest. The effect of strength irregularity was larger than the effect of stiffness irregularity. The effect of combined stiffness and strength irregularity was found the largest.

e) Das and Nau (2003) concluded that the restrictions on the applicability of the equivalent lateral force procedure are unnecessarily conservative for certain types of vertical irregularities considered.

f) Athanassiadou (2008) concluded that the seismic response of geometrically irregular structures was satisfactory.

g) Varadharajan et al. (2013) concluded that the fundamental period and inter-story drift ratio were affected by the setback irregularity configuration. They proposed equations that can estimate realistic periods of setback frames incorporating the cracking effects.

2.6 Soft storey

2.6.1 Reasons of soft storey action

Stiffness irregularity occurs when there is a difference of lateral storey stiffness between the adjacent floors. Soft storey mechanism occurs due to stiffness irregularity. According to seismic code, the soft storey condition will be prevail when the stiffness of a storey is less than 70 percent of an adjacent storey. There are numerous possible configurations of soft stories in a building. Soft storey exists in a building due to:

- Different in inter-storey height at a particular storey as compared to adjacent storey, as shown in Figure 2.10(a).
- Modification of member properties, member sizes or material at a particular storey, as shown in Figure 2.10(b).
- Lack of infill wall or open storey, as shown in Figure 2.10(c).
- Vertical discontinuities of structural members at a particular storey, as shown

in Figure 2.10(d).

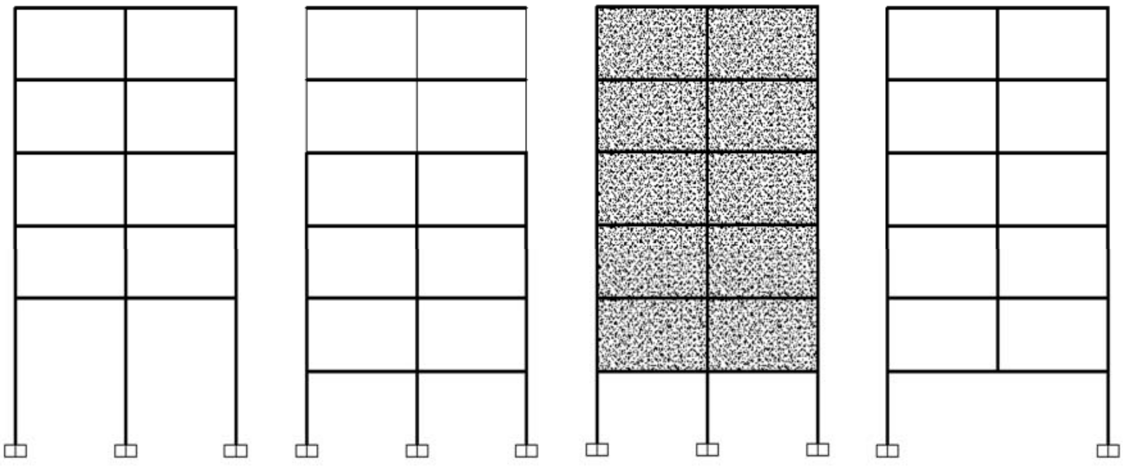

Figure 2.10: Examples of probable soft storeys by Sadashiva (2002)

Draft BNBC 2017 provides special attention to soft storey action due to open ground floor as it has become a common practice in Bangladesh for providing parking facility at the ground floor.

2.6.2 Design approach for soft storey action

Buildings with open parking spaces at the ground floor have a major source of soft storey action during an earthquake. According to draft BNBC 2017 (art. 2.5.17), a special arrangement is needed to increase the lateral strength and stiffness of the soft or open storey. The following two approaches have been suggested in draft BNBC 2017:

Approach-01: Dynamic analysis of such building may be carried out incorporating the strength and stiffness of infill walls and inelastic deformations in the members, particularly those in the soft storey, and the members designed accordingly.

Approach-02: Alternatively, the following design criteria are to be adopted after carrying out the earthquake analysis, neglecting the effect of infill walls in other storeys. Structural elements (e.g columns and beams) of the soft storey are to be designed for 2.5 times the storey shears and moments calculated under seismic loads neglecting effect of infill walls.

The Indian code IS 1893:2002 also recommends the similar two approaches as draft BNBC-2017. However, Eurocode 8 does not recommend any dynamic analysis.

Eurocode 8 also does not recommend any quantitative limit criteria to check stiffness irregularity or soft storey. If in case there is a drastic reduction of infill walls in any storey compared to the adjoining storeys, seismic forces in the less infilled storey shall be increased by a multiplication factor (MF) as given by the following expression

$$\eta = \left(1 + \Delta V_{RW} / \sum V_{ED}\right)$$

where, η is the multiplication factor, ΔV_{RW} is the total reduction in the lateral resistance of masonry infill wall in the concerned storey compared to the adjoining upper storey and $\sum V_{ED}$ is the design seismic force of the storey. Yadab and Mishra (2017) assessed the MF of 2.5 to be applied in the open ground storey column and beam recommended by IS 1893:2002. They performed equivalent static and response spectrum analysis for 4-storied moment resisting frame structure with no infill at the ground floor. They concluded that MF of 2.5 was seen too high for the open ground storey of the low rise buildings.

Davis et al. (2008) carried out nonlinear dynamic analysis including hysteresis effect of frame and infill on a four-storied and a seven-storied building for various infill wall arrangements. They suggested that there is no need for applying MF for low rise buildings. In case of the seven-storied building, they found MF in a range of 1.14 to 1.29. Karemore and Rayadu (2015) studied G+3 open ground floor system building by both linear and nonlinear analyses. They stated that MF of 2.5 to be applied on calculated shear force and bending moment is very conservative. They also concluded that the MF for bending moment is in the range of 1.06-1.98 for columns and for beam it is in the range of 0.92-1.06 for the soft storey level. MF for shear force was in the range of 1.42-1.52 for the column and for beam it was in a range of 0.97-1.07 for the soft storey. Misra and Jaisal (2017) found the MF for columns and beams ranged from 1.28-1.6 and 1.16-1.24, respectively for the maximum bending moment. They found magnification factor for columns and beams were in a range of 1.21-1.31and 1.12-1.14, respectively for the maximum shear force. Therefore, different codes and researchers proposed and stated out different approaches and different magnification factor in designing the open soft storey.

Draft BNBC 2017 proposed guidelines for designing structural elements (e.g. columns and beams) of the soft storey with a magnification factor of 2.5 for storey shears and moments when dynamic analysis will not be carried out considering the effect of infill. The current study is aim to evaluate the value of this magnification factor for the considered vertically irregular building structures.

Chapter 3

MASONRY INFILL WALL

3.1 General

Brick masonry partition wall is commonly used in reinforced concrete (RC) frame structure in Bangladesh. It is shown that these walls consist of relatively strong brick units and weak mortar joints. Since these are usually considered as non-structural elements, their interaction with the frame is often ignored in the design phase. But it was found that masonry infill wall has a contribution in response of the structure due to lateral force induced in an earthquake and may be related to safety of the occupants. Moreover, in Bangladesh and many other countries, construction of multistoried building with open ground storey for car parking or other utility services is a common practice. These building are designed as RC frame structures without considering the structural action of infill located on the upper floors in case of lateral load resisting system. Since the mass is concentrated at upper floors, it makes upper floors heavier than the ground open floor and creates the action of inverted pendulum. Infill on the upper floors makes the floors much stiffer in resisting the lateral seismic loads compared to that of the open ground floor. As a result, ground floor acts as a soft storey and consequently collapse of the ground floor occurs during an earthquake event.

3.2 Behavior of masonry infill wall

Observations from past earthquakes show that masonry infill wall plays an important role in controlling the seismic behavior of the structure. According to Murty and Jain (2000), the presence of masonry infills in RC frames changes the lateral load transfer mechanism of the structure from frame action to truss action as shown in Figure 3.1. Hence, reduction in bending moments and increase in axial forces occur in the frame members. Masonry infill walls confined by reinforced concrete frames plays a vital role in resisting the lateral seismic loads on buildings. The behavior of masonry infilled frames has been extensively studied in attempts to develop a rational approach for design of such masonry infilled frames.

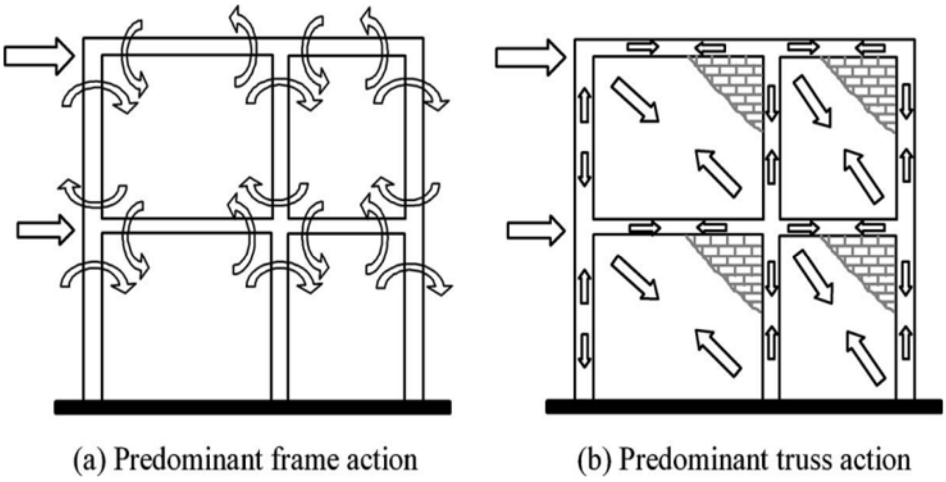

Figure 3.1: Change in lateral load transfer mechanism due to masonry infills by Murty and Jain (2000)

Moghaddam and Dowling (1987) found masonry infill walls having a very high initial lateral stiffness and low deformability. The beneficial effects of the interaction between masonry infills and structural elements for seismic performance of existing frame buildings were noticed notably.

Researchers have concluded that proper use of infills in frames could result in significant increases in the strength and stiffness of structures subjected to seismic excitations. However, the locations of infill in a building must be carefully selected to avoid or minimize the soft story effect.

The failure mechanisms of the masonry infilled frames are complex because of the high number of parameters involved in the seismic response of the structure such as the material property, configuration, and relative stiffness of the frame to the infill. The failure criteria of the masonry infill wall:

- Infill corner crushing with flexural failure in the columns. This mechanism is most likely in strong and ductile frames with strong infill as shown in Figure 3.2(a).
- Horizontal sliding of the masonry with flexural or shear failure of the columns as shown in Figure 3.2(b). Infill crushing is sometimes observed in this failure. This failure mechanism was observed in the weak frames with weak panels and also in the strong and ductile frames with weak infill panels.

- Diagonal cracking in the infill with column shear failure making plastic hinges in columns as shown in Figure 3.2(c). This failure typically occurs in non-ductile frames with strong infill.

- Column flexural failure can occur in case of strong frames with weak connections or weak frames infilled with very strong masonry as shown in Figure 3.2(d). This failure mode takes place in the form of premature flexural failure of columns or of beam-column connections.

- Column shear failure can be occurred in infilled concrete frame columns just after the formation of horizontal sliding shear failure as shown in Figure 3.2(e). In this case, the two masonry sub-panels above and below the horizontal sliding plane in HSS mode would act as two knee bracing members resulting in column shear failure.

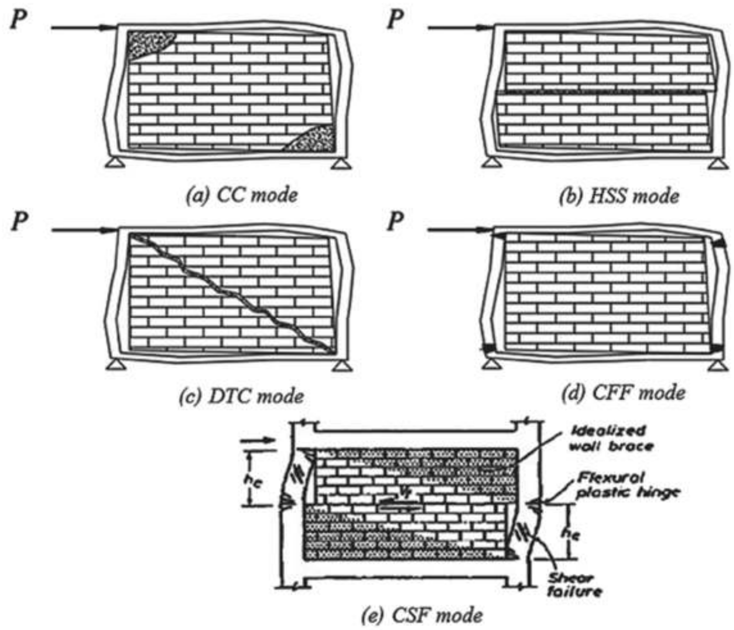

Figure 3.2: Different failure modes of infilled frame: (a) corner crushing; (b) horizontal sliding shear; (c) diagonal tension cracking; (d) column flexural; and (e) column shear from Penava et al. (2018)

3.3 Review of previous research on masonry infill wall

Several attempts have been made to define the seismic behavior of the reinforced concrete moment resisting frames with masonry panels and to develop methods for simulating the behavior of this kind of structure in the past 60 years. Most of these research works were concentrated on evaluating the stiffness of the infilled frame. In many works, infill-frame interaction is also addressed. The efforts conducted on the masonry infilled frames can be divided into three areas including experimental investigations and two types of analytical investigations, involving macro or micro-modeling approaches. Past researches in each of these areas are reviewed and details are presented in the following sections.

3.3.1 Experimental and numerical investigations

This section reviews experimental studies that have been conducted on masonry infilled reinforced moment resisting concrete frames. Some previous experimental investigations on the behavior of infilled frames are described below in chronological order.

Sachanski (1960) investigated the interaction between reinforced concrete frame and masonry infill wall. He conducted a set of static monotonic tests on full-scale infilled RC frames to check the theoretical approach to compute the stiffness of the combined frame-infill system and distribution of lateral force between the frame and infill. His method was applied to an infilled frame having homogeneous, isotropic infill with no separation between the frame and wall. The lateral load carrying capacity of the masonry wall was based on the criterion of maximum principal stresses i.e. when the first crack appeared in the masonry wall.

Fiorato et al. (1970) performed monotonic tests on several 1/8-scale infilled non-ductile RC frames. The specimens were different in terms of the number of stories, number of bays and the reinforcement arrangements. They concluded that existence of the masonry infill wall increases the stiffness and strength of the infilled frame, but decreases the ductility of the frame.

In order to assess the behavior of masonry infilled frame structures, Klingner and Bertero (1978) tested specimens under the monotonic loading. Infill materials were typically clay bricks. They concluded that presence of the reinforced infill panels decreases the risk of incremental collapse compared to the bare RC frame.

Buonopane and White (1999) conducted a two-story, two-bay reinforced concrete frame infilled with masonry by pseudo-dynamic testing of a half-scale specimen. There were provisions for window openings in the second story. They investigated the relationships between the type of cracking and storey drift-storey shear response. They concluded that the ability of the structure to resist lateral loads without excessive drift by mobilizing and maintaining effective compressive strut action was closely related to the type of cracking. They found diagonal cracking in the upper storey and horizontal bed joint shear cracking in the lower storey. This change in the cracking mode in the infill implies the use of other strut configuration than single diagonal strut in the modeling. They also concluded that that window openings in unreinforced masonry infill lead to a more desirable cracking pattern than that of the extensive bed joint cracking which occurs in full-panel infills. They also suggested using different strut configurations for modeling infill panel with openings.

Al-Chaar et al. (2003) tested five half-scale, single-story masonry infilled non-ductile concrete frames with different number of bays under monotonic static loading to provide guidelines for evaluating strength and stiffness of the unreinforced masonry infill panels in structures subjected to lateral forces. Their investigated models which were single bay bare frames, single bay with concrete masonry unit infill, single bay with brick infills, double-bay with concrete masonry unit infill and triple-bay with brick infill. Their results showed a significant increase in stiffness, ultimate and residual strength of the infilled frame compared to those of the bare frame. They also reported that the maximum strength and stiffness of the infilled frame increase with the increase in the number of span, but the behavior is not linear. They also concluded that infill wall may result in short column effect and generate torsional responses.

Hashemi and Mosalam (2006) conducted a shake-table test on a hypothetical 5-storey prototype structure with reinforced concrete frame and unreinforced masonry wall. The results of the shake-table tests in terms of the global and local responses were determined. They observed the effects of the masonry infill wall on the structural behavior and the dynamic properties of the test structure. They concluded that the masonry infill in the frame increases the strength and ductility of the test structure and shortens the fundamental periods.

Stavridis et al. (2012) conducted shake-table tests on a 2/3-scale, two-bay, three-story masonry infilled non-ductile RC frame which was the representative of a 1920's building in California. They used 14 scaled historical earthquake ground motion records with different intensities. The reinforced concrete frame had non-ductile reinforcement detailing. It was infilled with solid masonry walls in one bay and infill walls with window openings in the other bay. They reported that with an increase of the intensity of the base motion, the cracks in the masonry walls gradually propagated. It caused the development of significant diagonal shear cracks in the RC columns when the level of shaking in terms of the effective spectral intensity exceeded the maximum considered earthquake by 43%. As the base motion was increased further, the structure was severely damaged and severe diagonal crack were developed in the columns at the first storey.

All these experimental studies conducted in the past decades to investigate the difference in the strength and stiffness of the masonry infilled frames compared to those of the bare frames. Most of these studies reported the formation of the compression struts due to the presence of infill wall. However, a change of failure mechanism at different floor levels was also reported for some experimental results.

3.3.2 Modeling of masonry infill wall

Masonry infill wall is a highly orthotropic material due to the existence of the mortar joint. In addition, the masonry infill wall can experience different failure mechanisms, such as cracking, sliding, and compression failure depending on the position and properties of materials. To simulate the behavior of the masonry wall, different types of models have been developed depending on the level of accuracy needed. In the literature different types of models can be found which can be subdivided in two classes: i) micro-modeling and ii) macro-modeling. A brief discussion on these two modeling approaches has been given in the next sub-sections.

i) Micro-modeling:

Micro-modeling is a modeling technique which considers the effect of mortar joints as a discrete element in the model. Considering the fact that mortar joint is the weakest plane in a masonry wall, micro-modeling can be considered to be the most exact modeling approach for the masonry wall. Micro-modeling can be conducted in two levels: detailed micro-modeling and simplified micro-modeling as shown in Figure 3.3. In detailed micro-modeling approach, the brick and mortar joints are modeled as continuum elements and interface between the brick and mortar is modeled by an interface element. Both the continuum elements and interface elements may be defined by nonlinear stress-strain relations. Different constitutive models are used to define 1) the bricks, 2) the mortar joint and 3) the interface between the mortar and bricks.

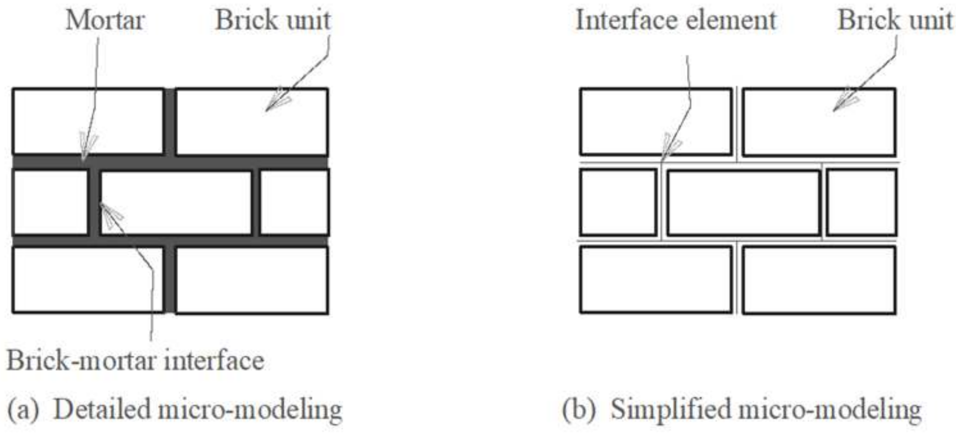

Figure 3.3: Different types of micro-modeling by Lourenço (1996)

In simplified micro-modeling approach, bricks are modeled by continuum elements, but the mortar joint and its interface with bricks is modeled together in an interface element.

ii) Macro-modeling:

In this approach, the masonry infill is modeled by one or more struts in each direction. The load path within infill mainly follows the diagonal. It is the most popular method for its simplicity in analysis to represent the masonry infill. According to this method, equivalent diagonal strut is used to represent the behavior of infill under lateral loads. A detailed discussion on this method has been given in the following section.

3.4 Equivalent strut model

Equivalent diagonal strut method is considered to be the most effective approach for representing the combined effect of frame-masonry infill for seismic actions. Under progressively increasingly lateral load, axial stresses along the diagonal becomes the dominant. Therefore, it is reasonable to model the infilled frame as a system braced by diagonal equivalent struts that simulate the axial behavior of the panels as given in Figure 3.4.

The fundamental factors that govern the equivalent strut model are the width of the strut (w) and the constitutive relationship of the panel. These two factors have been discussed in the following section.

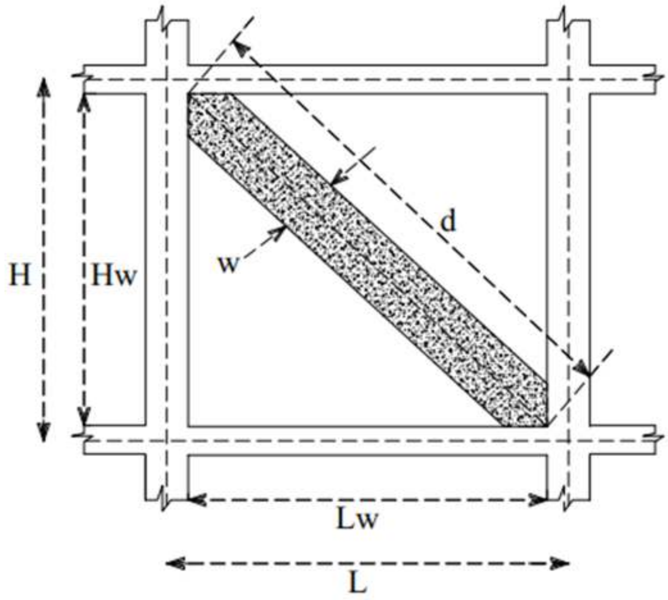

Figure 3.4: Equivalent strut model

3.4.1 Equivalent strut width estimation

In macro modeling of masonry infill wall, the strut width plays a major role in controlling the stiffness and strength of the infilled frame. The thickness of the strut is usually assumed as the same of the masonry panel, whereas different proposals have been suggested with regard to the width. Basically, there are two main approaches. The first one defines the strut width simply as a function of diagonal length, giving more emphasis on geometric aspects of the panel rather than its mechanical properties. The second approach defines it on the basis of the both geometry and mechanical properties of infilled frame materials. A brief discussion of the most representative proposals for both approaches has provided below.

Paulay and Priestley (1992) proposed replacing the infill by an equivalent diagonal strut made with the same material having pin joints at its ends and having the same thickness as the infill panel and a width *'w'* defined by:

$$\frac{w}{d} = \frac{1}{4}$$

where, d is the diagonal length of masonry panel as shown in Figure 3.4.

Later, many researchers worked on the strategy of Paulay and Priestley (1992) focusing on the diagonal length of the panel only. Among them, Kappos et al. (1998)

recommended it as 0.2d.

On the other hand, some researchers considered the mechanical properties of infill materials and geometric properties of the infill panel. This approach is more justified as it considered the level of degradation and the cracking of the panel which is important to define the stiffness and strength of the infill panel. The first author to work in this approach was Smith and Carter (1969). They recommended a theoretical relationship for the width of the diagonal strut connected to infill–frame stiffness parameter λ_h, and revealed that the effective width of the strut was not a constant value for a particular infill but decreased as the load increased. They proposed the equivalent width as function of the relative panel-to-frame-stiffness parameter, in terms of:

$$w = 0.58\left(\frac{1}{H_w}\right)^{-0.445} \left(\lambda_h H\right)^{0.335d\left(\frac{1}{H_W}\right)^{0.064}}$$

where, H_w is the infill wall height, H is the column height, $\lambda_h = \sqrt[4]{\frac{E_w t_w \sin 2\theta}{4E_c I_c h_w}}$ in which E_w is the modulus of elasticity of masonry panel, t_w is the thickness of infill panel and equivalent strut, $E_c I_c$ is the flexural rigidity of the columns, and θ the angle, whose tangent is the infill height to length aspect ratio, is equal:

$$\theta = \tan^{-1}\left(\frac{h_w}{L_w}\right)$$

where, L_w is the length of infill panel. All the above parameters are explained in Figure 3.4.

Klingner and Bertero (1978) performed laboratory tests on scaled models produced by RC frame and infill panels made by clay bricks. They obtained the following expression for the width of the equivalent strut:

$$\frac{w}{d} = 0.175(\lambda_h h_w)^{-0.4}$$

According to Abdul-Kadir (1974), the width of the strut was influenced not only by the adjacent columns, but also affected by the top beam. Therefore, he divided the parameter λ into two different factors λ_T and λ_P that were correlated to the adjacent columns and to the upper beam, respectively, and developed a relation for the width of the equivalent strut, as a function of the two different factors λ_T and λ_P as follows:

$$w = \frac{\pi}{2}\sqrt{\left(\frac{1}{\lambda_T}\right)^2 + \left(\frac{1}{2\lambda_P}\right)^2}$$

where,

$$\lambda_T = \sqrt[4]{\frac{E_w t_w \sin 2\theta}{4E_c I_T h_w}} \text{, and } \lambda_P = \sqrt[4]{\frac{E_w t_w \sin 2\theta}{4E_c I_P h_w}}$$

Durrani and Luo (1994) conducted a comprehensive numerical finite element analysis. Their expression was somewhat too complex to use as the equation considered the beam stiffness, column stiffness, and both infill and panel aspect ratios. Their proposed formula in which the effects of frame geometry and material properties were considered through the coefficient m and γ is as follows:

$$w = \gamma\sqrt{L^2 + H^2}\, \sin 2\theta$$

where, $\gamma = 0.32\sqrt{\sin(2\theta)}\left(\frac{E_w t_w h^4}{m I_c E_c h_w}\right)^{-0.1}$ and $m = 6\left(1 + \frac{6E_c I_b h}{\pi E_c I_c L}\right)$

Mainstone and Weeks (1970), based on experimental and analytical data, proposed the following empirical data for the calculation of the equivalent width:

$$\frac{w}{d} = 0.175(\lambda_h h)^{-0.4}$$

This equation was included in FEMA 306 (1998) as it has been proven to be the most effective over the years. This equation was accepted by the majority of researchers dealing with the analysis of infilled frames.

3.4.2 Stiffness of the equivalent strut

It is well acknowledged that the presence of masonry infill wall in a frame modifies the strength and stiffness of the system by altering the seismic response. In literature, different proposals are available for quantifying the strength and stiffness of infill. Actually, in all the formulations discussed in above section, the width of the equivalent strut is not related to progressive degradation of the strength and stiffness of infill panel under cycling loading. But this is a very important issue which affects the performance of the structure.

One of the early attempts to define the complete force-displacement behavior of the masonry infill panel was conducted by Klingner and Bertero (1978). They proposed a nonlinear hysteretic response for the equivalent diagonal strut model based on the findings of the experiments conducted on masonry infilled RC frames. They considered the strength degradation and reloading stiffness deterioration in their cyclic model, as shown in Figure 3.5.

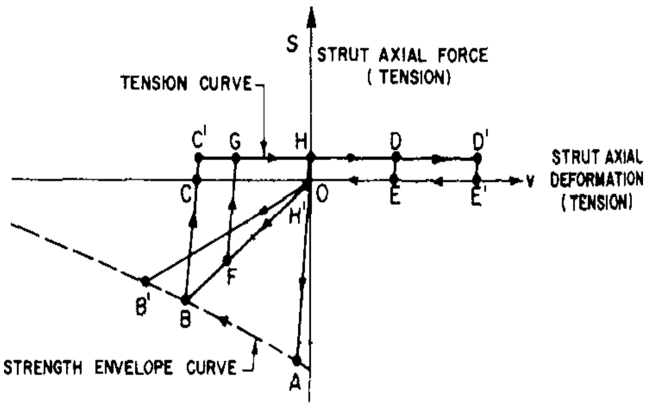

Figure 3.5: Force-displacement response of the strut by Klingner and Bertero (1978)

A constitutive formula was proposed by Panagiotakos and Fardis (1996) by studying the global response of RC frame structure through nonlinear dynamic response spectrum analysis. They obtained the curve as shown in Figure 3.6 having four segments. The first segment represents the initial shear behavior of uncracked panel. The second segment depends on the equivalent diagonal strut formation in the panel after the separation of infill from boundary frame. The third segment defines the infill wall softening behavior after the critical displacement S_m and is characterized by the K_3 slope. The last horizontal part defines the final state of the panel and is characterized by a constant residual resistance.

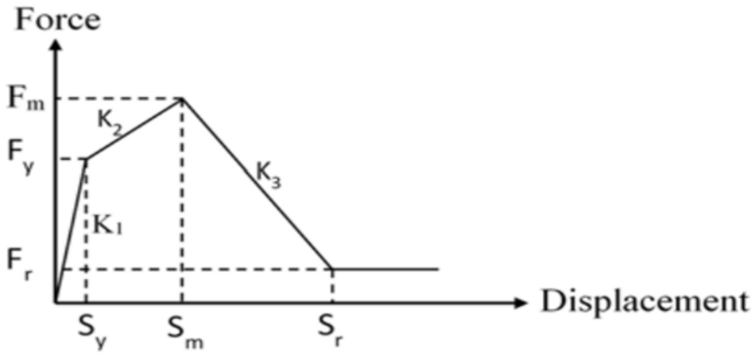

Figure 3.6: Force-displacement response of the strut by Panagiotakos and Fardis (1996)

However, some authors neglect the final part assuming a softening line that reaches a zero-residual strength. Thus, the initial shear stiffness of uncracked panel (K_1), yielding force at first cracking of infill panel (F_y), displacement corresponding to yielding (S_y), axial stiffness of equivalent strut (K_2) and displacement corresponding to maximum force are given below:

$$K_1 = \frac{G_w T_w L_w}{H_w}$$

$$F_y = f_{tp} T_w L_w$$

$$S_y = \frac{F_y}{K_y}$$

$$K_2 = \frac{E_m b_w T_w}{d}$$

$$S_m = S_y + \frac{F_m - F_y}{K_2}$$

where, G_w is shear modulus; f_{tp} is tensile strength of infill panel; L_w, H_w and T_w are the clear length, height and thickness of infill panel, respectively.

Dolsek and Fajfar (2005) simplified the equation provided by Panagiotakos and Fardis (1996) in 2005. In their proposed equation, the residual force (F_r) was considered as zero and the ratio of yield and maximum force was taken as 0.6 and the ratio between the displacements at the collapse force to the maximum force was considered as 5.

Chapter 4

RESPONSE REDUCTION FACTOR

4.1 General

Due to economic and architectural demand, civil engineers are obliged to design structural systems which are aesthetical in view, cost effective as well as adequately safe for inhabitants. Scare resources of construction materials, technological advancement and time lead the engineers to design the structure in a cost-effective way. The basic principle of earthquake resistance design of structures is that the structure should not be collapsed but small damage to the structural and non-structural elements is permitted. However, by allowing some structural and non-structural damage, a high level of life safety can be economically achieved in structures by allowing inelastic energy dissipation. As a result of this design philosophy, the design lateral strength prescribed in seismic codes is lower than the lateral strength required to maintain the structure in the elastic range.

Conventional seismic design in codes of practice is entirely force-based. This design method is suited to design for loads that are permanently considered. Members are designed to resist the effects of these loads. But, seismic design should consider the fact that inelastic deformations may be utilized to absorb certain levels of energy leading to reduction in the forces for which structures are designed. This leads to the idea of response reduction factor (R). This factor is used to account for expected overstrength, energy absorption and dissipation i.e. ductility and structural capacity to redistribute forces from highly stressed regions to other less-stressed locations in the structure. This term is also known as force reduction factor which reflects the capability of the structure to dissipate energy through inelastic behavior.

4.2 Definition and formulation of response reduction factor (R)

Reduction factor defines the level of inelasticity expected in structural systems during an earthquake event. With some major assumptions and experiences, R factor is first introduced by ATC in 1978, served to reduce the base shear force calculated by elastic analysis using a 5% damped acceleration response spectrum for the purpose of calculating design base shear. National Earthquake Hazards Reduction Program

(NEHRP) provision defines R factor as “R factor is intended to account for both damping and ductility inherent in structural systems at the displacements great enough to approach the maximum displacement of the systems”. This definition provides some guidelines into the understanding of the seismic response of buildings and the expected inelastic behavior of a code-compliant building in the design earthquake. R factor is widely used into the static elastic analysis of structures to account for inelastic response.

In the mid-1980s, data from an experimental research program at the University of California at Berkeley were used to develop an improved understanding of the seismic response. Using the experimental data, the Berkeley researchers proposed a draft formulation for the response reduction factor. Base shear-roof displacement relationships were established using data acquired from the earthquake simulator testing of two code-compliant framing systems. The Berkeley researchers described R factor as the product of three factors that accounted for overstrength, ductility and added viscous damping:

$$R = R_S . R_\mu . R_\xi$$

In the above equation, R_S is overstrength factor, R_μ is ductility reduction factor and R_ξ is damping factor. The overstrength factor was calculated to be equal to the maximum base shear force at the yield level (V_y) divided by the design base shear force (V_d) as shown in Figure 4.1. The ductility reduction factor was calculated as the base shear (V_e) for elastic response divided by the yield base shear force (V_y). The damping factor R_ξ is intended to account for the influence of supplemental viscous damping devices. The damping factor R_ξ was set equal to 1.0 as there was no provision of supplementary damping device.

Further research has been completed since the first proposal for splitting R into three component factors. Studies conducted by ATC 19 (1995) proposed a new formulation for R in which R is expressed as the product of overstrength factor, ductility factor and redundancy factor. Values of redundancy factor as suggested by ATC 19 are 0.71, 0.86 and 1.0 for 2, 3 and 4 or more vertical lines of framing, respectively. The equation was as follows:

$$R = R_S . R_\mu . R_R$$

where, R_S is overstrength factor, R_μ is period dependent ductility factor and R_R is redundancy factor. This formulation, with the exception of the redundancy factor, is almost similar to those proposed by the Berkeley researchers.

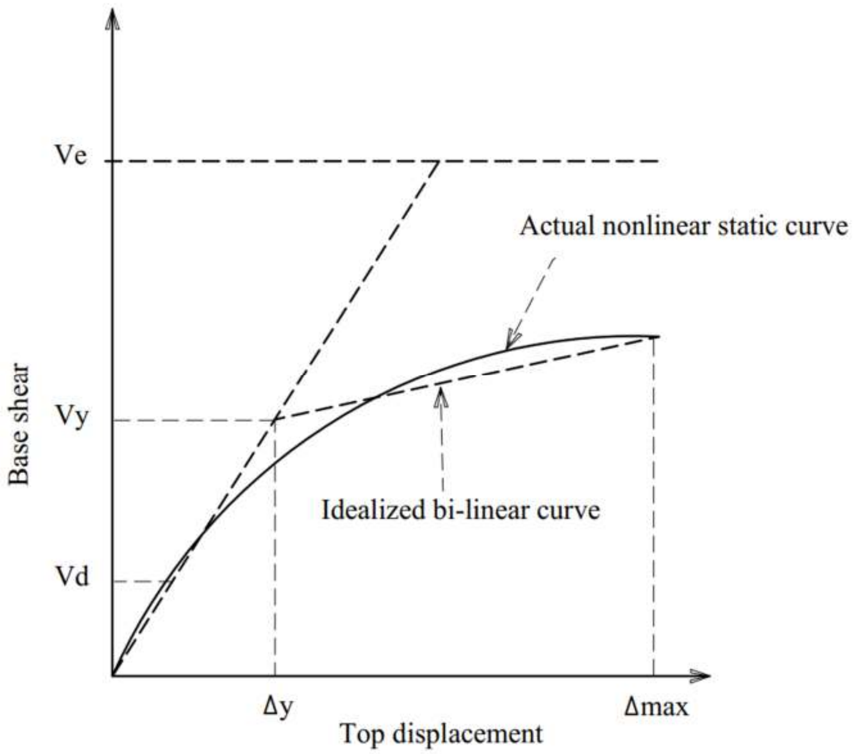

Figure 4.1: Force-Displacement relationship for R factor

4.3 Overstrength factor (R_s)

The real strength of a structure will more likely be higher than its design strength. This is due to overall design simplifications and assumptions that are incorporated through the process. These assumptions and design practices are usually in favor of conservative design as to stay on the safe side. The design code can mandate a strength level for the material while the actual strength is higher.

Overstrength of a structure due to its inelastic behavior under lateral loading can be assessed by numerical analysis. Non-linear static or pushover analysis procedure is a functional tool for estimating the lateral yield strength of the structure. Significant yield point is determined by idealizing the resultant capacity curve of the structure. Base shear vs. roof displacement graph is reformed as a bilinear curve where the junction between the two curves indicates the yield displacement and the yield base shear. Overstrength factor (R_s) is the ratio between the yield base shear to design base shear as provided in below:

$$R_S = \frac{V_y}{V_d}$$

An example illustration for significant yield point can be seen in Figure 4.1 at point (V_y, Δ_y). In the following sub-section, some research works regarding the overstrength factor for RC buildings have been reviewed.

4.3.1 Previous studies on overstrength factor (R_s)

Mitchell and Paultre (1994) studied the influence of ductility and structural overstrength in the seismic design of reinforced concrete structures. They summarized some factors contributing to overstrength and factors that limit overstrength. They also stated that some factors such as non-structural elements can provide additional strength but can be detrimental for the case of low period structures. In addition, the presence of partial masonry infills can create “short columns” which may be susceptible to brittle shear failures. Design and detailing provisions in all seismic codes require minimum amounts and maximum spacing of reinforcement and these requirements are the main source of overstrength for the structure.

Kappos (1999) evaluated the behavior factors for seismic design of structures considering both of ductility and overstrength of the structure. He examined one five storied reinforced concrete structure which was consisting of beams, columns, and structural shear walls. He found that the overstrength was higher in the case of low-rise structures and the values up to 2.7 were reported, compared to about 1.5 for medium and high-rise structures.

Massumi et al. (2004) investigated structural overstrength factor of a large number of multi-bay and multi-storied buildings ranges from 1 to 10 storeys using both dynamic inelastic time history and static inelastic pushover analyses. A large number of actual earthquake records were used in dynamic analysis. They found that number of bays did not affect overstrength factor significantly. Low-rise buildings had higher overstrength factor. The overstrength factors were found ranges from 1.7 to 3.3 approximately when ultimate strength design approach was considered whereas approximately 2.5 to 5 were found when working stress design approach were considered.

Lee et al. (2005) investigated overstrength factors for 5, 10 and 15-storied moment resisting RC buildings designed in low and high seismicity regions using nonlinear static analysis. They concluded that overstrength factors in low seismicity regions are larger than those of high seismicity regions for structures designed with the same response reduction factor. They found overstrength factors ranging from 2.3 to 8.3.

Mwafy (2013) carried out elastic and inelastic analysis to investigate the overstrength factor of a wide range of reinforced concrete buildings of different characteristics ranging from 8 to 60-storied. Realistic input ground motions were adopted based on design spectra and seismicity of the regions from where the buildings were selected. The found overstrength factor in a range of 2.1 to 2.42 for the considered reinforced moment resisting frame structures.

Chaulagain et al. (2014) explore the effect of the overstrength factor on the ductility factor, beam column capacity ratio on building ductility and load path on response reduction factor. They considered twelve irregular engineered RC buildings in Kathmandu, Nepal. They found overstrength factor in a range of 2.1 to 4.28 for the considered buildings.

Hanafy et al. (2017) investigated overstrength factors of 2 and 3-storied moment resisting RC buildings for six different seismic zones according to Egyptian Code. They found overstrength factor in a range of 1.06 to 1.21 for 2-storied buildings and 1.03 to 1.19 for 3-storied buildings.

4.4 Ductility factor (R_μ)

The extent of inelastic deformation experienced by the structural system subjected to a given ground motion or a lateral loading is given by displacement ductility ratio (μ). It is defined as the ratio of maximum absolute relative displacement (Δ_{max}) to its yield displacement (Δ_y).

$$\mu = \frac{\Delta_{max}}{\Delta_y}$$

Ductility factor (R_μ) is defined as a function of the period of the structure, the damping, the type of behavior and the displacement ductility ratio. It is primarily influenced by the period of vibration and the level of inelastic deformation, and to a much lesser degree by the damping and the hysteretic behavior of the system. Therefore, it can be expressed as:

$$R_\mu = R_\mu (T_i, \mu)$$

For very rigid structures where its natural period converges to zero, the inelastic strength demand in these systems is the same as the elastic strength demand, so the ductility factor must satisfy the following equation:

$$R_\mu = R_\mu (T_i = 0, \mu_i) = 1$$

For flexible structures where its natural period is higher, ductility factor will be the same as the displacement ductility. So, the system will satisfy the following equation:

$$R_\mu = R_\mu (T_i \to \infty, \mu_i) = \mu_i$$

4.4.1 Previous studies on ductility factors (R_μ)

In this section, some of the previous studies about ductility factors (R_μ) are reviewed and proposed formulations and plots of ductility factor are presented.

Based on elastic and inelastic response spectra of the El Centro, California earthquake Newmark and Hall (1982) observed that for the high and medium period structures, elastic and inelastic systems have the same maximum displacement. For the case of extreme low period structures, elastic and inelastic systems have the same forces. As a result of their observations, the authors provided a relationship as shown in Figure 4.2 that can be used to estimate ductility reduction factors (R_μ) for elasto-plastic SDOF systems as follows:

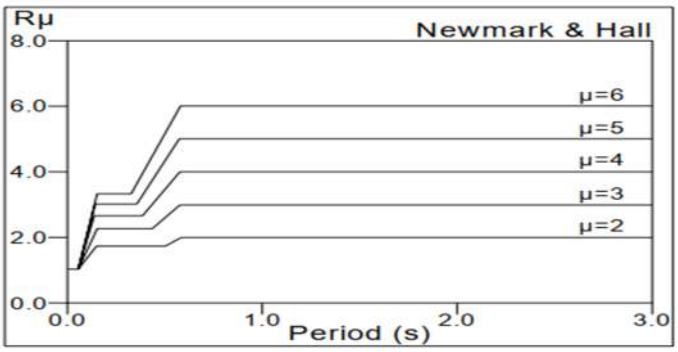

Figure 4.2: Relationship for ductility vs. period (Newmark and Hall (1982))

For structures having periods (T) below 0.03 second:

$$R_{\mu} = 1$$

For structures having periods (T) between 0.12 second and 0.5 second:

$$R_{\mu} = \sqrt{2\mu - 1}$$

For structures having periods (T) exceeding 1 second:

$$R_{\mu} = \mu$$

Nassar and Krawinkler (1992) developed a $R_{\mu} - \mu - T$ relationship for single degree freedom (SDOF) systems on rock or stiff soil sites. They used the result of statistical study based on 15 western United States ground motion records from earthquake ranging in a magnitude from 5.7 to 7.7. They developed an equation for ductility factor assuming 5% damping ratio as follows:

$$R_{\mu} = \left[c(\mu - 1) + 1 \right]^{1/c}$$

where,

$$c(T, \alpha) = \frac{T^{a}}{1 + T^{a}} + \frac{b}{T}$$

Parameters a and b were obtained for different strain-hardening ratios as follows:

$\alpha = 0.00$;   a = 1,   b = 0.42,

$\alpha = 0.02$;   a = 1,   b = 0.37,

$\alpha = 0.10$;   a = 0.8, b = 0.29

Here it is noted that when $\alpha = 0.00$ corresponds to an elastic-plastic system. The resulting $R_{\mu} - \mu - T$ relationship for a strain-hardening ratio of 0.1 is presented in Figure 4.3.

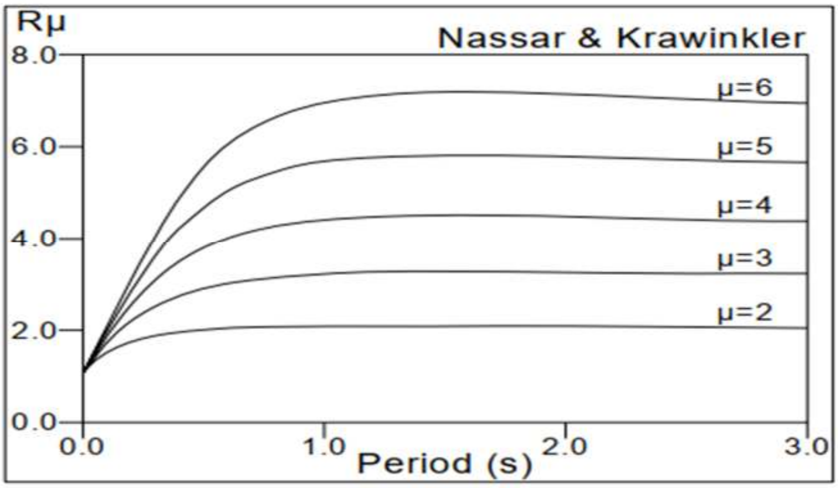

Figure 4.3: Relationship for ductility vs. period (Nassar and Krawinkler (1992))

Miranda and Bertero (1994) utilized 124 ground motions recorded on rock, alluvium and soft soil conditions belonging to various earthquakes. Ductility reduction factors were computed for 5% damped bilinear single degree of freedom (SDOF) systems and displacement ductility ratios were assumed between 2 and 6. Their equation for ductility factor is:

$$R_{\mu} = \frac{\mu - 1}{\phi} + 1$$

where,

For rock soils: $$\phi = 1 + \frac{1}{10T - \mu T} - \frac{1}{2T} exp\left[-\frac{3}{2}\left(ln\, T - \frac{3}{5} \right)^2 \right]$$

For alluvium soil: $$\phi = 1 + \frac{1}{12T - \mu T} - \frac{2}{5T} exp\left[-2\left(ln\, T - \frac{1}{5} \right)^2 \right]$$

For soft soil: $$\phi = 1 + \frac{T_g}{3T} - \frac{3T_g}{4T} - exp\left[-3\left(ln \frac{T}{T_g} - \frac{1}{4} \right)^2 \right]$$

Here, ϕ is a function of soil condition and T_g is defined as the predominant period of the motion. Figure 4.4 shows the $R_{\mu} - \mu - T$ relationship proposed by Maranda and Bertero (1994) for alluvium soil.

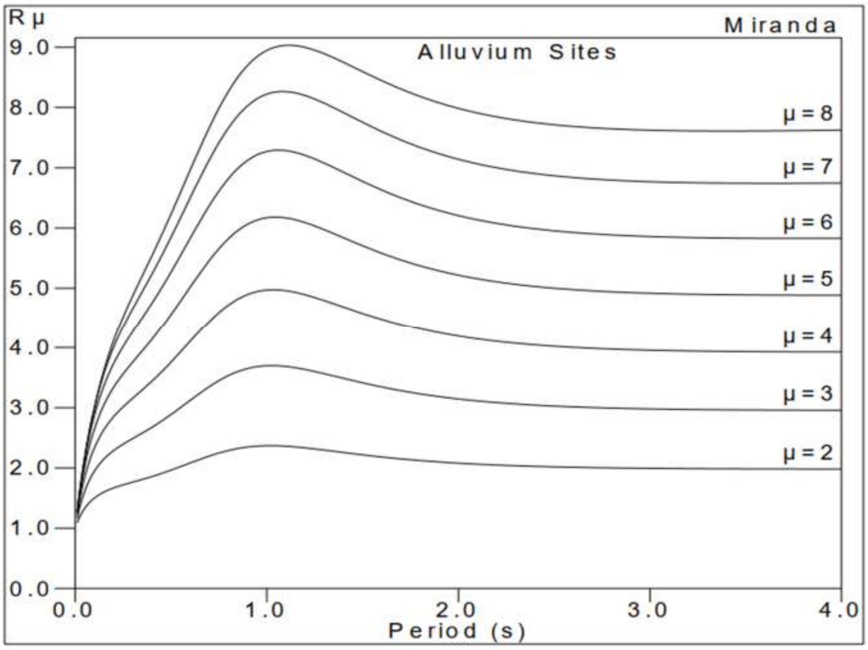

Figure 4.4: Relationship for ductility vs. period (Maranda and Bertero (1994))

AlHamaydeh (2011) investigated the seismic design factors for three reinforced concrete (RC) framed buildings with 4, 16 and 32-storied in Dubai, UAE, by conducting nonlinear analysis. The buildings were designed according to the response spectrum procedure defined in the International Building Code (IBC 2009). Two ground motion records with 10% and 2% probability of exceedance in 50 years were used. They found ductility factors in a range of 2.1 to 3.7 for 2% probability of exceedance and 1.25 to 2.4 for 10% probability of exceedance.

Sharifi and Toopchi-Nezhad (2018) investigated the seismic design factors for a group of 2D frame structures of 1, 2, 3, and 4 bays of 3, 5, 7, and 9-storied structures. To calculate the ductility factor and other factors, nonlinear static pushover analysis was conducted on each frame structure. They found ductility factors in a range of 4.05 to 7.7 for SMRF frames and 1.77 to 4.5 for OMRF frames.

4.5 Bi-linear approximation of capacity curve

Base shear vs. roof displacement curve or pushover curve is found from nonlinear static analysis. In order to extract meaningful and practical information, it is often required to develop an equivalent bilinear approximation of pushover curve. Bi-linear idealization provides the key components, which are the significant yield strength, the significant yield displacement as well as the predetermined design strength and the ultimate displacement. Equal-energy method is widely used for bilinear approximations to extract the relevant information from pushover curve proposed by ATC.

Bilinear curve is fitted in the pushover curve in such a way that the first segment starts from the origin and intersects with the second segment at the significant yield point. The second segment ends at displacement corresponding to a limit state or ultimate displacement. First segment, referred to as elastic portion, is then obtained with a mean slope of the successive parts of the curve until a remarkable change occurs. The second segment, referred to as post-elastic portion, is plotted by acquiring the significant yield point by means of equal energy concept in which the area under the pushover curve and the area under the bi-linear curve is kept equal. A generic illustration of the bi-linear approximation using equal energy concept is given in Figure 4.5.

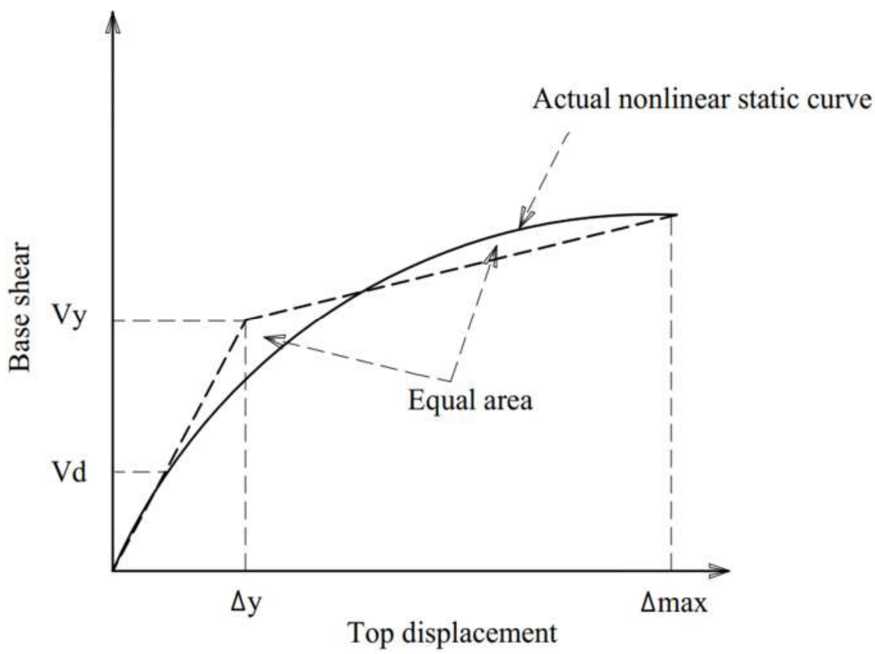

Figure 4.5: Bi-linear approximation of pushover curve

Chapter 5

STRUCTURAL MODELING AND ANALYSIS

5.1 General

The chapter presents a summary of various parameters defining the finite element models, the basic assumptions for seismic analysis and the building geometries considered for this study. For the design of the structures and their performance evaluation, finite element modeling of the structural systems is required. In the current study, integrated software for structural analysis and design ETABS 16.2.1 was used. Details of analysis procedures and important parameters considered in equivalent static, response spectrum, time history and non-linear static or pushover analysis for capacity evaluation of the considered frames have been discussed in this chapter. An accurate modeling is very important for the seismic analysis and performance evaluation of the structures. Therefore, validation of the model has been performed and comparison of obtained results are provided.

5.2 Estimation of fundamental period (T)

The most important structural parameter in the estimation of the seismic demand on a building is the natural period of the building. There are several existing empirical, analytical, and experimental methods which can be used to estimate the fundamental period of a building. According to draft BNBC 2017 (sec. 2.5.7.2), the fundamental period (T) of the building in the horizontal direction under consideration shall be determined using the following guidelines:

(a) Structural dynamics procedures (such as Rayleigh method or modal eigenvalue analysis), using structural properties and deformation characteristics of resisting elements, may be used to determine the fundamental period T of the building in the direction under consideration. This period shall not exceed the approximate fundamental period determined by Equation (1) by more than 40 percent.

(b) The building period T (in secs) may be approximated by the following formula:

$$T = C_t \left(h_n\right)^m$$

where, h_n is the height of buildings in meters or from top of the rigid basement.

The value of C_t and m are obtained from draft BNBC 2017.

In this study, fundamental period (T) of the considering structures were estimated by following two above mentioned methods. The following equation was used to estimate T using modal eigen value analysis method using the method (a):

$$T = \frac{2\pi}{\omega_n}$$

where, ω_n is the angular frequency of structure for the first mode of vibration.

5.3 Estimation of lateral storey stiffness

Presence of stiffness irregularity along the height leads to undesirable behavior of the building during an earthquake. Thus, seismic code recommends to identify the presence of stiffness irregularity of a building. This requires estimation of the lateral storey stiffness along the height of the building. In practice, several methods are used to estimate storey stiffness and different methods provide different results. In this thesis, lateral load displacement method has been used to estimate storey stiffness. As per code, the soft storey condition will be prevail if the stiffness ratio of a particular storey and its adjacent above storey (K_i / K_{i+1}) is less than 0.7. The extreme soft storey condition will be prevail if the stiffness ratio is less than 0.6.

Lateral load displacement method

Vijayanarayanan et al. (2017) proposed lateral load displacement method to define lateral stiffness. Stiffness is technically defined as the force per unit deformation. Using this complementary concept, they defined the lateral stiffness of a storey as the force per unit displacement. It is the ratio of cumulative storey shear force to the inter-storey lateral displacement. In this method, design earthquake loads are used to estimate storey stiffness. This method seems very easy and time savings. Designers does not require to perform too much analysis to estimate lateral stiffness of a storey. Step by step procedure to estimate lateral stiffness in lateral load displacement method has been shown in Figure 5.1.

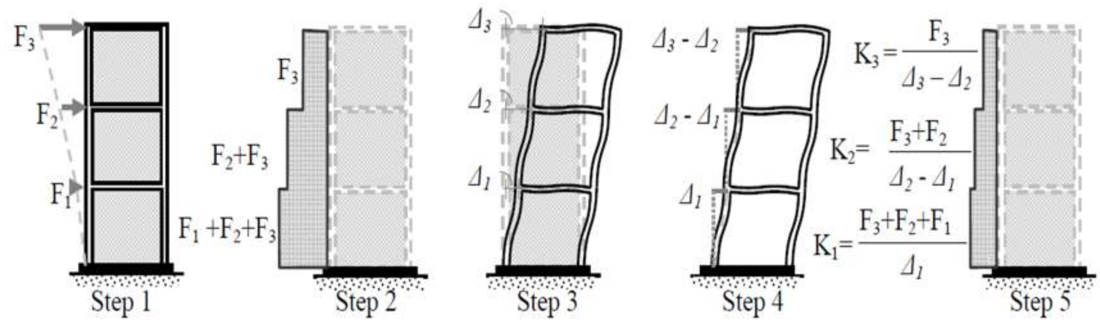

Figure 5.1: Lateral storey stiffness by Vijayanarayanan et al. (2017)

5.4 Nonlinear static or pushover analysis

Nonlinear static analysis or pushover analysis has become the preferred analysis procedure for design and seismic performance evaluation purposes. This procedure is relatively simple and considers post-elastic behavior. It is the procedure in which the magnitude of the lateral force is incrementally increased, maintaining the predefined distribution pattern along the height of the building. The base shear versus roof displacement relationship, referred to as the capacity curve, is the fundamental product of a pushover analysis because it characterizes the overall performance of the building. With the increase in the magnitude of the loads, weak links and failure modes of the building are found. Pushover analysis can determine the behavior of a building, including the ultimate load and the maximum inelastic deflection. Local nonlinear effects are modeled and the structure is pushed until a collapse mechanism gets developed. At each step, the base shear and the roof displacement can be plotted to generate the pushover curve. It gives an idea of the maximum base shear that the structure can capable of resisting at the time of the earthquake.

One of the most important issues in the pushover analysis is the load pattern applied to the structure. There are many acceptable applied load patterns to determine the pushover curve. The uniform and triangular lateral load patterns are recommended by the FEMA 356. In this thesis, lateral load pattern consistent with the fundamental mode shape of the building has been used. This lateral load pattern represents the distribution of lateral load according to following equation:

$$F_i = V \frac{W_i h_i^k}{\sum_{i=1}^{n} W_i h_i^k}$$

$K = 0.5T + 0.75$

where, W_i is the weight of the i- th storey, h_i is the height of the i-th storey, T is the fundamental period of the structure and V is the design lateral load. Axial force biaxial moment interaction hinges (P-M2-M3) were assigned for the columns, and moment hinges (M3) were assigned for the beams. The plastic hinges were assigned to the end of the members. Furthermore, axial force (P) hinges were assigned at the middle of the strut. Hinge properties were considered according to FEMA 356 (2000).

5.5 Building structures considered in the study

5.5.1 Structural geometry of the building models

The effects of vertical irregularity on seismic behavior of reinforced concrete (RC) frame structures have been investigated in this study. There are different types of vertical irregularity which has been discussed in section 2.1. Stiffness irregularity is one of them. In this thesis, stiffness irregularities due to sudden absence of infill wall at the ground floor level have been considered. Different types of RC moment resisting framing structures having different types of vertical irregularities are considered. All the studied structures had the same symmetric plan configuration with 4 nos. of bays along each direction as shown in Figure 5.2. Bay width was considered 5m. Figure 5.3 shows the three-dimensional view of 4, 6 and 10-storied RC frame buildings. Figure 5.4 shows the masonry infill configurations for the considered building models.

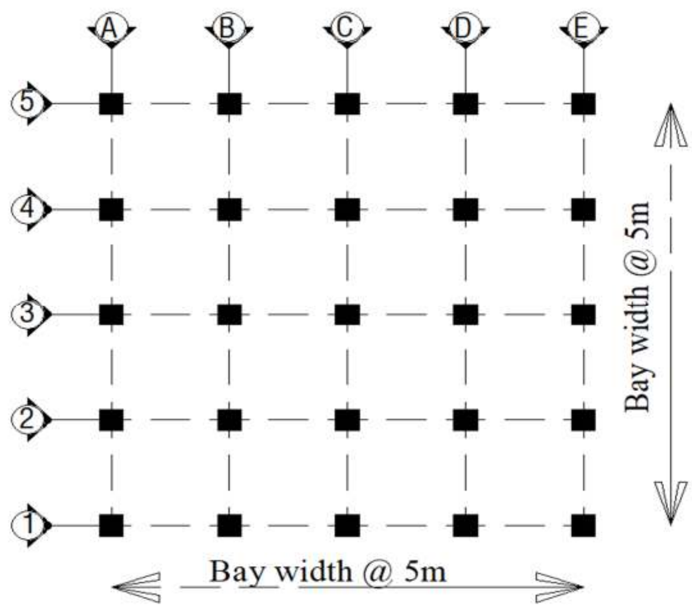

Figure 5.2: Plan view of 4, 6 and 10-storied buildings

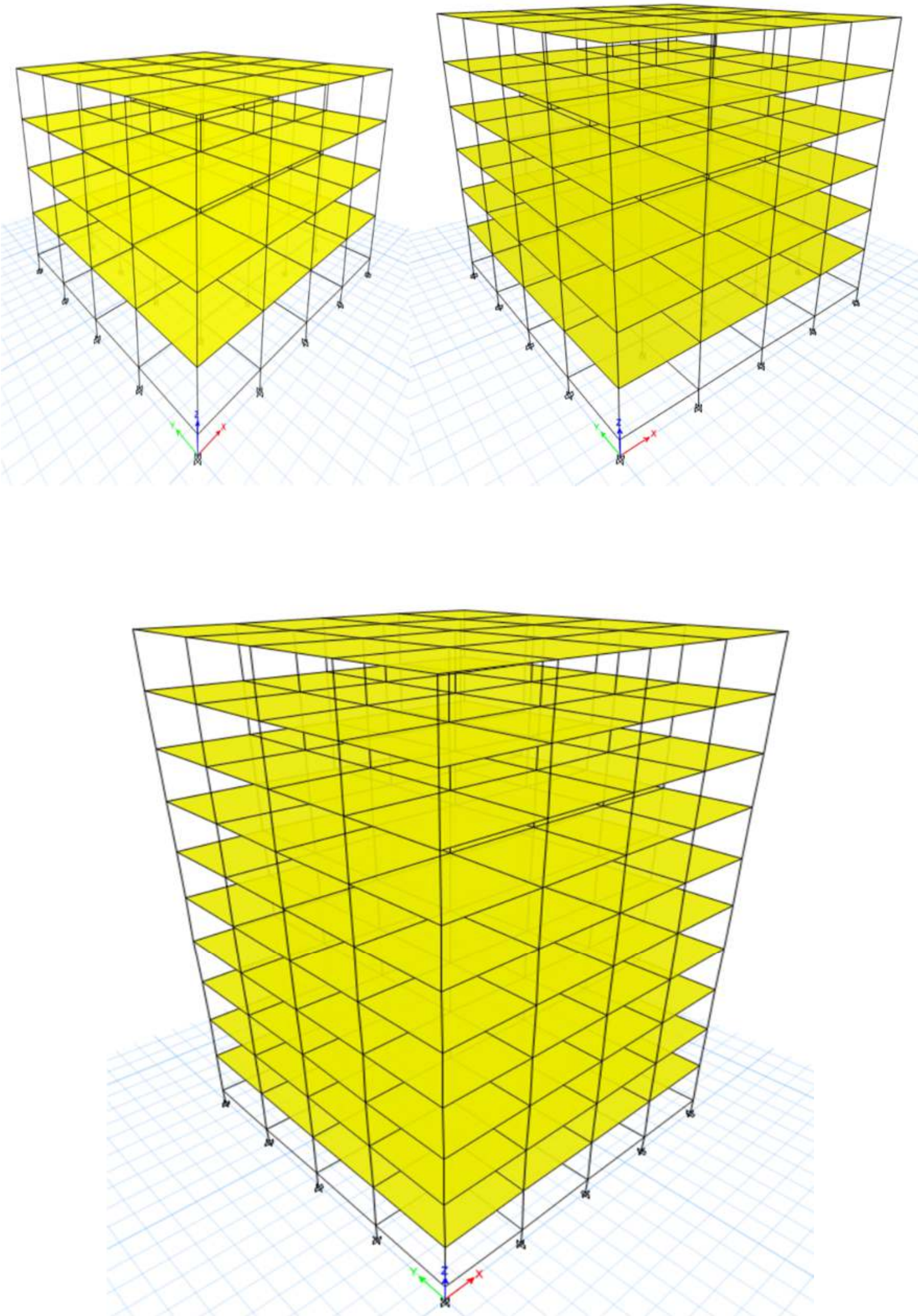

Figure 5.3: 3D views of 4, 6 and 10-storied buildings

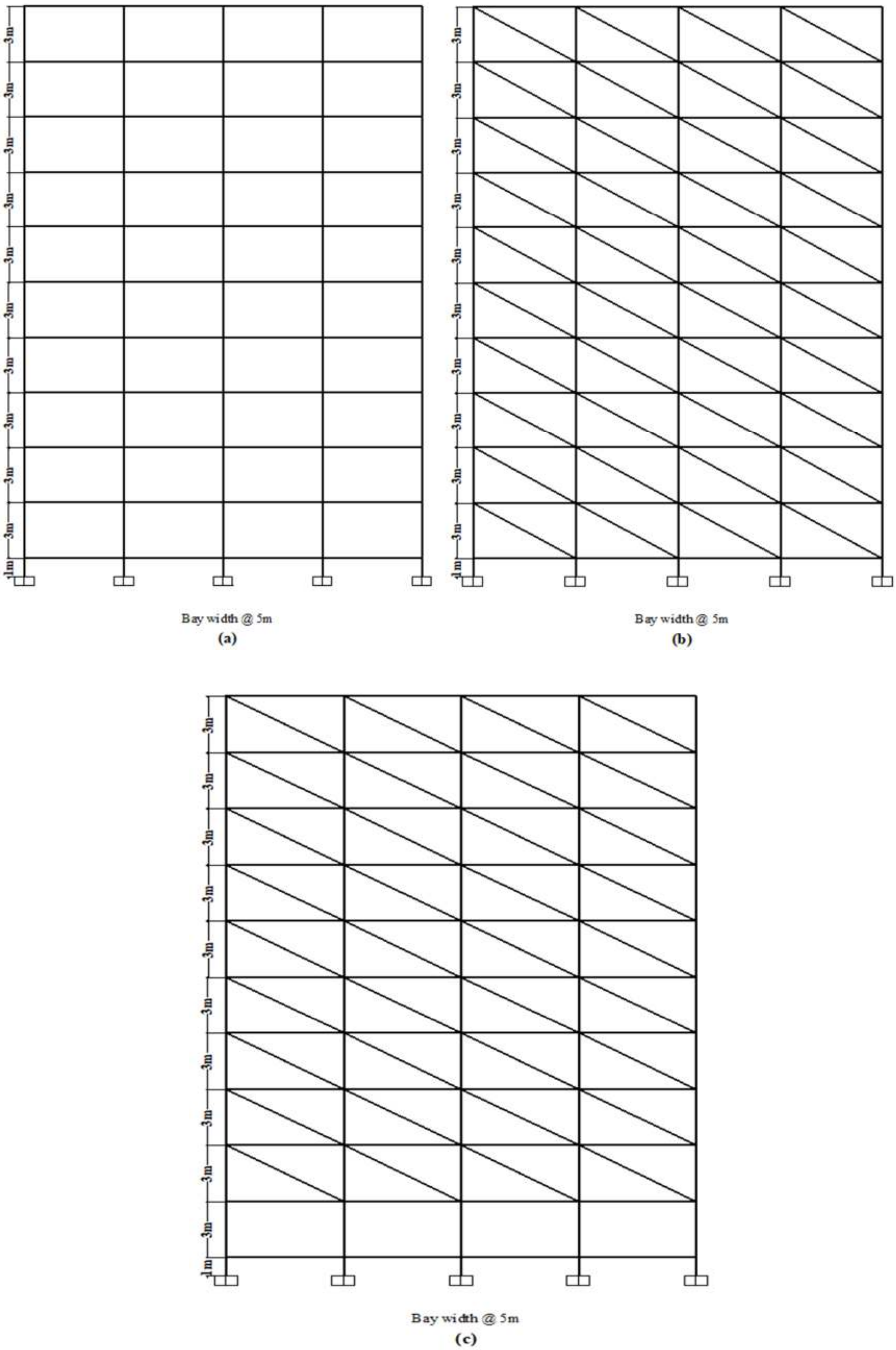

Figure 5.4: Elevation of 10-storied (a) Bare frame, (b) Fully infilled frame and (c) OGF frame

In case of all types of regular 4, 6 and 10-storied buildings, typical storey height was 3m. Grade beams were provided at 1m height. For each type of building, three patterns of infill configurations such as (i) bare frame, (ii) fully infilled frame and (iii) open ground floor (OGF) frame are considered. In fully infilled frame, the masonry infill exists in all floors and OGF frame, the masonry infill walls exist in all floor level except the ground floor. Tables 5.1 and 5.2 present the sizes and reinforcement requirements for columns and beams of the buildings, respectively as per draft BNBC 2017.

Table 5.1: Column sections of 4, 6 and 10-storied buildings

Building	Floors	Sizes (mm)	Rebar Percentage
4-storied	Base to grade beam	425 x 425	1.00 %
	Ground Floor	375 x 375	2.48 %
	1st Floor to roof	375 x 375	1.00 %
6-storied	Base to grade beam	500 x 500	1.00 %
	Ground Floor	450 x 450	2.13 %
	1st Floor to roof	450 x 450	1.00 %
10-storied	Base to grade beam	600 x 600	1.02 %
	Ground Floor	550 x 550	1.87 %
	1st Floor to roof	550 x 550	1.00 %

Table 5.2: Beam sections of 4, 6 and 10-storied buildings

Building	Beams	Sizes (mm)	Top Rebar (mm^2)	Bottom Rebar(mm^2)
4-storied	Grade Beams	250 x 375	352	193
	Floor Beams	250 x 375	1080	452
6-storied	Grade Beams	300 x 450	390	215
	Floor Beams	300 x 450	1140	575
10-storied	Grade Beams	300 x 450	390	186
	Floor Beams	300 x 450	1288	698

5.5.2 Loads on the building structures

For basic design and evaluation of the structures the various loading conditions have been considered. Basic Load cases considered as Dead Load (DL), Live Load (LL), and Earthquake Load (EQ). These load cases are combined according to draft BNBC 2017.

The basic loads are:

- Dead load (DL)
- Live load (LL)
- Earthquake load (EQ)

Dead load (DL): Dead load is the vertical load due to the weight of permanent structural and non-structural components of a building. For the present study only self-weight of beams, columns, slabs, floor finish and masonry infill walls are considered as dead load case of the structure. All vertical dead loads except self-weight of beam, columns and slab are applied as superimposed dead load on the structure. Total vertical load for floor finish applied on the structure is 1.5 kN/m^2. Thicknesses of the slab and masonry infill partition wall are 0.15m and 0.125m, respectively.

Live load (LL): The temporary load acting on structure as occupancy load is called live load and considered as uniformly distributed surface load in gravity direction. In this study, live load applied on the floor levels is 2 kN/m^2 and on the roof is 1 kN/m^2.

Earthquake load (EQ): Earthquake load (EQ) has been considered as per draft BNBC 2017. Equivalent static load method has been used with response reduction factor, $R = 5$ and associated other factors. In calculating seismic weight, a 25% of live load was considered. Other parameters used in seismic load calculation are $Z = 0.2$, $I = 1.00$, $S = 1.15$ as per draft BNBC 2017.

5.5.3 Load combinations

Ultimate Strength Design (USD) method was used to design the structural members. Following load combinations were used in this study according to BNBC 2017 (art. 2.7.3.1):

(a) 1.4 DL

(b) 1.2 DL + 1.6 LL

(c) 1.2 DL + 1.0 EQ + 1.0 LL

(d) 0.9 DL + 1.0 EQ

5.6 Earthquake load analysis

Several earthquake analysis procedures have been asserted in draft BNBC-2017. In this study, equivalent static analysis and response spectrum analysis have been performed. A short description of these two earthquake analyses method has been given in the following section.

5.6.1 Equivalent static analysis

Although seismic analysis of buildings subjected to dynamic earthquake loads should theoretically require dynamic analysis procedures, for certain type of building structures subjected to earthquake shaking, simplified static analysis procedures may also provide with reasonably good results. The equivalent static force method is such a procedure for determining the seismic lateral forces acting on the structure. This procedure is widely used by professional engineers to design the structures. In this procedure, the earthquake load mainly depends on the mass and seismic coefficient of the structure and the latter in turn depends on properties like seismic zone in which structure lies, fundamental period of the structure, importance of the structure and the soil on which it rests.

The total design seismic base shear (V_d) along any principal direction according to draft BNBC 2017 shall be determined by following expression:

$$V_d = S_a.W$$

where, W is the total seismic weight of the building and S_a is the lateral seismic force coefficient.

Seismic weight (W) includes all the dead loads and applicable portions of other imposed live loads listed below:

(a) For live load up to and including 3 kN/m^2, a minimum of 25 percent of the live load shall be applicable.

(b) For live loads above 3 kN/m^2, a minimum of 50 percent of the live load shall be applicable.

(c) Total weight (100 percent) of permanent heavy equipment or retained liquid or any imposed load sustained in nature shall be included.

Where the probable imposed loads (mass) at the time of earthquake are more correctly assessed, the designer may go for higher percentage of live load.

In this study, 25% of the live load has been added to total dead load as seismic weight, as the live load is 2 kN/m^2, which is less than 3 kN/m^2.

The lateral seismic force coefficient is given in the draft BNBC 2017 by following equation:

$$S_a = \frac{2}{3}\frac{ZI}{R}C_s$$

where, Z is the seismic zone coefficient, I is the structure importance factor, R is the response reduction factor and C_s is the normalized response spectrum factor. Figure 5.5 shows the normalized design acceleration for different site classes.

C_s depends on S, η and values of T_B, T_C and T_D. Here, S is the soil factor which depends on site class and η is the damping correction factor which can be expressed by the following expression:

$$\eta = \sqrt{10/(5+\xi)} \geq 0.55$$

where, ξ is the viscous damping ratio of the structure. η value 1 (one) for the 5% viscous damping.

Table 5.3 presents the soil factor, S and other parameters associated with normalized response spectrum factor as per draft BNBC 2017.

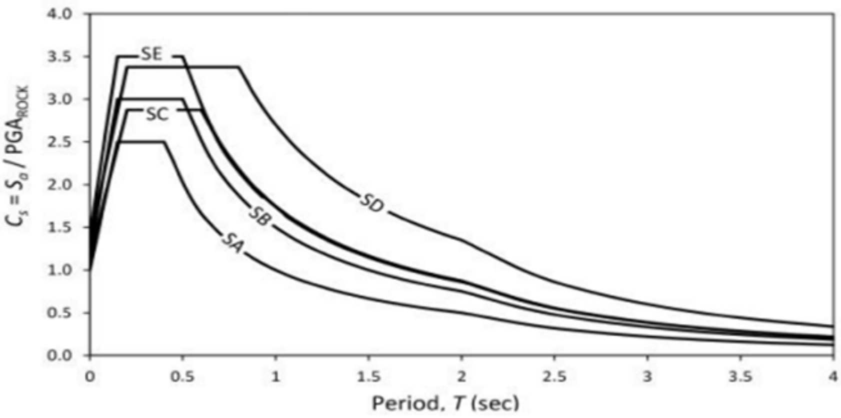

Figure 5.5: Normalized design acceleration for different site classes for draft BNBC 2017

C_s is defined by the following equations:

$$C_s = S\left(1 + \frac{T}{T_B}(2.5\eta - 1)\right) \quad \text{for} \quad 0 \le T \le T_B$$

$$C_s = 2.5S\eta \quad \text{for} \quad T_B \le T \le T_C$$

$$C_s = 2.5S\eta\left(\frac{T_C}{T}\right) \quad \text{for} \quad T_C \le T \le T_D$$

$$C_s = 2.5S\eta\left(\frac{T_C T_D}{T^2}\right) \quad \text{for} \quad T_D \le T \le 4\,sec$$

Values of soil factor (*S*) and other parameters defining C_s is given in the following Table 5.3:

Table 5.3: Soil factor (*S*) and other parameters defining C_s

Soil Type	***S***	$\boldsymbol{T_B}$	$\boldsymbol{T_C}$	$\boldsymbol{T_D}$
SA	1.0	0.15	0.40	2
SB	1.2	0.15	0.50	2
SC	1.15	0.20	0.60	2
SD	1.35	0.20	0.80	2
SE	1.4	0.15	0.50	2

The intent of the seismic zoning map is to give an indication of the Maximum Considered Earthquake (MCE) motion at different parts of the country. In probabilistic terms, the MCE motion may be considered to correspond to having a 2% probability of exceedance within a period of 50 years. The country has been divided into four seismic zones with different levels of ground motion as shown in Figure 5.6. The zone coefficients (Z) of the four zones are: Z = 0.12 (Zone 1), Z = 0.20 (Zone 2), Z = 0.28 (Zone 3) and Z = 0.36 (Zone 4). Dhaka city falls in the moderate seismic intensity zone with Z = 0.2 and in this study this zone has been selected.

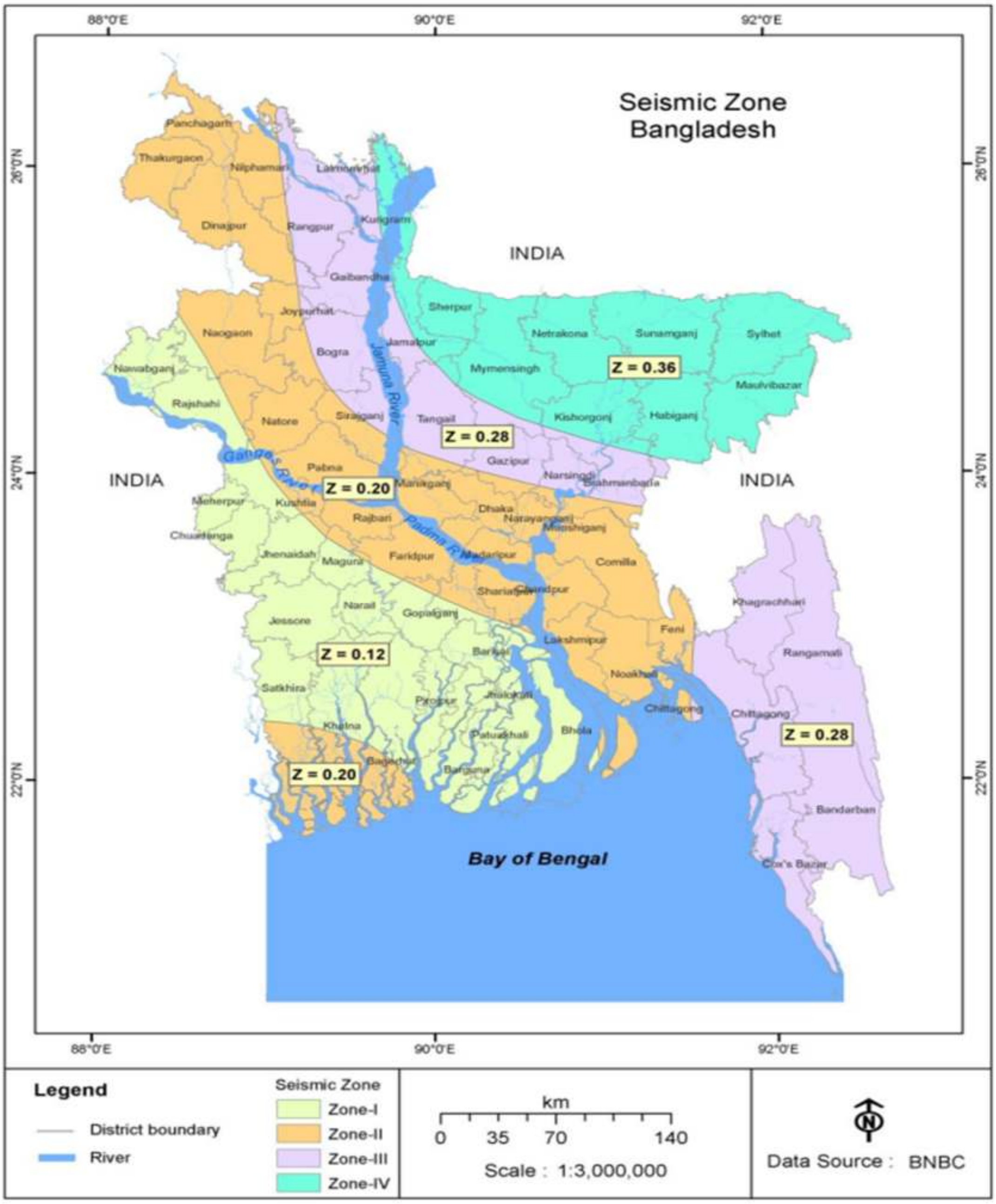

Figure 5.6: Seismic zoning map of Bangladesh as per draft BNBC 2017

The design base shear (V_d) shall be distributed along the height of the building using following equation:

$$F_x = V_d \frac{W_x h_x^k}{\sum_{i=1}^{n} W_i h_i^k}$$

where,

$V_d =$ Total design base shear.

$F_x =$ Part of base shear force induced at level x.

W_i & $W_x =$ Part of the total effective seismic weight of the structure (W) assigned to level i or x.

h_i & $h_x =$ The height from the base to level i or x.

$K =$ 1 for structure period $\leq 0.5s$

$=$ 2 for structure period $\geq 2.5s$

$=$ Linear interpolation between 1 and 2 for other periods.

$n =$ Number of stories.

5.6.2 Response spectrum analysis (RSA)

A response spectrum analysis (RSA) shall consist of the analysis of a linear mathematical model of the structure to determine the maximum accelerations, forces, and displacements resulting from the dynamic response to ground shaking represented by the design acceleration response spectrum. It is also called modal analysis procedure as it considers different modes of vibration of the structure and combines the results of different modes. The analysis shall include a sufficient number of modes to obtain a combined modal mass participation of at least 90 percent of the actual mass. The combination shall be carried out by taking the square root of the sum of the squares (SRSS) of each of the modal values or by the complete quadratic combination (CQC) technique. As per draft BNBC 2017, when the base shear V_{rs} calculated by RSA is less than the V_d calculated by equivalent static analysis method, all the forces obtained by the RSA shall be multiplied by $\frac{0.85V_d}{V_{rs}}$.

5.6.3 Base shear as per draft BNBC 2017 and BNBC 2006

In this study, it was considered that the structures were located in Zone-2 which is medium seismic intensity zone as per draft BNBC 2017. The modal combination were carried out by CQC technique. Soil type SC was considered which is stiff clay or medium dense sand type soil. Normalized design acceleration response spectrum curve C_S vs. T (sec) graph for this class of soil was shown in draft BNBC 2017 (sec.2.5.4.3) as shown in Figure 5.7. Using this C_S vs. T (sec) graph, spectral acceleration $S_a(g)$ vs. period (T) graph was generated. The relationship between C_S and S_a are as follows:

$$C_S = S_a / PGA_{rock}$$

where, $PGA_{rock} = \frac{2}{3}\frac{ZI}{R}$

Here, Z = 0.2 (zone-2), I = 1 and R = 5 was considered. Chart of period and spectral acceleration is given in Table 6.3.2.1 of the draft BNBC 2017 as shown in Figure 5.7. Using these data, $S_a(g)$ vs. T graph was generated which has been shown in Figure 5.8.

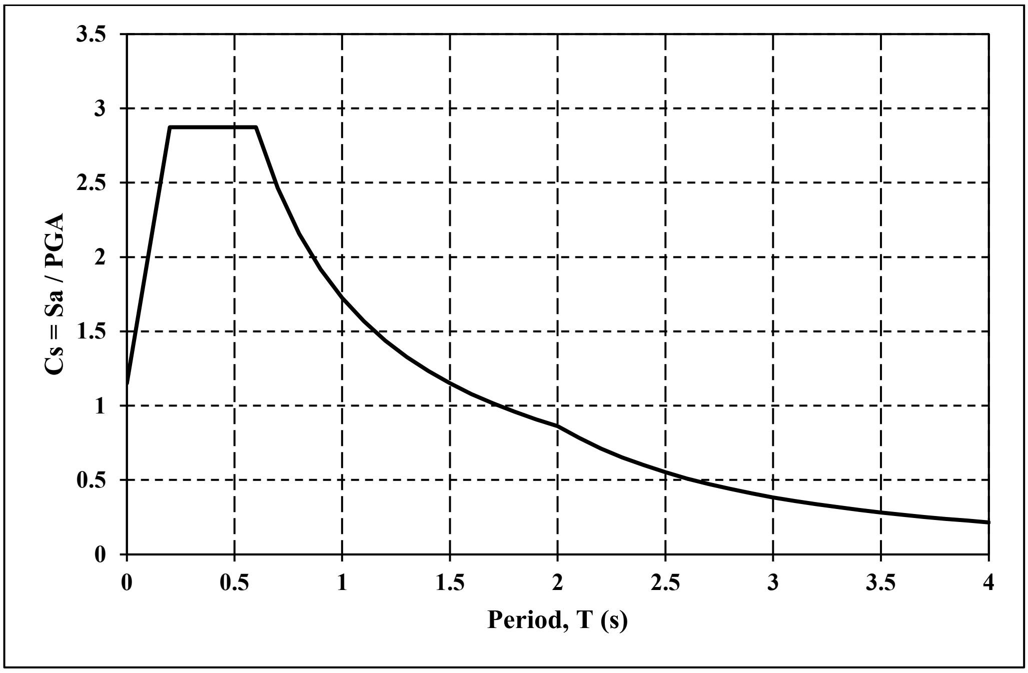

Figure 5.7: *Cs* vs. *T* graph for soil type C

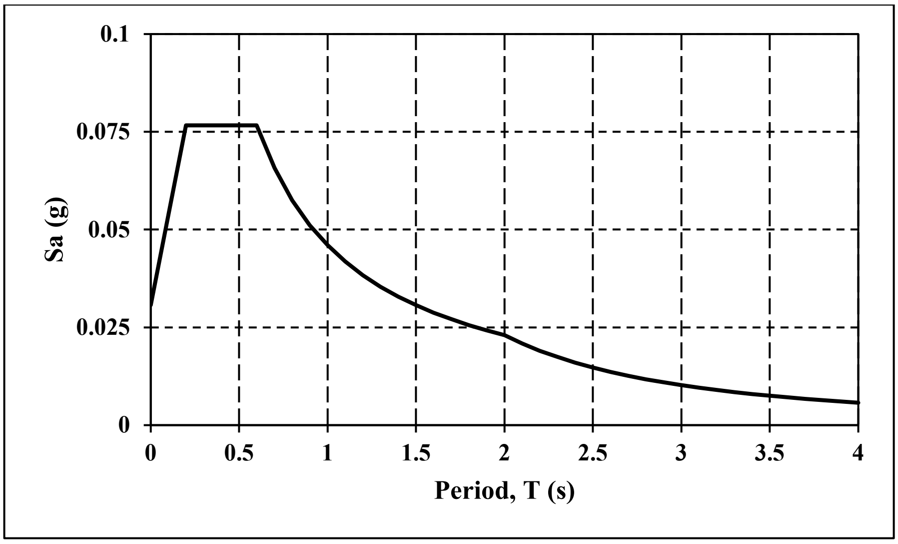

Figure 5.8: Generated $S_a(g)$ vs. T graph for response spectrum analysis

The generated $S_a(g)$ vs. T graph can be checked by the value of lateral seismic force coefficient (S_a) used in the equivalent static analysis method to estimate the design force. As per draft BNBC 2017, the design base shear force in a given direction shall be determined from the following given equation:

$$V_d = S_a W$$

where, S_a is the lateral seismic force coefficient calculated using the equation defined in the code and W is the total seismic weight. The value of lateral seismic force coefficient (Sa) for the 4, 6 and 10-storied moment resisting framed buildings were found as 0.0766, 0.0697 and 0.0449, respectively as per draft BNBC 2017.

The structural period T in seconds can be determined by the following formula:

$$T = C_t \left(h_n\right)^m$$

For the concrete moment resisting frame structures (RC MRF), the value of C_t and m are 0.0466 and 0.9, respectively as per draft BNBC 2017.

For the RC MRF, the value of C_t and m as shown above are considered 0.073 and 0.75, respectively as per BNBC 2006. Equation of S_a as per BNBC 2006 is as follows:

$$S_a = \frac{ZIC}{R}$$

were, $Z = 0.15$ for Dhaka city, importance factor, $I = 1$ and $R = 8$ for concrete intermediate moment resisting frame structure.

Values of S_a for 4, 6 and 10-storied buildings were found 0.056, 0.046 and 0.036, respectively as per BNBC 2006. Values of S_a for 4-, 6- and 10-storied buildings were found 0.077, 0.070 and 0.045, respectively as per draft BNBC 2017. Therefore, it seems that S_a values found from draft BNBC 2017 were 27%, 34% and 19% larger than those values as per BNBC 2006 as shown in Figure 5.9. Although, S_a values vary but their overall effect under the load combination seems to be almost the same as earthquake load factor of 1.4025 used as per BNBC 2006 and 1.0 as per draft BNBC 2017.

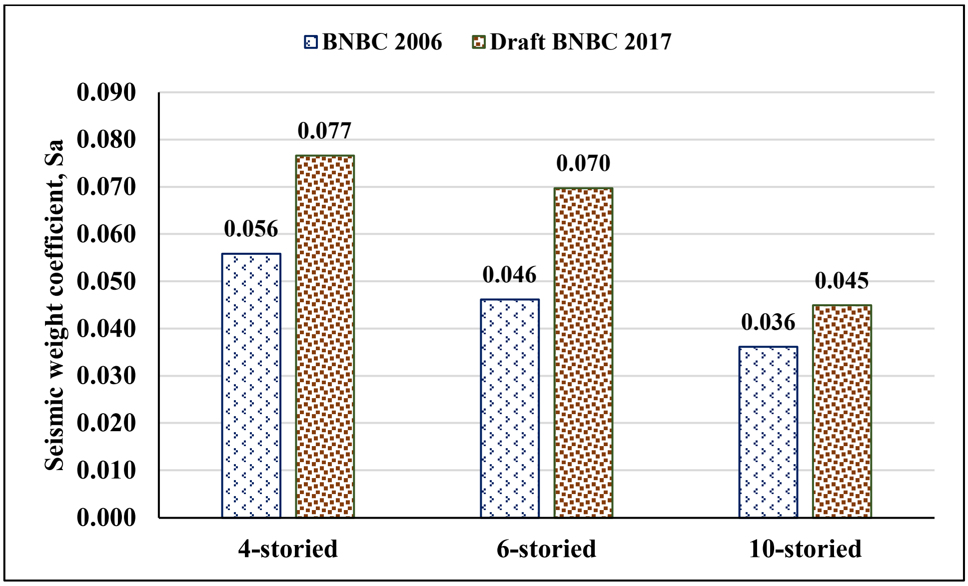

Figure 5.9: S_a value from BNBC 2006 and draft BNBC 2017

5.6.4 Time History Analysis

Nonlinear Time History Analysis (NTHA) is one of the most powerful dynamic analysis methods for assessment of seismic behavior of a building. It is a dynamic analysis of a structure represented by mathematical modelling through applying ground motion acceleration at its base level. The seismic response of a structure at every time interval is recorded for the whole earthquake period and the statistical average is represented.

Time history (TH) analysis was performed with appropriate horizontal ground-motion time history components that were selected and scaled from different recorded events. Appropriate time histories have magnitude, fault distance and source mechanism that are consistent with those that control the design basis earthquake. In this study, three different ground accelerations were used to assess the seismic response of vertically irregular structures. These records were obtained from Pacific Earthquake Engineering Research Center (PEER) ground motion database.

5.6.4.1 El Centro (1940) Earthquake

El Centro is the largest city in the Imperial Valley which is located in the far corner of California. On May 18th, 1940, an earthquake occurred near the international border, in the Imperial Valley in Southern California. It measured 7.1 on the Richter scale and affected both the United States and Mexico, with the city of El Centro. It was also the first major earthquake to be recorded by strong-motion accelerographs. The N-S component recorded at a site in El Centro Terminal Substation building has become a popular point of reference for dynamic analyses. Figure 5.10 shows the ground motion acceleration of El Centro 1940 earthquake where vertical axis shows the acceleration and horizontal axis shows the time in seconds.

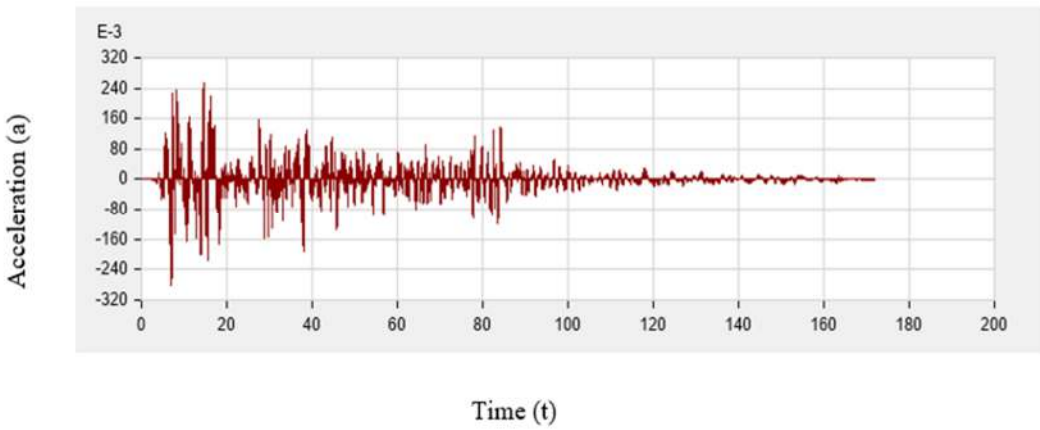

Figure 5.10: Ground motion acceleration of El Centro (1940) earthquake

5.6.4.2 Imperial Valley (1979) Earthquake

The Imperial Valley earthquake occurred on 15 October 1979 in south side of Mexico – United States border. The earthquake was measured 6.6 on the Richter scale. Figure 5.11 shows the ground motion acceleration of Imperial Valley 1979 earthquake where vertical axis shows the acceleration and horizontal axis shows the time in seconds.

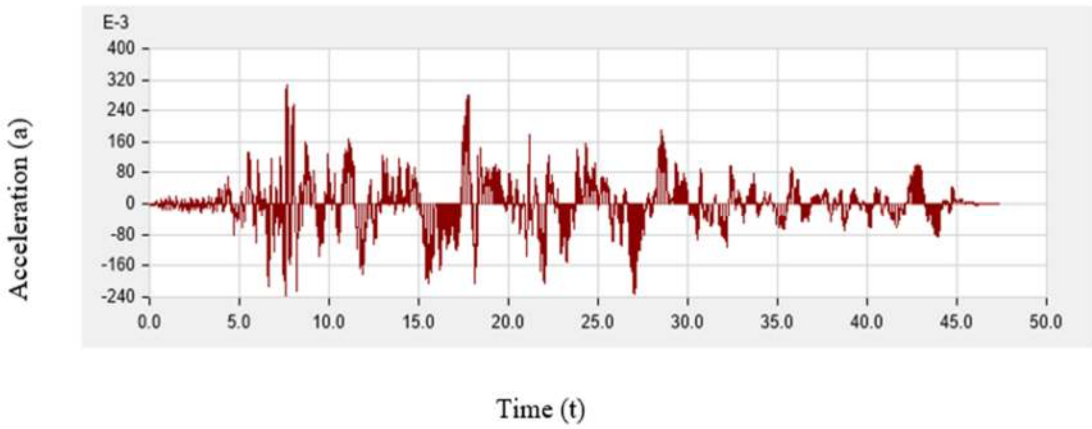

Figure 5.11: Ground motion acceleration of Imperial Valley (1979) earthquake

5.6.4.3 Kobe (1995) Earthquake

Kobe is located in the south east of Japan. The earthquake hit Kobe on 17th January 1995 measured a massive 7.2 on the Richter scale. More than 150,000 buildings were destroyed in Kobe earthquake. Figure 5.12 shows the ground motion acceleration of Kobe (1995) earthquake.

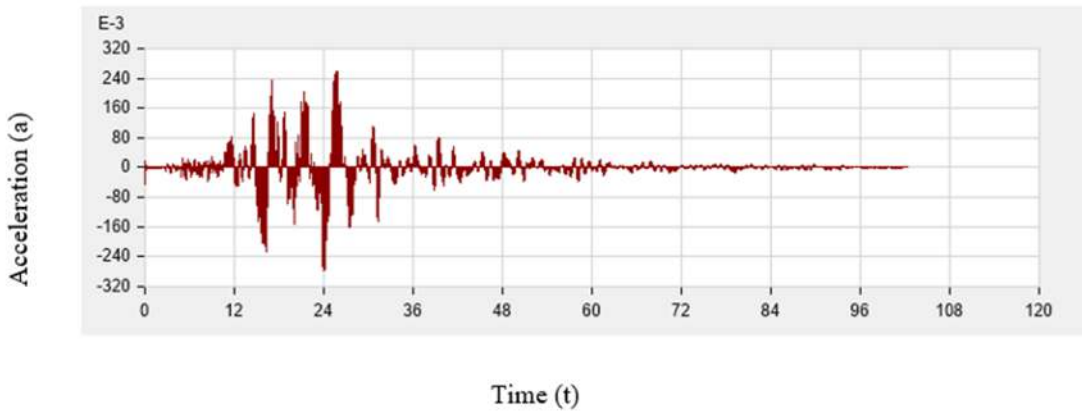

Figure 5.12: Ground motion acceleration of Kobe (1995) earthquake

A summary of earthquake records used in the current study has been provided in Table 5.4 below:

Table 5.4: Details of earthquake records used in the study

Earthquake	Magnitude	Year	Recording station	PGA (g)
El Centro	6.95	1940	El Centro Array #9	0.30
Imperial Valley	6.53	1979	Aeropuerto Mexicali	0.32
Kobe	6.90	1995	Kobe university	0.27

5.6.4.4 Conditions for the requirement of dynamic analysis

Dynamic analysis method involves applying principles of structural dynamics to compute the response of the structure to applied dynamic (earthquake) loads. This method should be performed for the following buildings:

(a) Regular buildings with height greater than 40 m in Zones 2, 3, 4 and greater than 90 m in Zone 1.

(b) Irregular buildings with height greater than 12 m in Zones 2, 3, 4 and greater than 40 m in Zone 1.

5.7 Estimation of strut widths for masonry infill wall

The mechanical properties of the masonry infill wall were used according to the draft BNBC 2017. The following values were considered in this study:

- Thickness of masonry wall, $t_w = 0.125$ m
- Mortar strength, (cement : sand = 1:4) $f_j = 7.5$ MPa
- Compressive strength of brick, $f_b = 17$ MPa
- Equation of Compressive strength of masonry by Kaushik et al. (2007),

$$F_m = 0.63(f_b)^{0.49}\ (f_j)^{0.32} = 0.63(17)^{0.49}\ (7.5)^{0.32} = 4.81 \text{ MPa}$$

- Elastic modulus, $E_m = 750(F_m) = 750 \times 4.81 = 3608$ MPa

Figure 5.13 shows the strut width values as per different research works and codes as described in Chapter-4 of this thesis. The obtained results provide a wide range estimation of the strut width considered for the masonry infill.

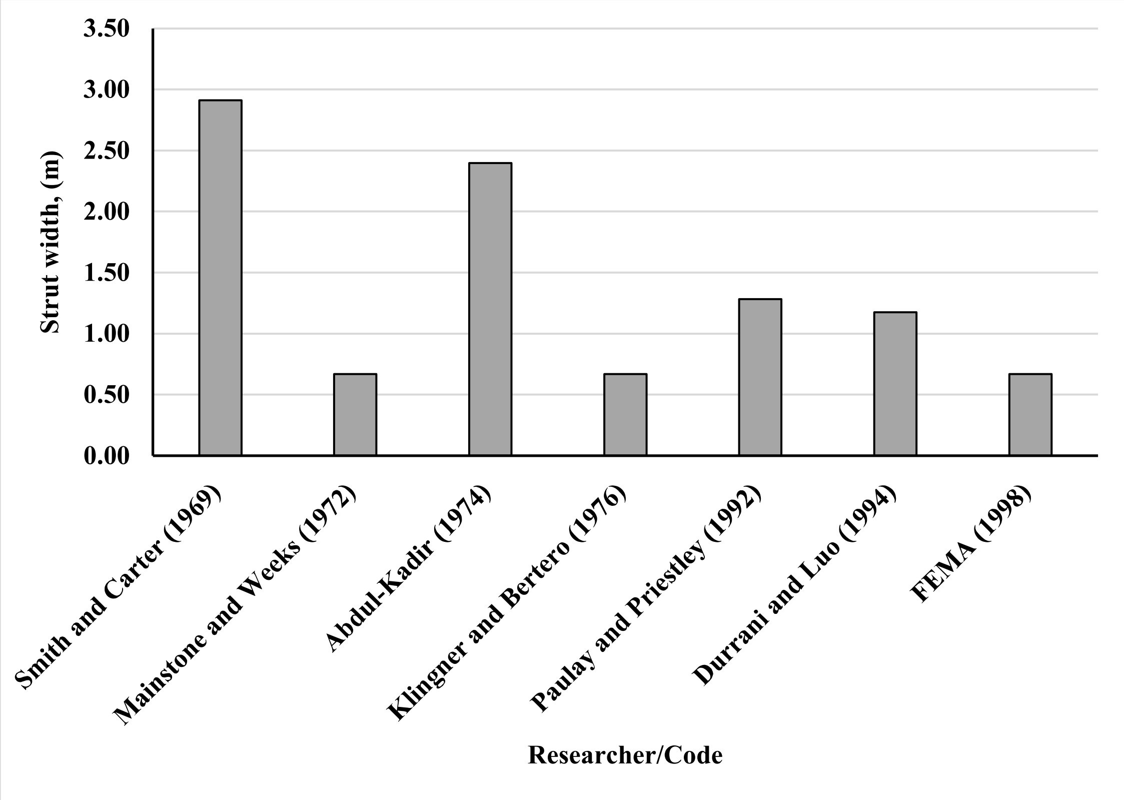

Figure 5.13: Strut widths of 10-storied buildings as per various researches and code

It was found that in case of 10-storied buildings, Smith and Carter (1969) provided the highest value of strut widths. FEMA guidelines always provided the lowest value of strut width in case of all 4, 6 and 10-storied buildings. Table 5.5 shows the strut widths used in this study considering the FEMA guidelines.

Table 5.5: Strut widths for 4, 6 and 10-storied buildings

Building	**Strut widths (w)**
4-storied	0.60 m
6-storied	0.63 m
10-storied	0.67 m

5.8 Mass irregular frames

As per draft BNBC 2017, mass irregularity occurs when the masses of any storey is more than twice of that of its adjacent storeys. This irregularity need not be considered in case of roofs. In this study, mass irregularity was considered at mid-storey level of 4, 6 and 10-storied buildings. The regular frames had an even distribution of masses in each floor. But when mass irregularity was considered, a special load of 10 kN/m^2 was considered at mid-storey level of 4 and 6-stroried buildings and 10.5 kN/m^2 was considered at mid-storey level of 10-storied building as shown in Figure 5.14. Column and beam sections were the same as regular bare frames buildings.

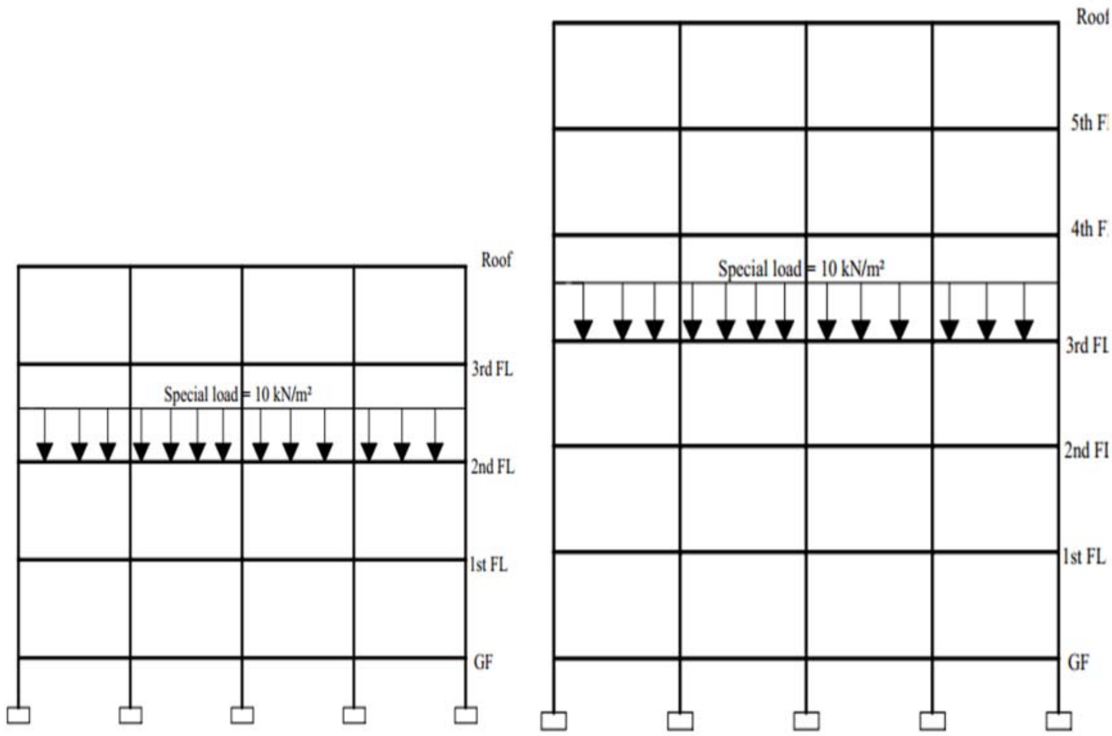

(a) (b)

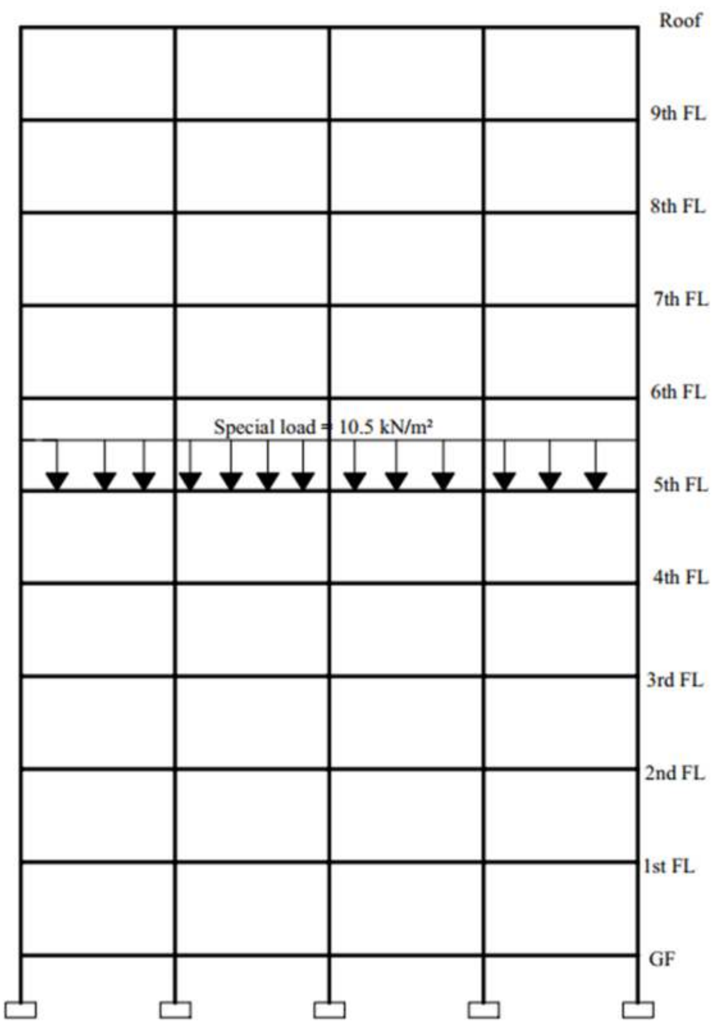

(c)

Figure 5.14: Mass irregular frames (a) 4-storied, (b) 6-storied and (c) 10-storied

5.9 Geometric irregular frames

Vertical geometric irregularity is generated for the presence of setback in the building. According to draft BNBC-2017, in case of one-stepped setback building, geometric irregularity will be considered when the horizontal dimension of lateral force resisting system in any storey is more than 130% of that in adjacent storey. Two types of geometric irregularity configurations (i) B1-upper and (ii) B1- mid were considered as shown in Figures 5.15 to 5.17 for 4, 6 and 10-storied buildings, respectively. Upper means the setback was provided at the roof level and mid means the setback was provided at mid storey level. Ratio of horizontal dimension of for 1 bay setback was 1.325. All the setbacks were provided at the same number of bay and at the same storey level from both x- and y- axis directions.

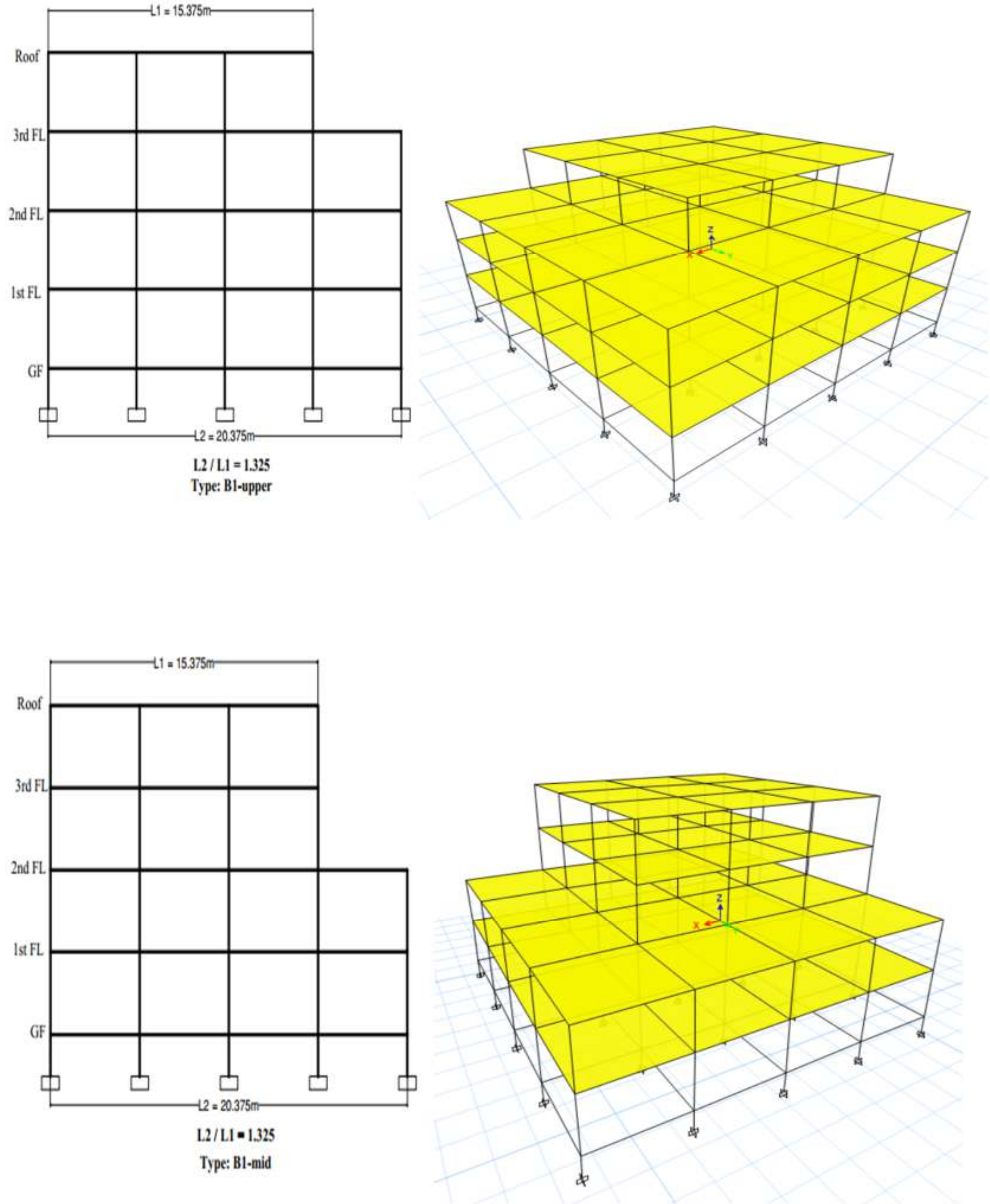

Figure 5.15: 2D and 3D views of 4-storied geometric irregular buildings

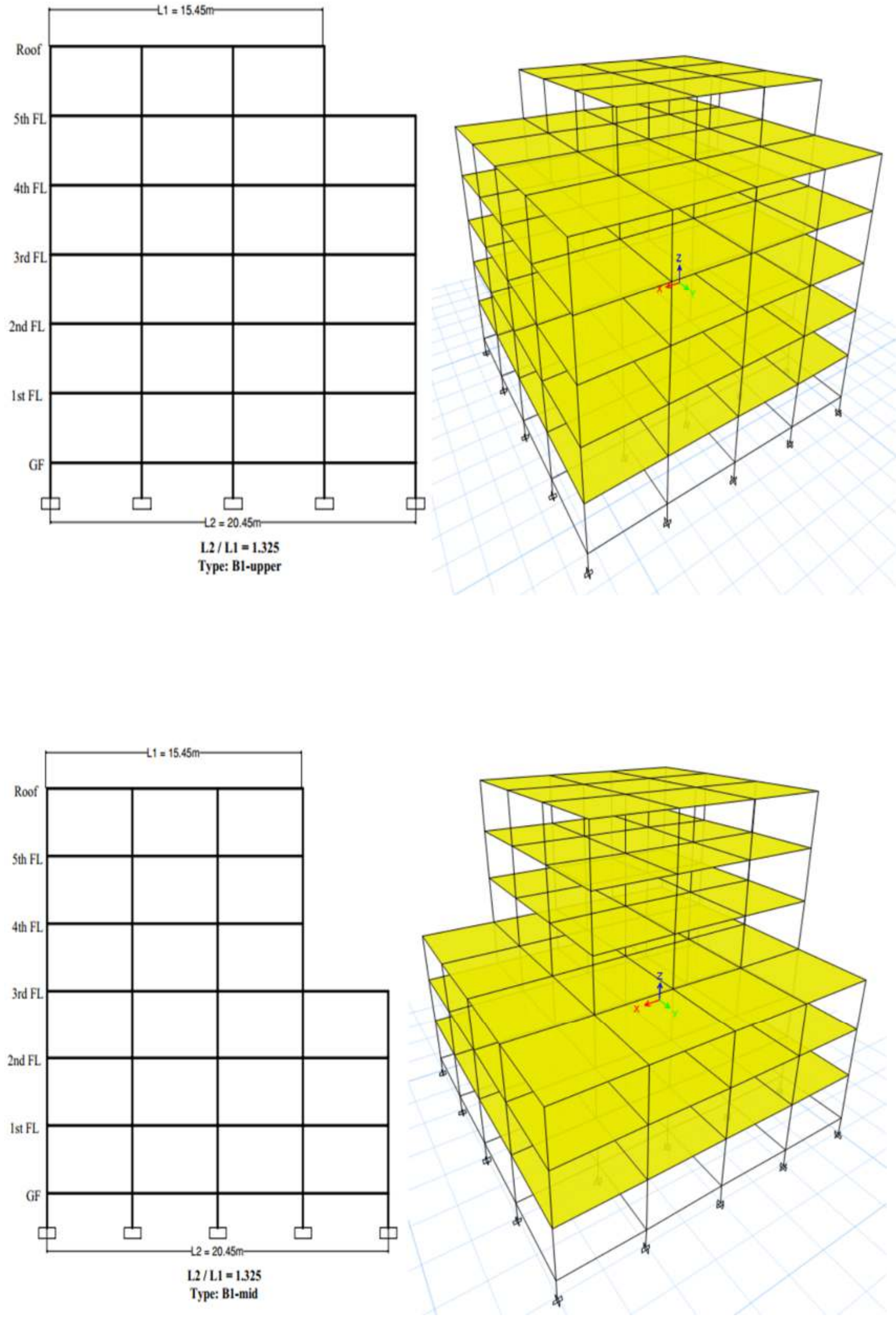

Figure 5.16: 2D and 3D views of 6-storied geometric irregular buildings

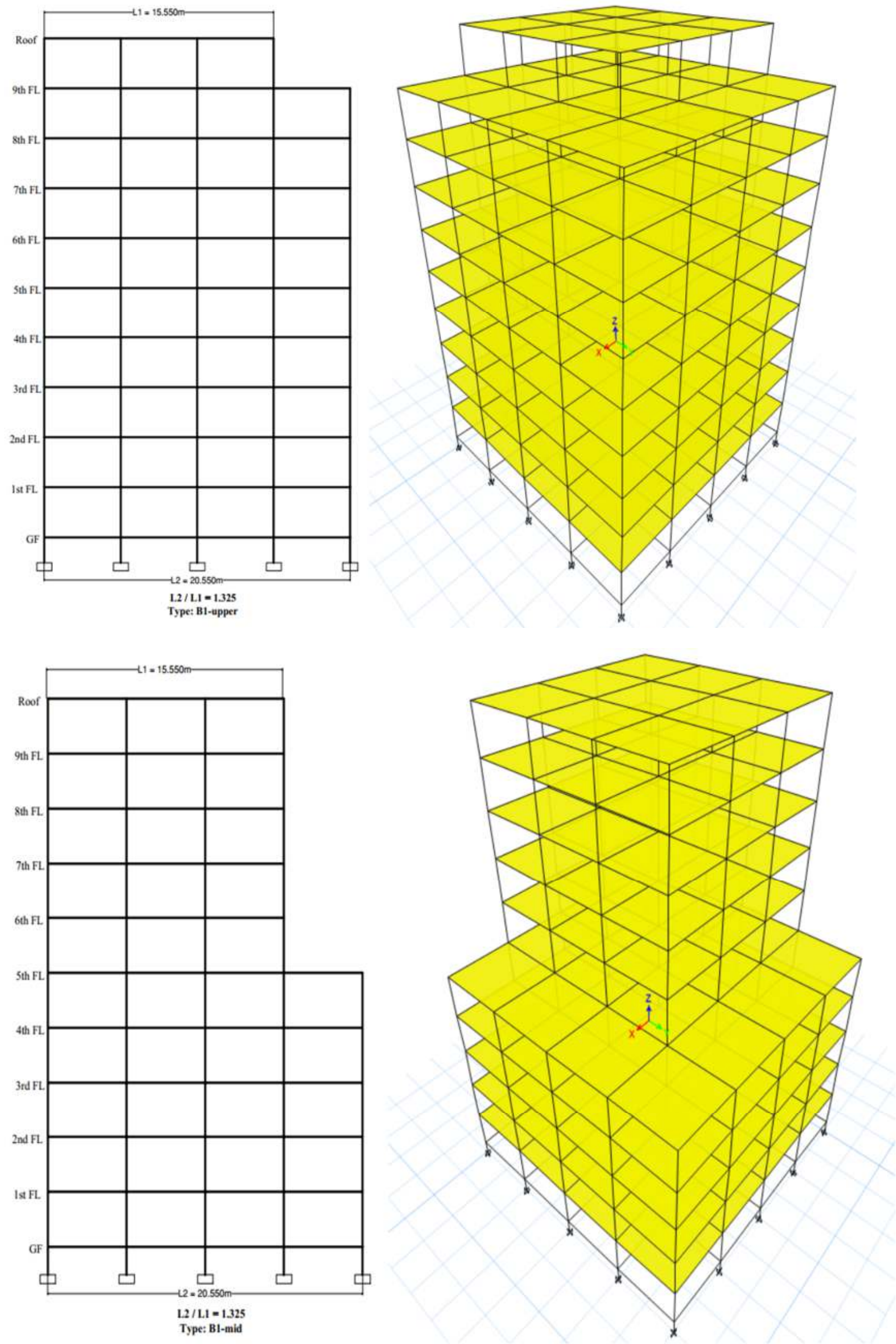

Figure 5.17: 2D and 3D views of 10-storied geometric irregular buildings

5.10 Model validation

Validation of the building models is an essential step towards having confidence in the results of the analysis performed on the structures. For this purpose, research and analysis work performed by Landi et al. (2015) was selected. They performed seismic analysis on five RC frame structures. Among these, three were vertically regular frames with three, six and nine storeys (called 3F, 6F and 9F) and two were vertically irregular frames as shown in Figure 5.18. One of the vertically irregular frames was a six floor soft storey frame (6FIR) and the other was a storied frame with a setback at the third storey (6FIM).

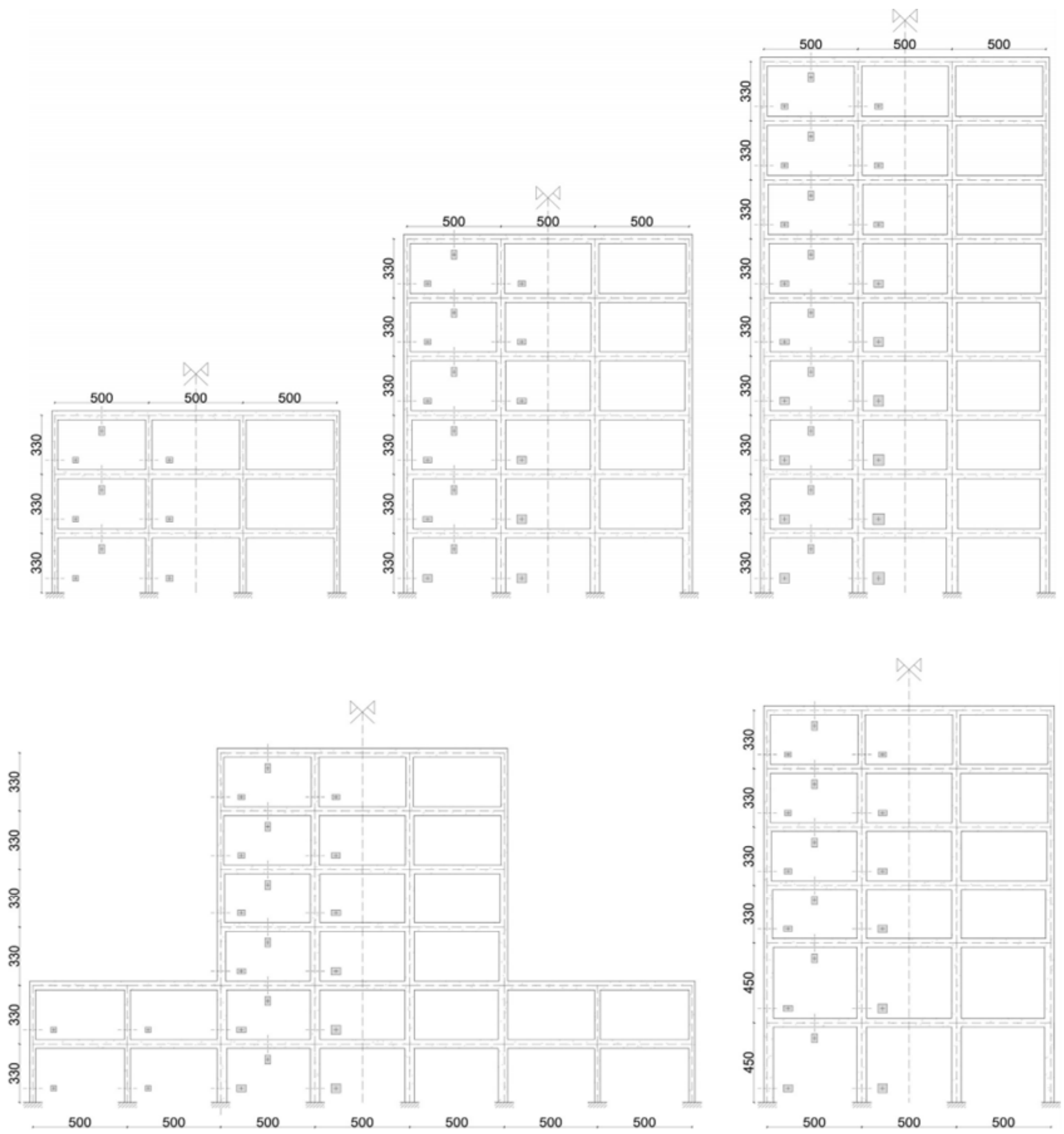

Figure 5.18: 3, 6 and 9-storied regular (3F, 6F and 9F) and 6 storied vertically irregular (6FIM and 6FIR) RC frames [Landi et al. (2015)]

All the bays were 500 cm length and the storeys were 330 cm in height except the irregular soft storey frame where the height of the first two storeys was 450 cm. All the beams were 30 cm wide and 50 cm deep. For all the regular frames and the irregular soft storey frame, the seismic weight, excluding the self-weight of beams and columns, was equal to 676.5 kN for the lower storeys and to 511.5 kN for the top storeys. For the frame with a setback at the third storey (6FIM), the seismic weight, excluding the self-weight of beams and columns, was equal to 1498.5 kN at the first floor and to 1318.5 kN at the second floor. For the self-weight of the structural elements, the unit weight of the reinforced concrete was 25 kN/m^3. Cylinder strength of the concrete was assumed as 25 MPa and the yield strength of the steel was assumed as 450 MPa.

Tables 5.6 and 5.7 show the comparison of the fundamental period and total effective modal masses of first three modes, respectively for the present analysis and Landi et al. (2015). From these two tables, it is found that the fundamental period and total effective modal masses of first three modes obtained from present analyses are in a good agreement with those values obtained from Landi et al. (2015).

Table 5.6: Comparison of fundamental period between present analysis and Landi et al. (2015)

Models	**Period by present analysis, Tp, (s)**	**Period by Landi et al. (2015), Tq, (s)**	**Comparison (Tp / Tq) x 100%**
3F	0.80	0.79	100.63
6F	1.13	1.11	101.48
9F	1.58	1.58	99.75
6FIM	1.05	1.04	100.87
6FIR	1.38	1.29	107.19

Table 5.7: Comparison of total effective modal mass of first three modes between present analysis and Landi et al. (2015)

Models	Effective modal mass by present analysis (%)				Effective modal mass by Landi et al. (2015) (%)				Comparison of total modal mass (Mp / Mq) x 100%
	Mode 1	Mode 2	Mode 3	Total modal mass, Mp	Mode 1	Mode 2	Mode 3	Total modal mass, Mq	
3F	88.4	9.6	2.0	100.0	88	9	2	99	100.99
6F	78.7	11.5	4.4	94.5	78	12	4	94	100.58
9F	75.9	11.5	4.4	91.7	76	11	4	91	100.82
6FIM	67.1	22.0	5.5	94.6	67	22	6	95	99.54
6FIR	86.1	7.4	3.4	96.9	86	8	4	98	98.88

Another model validation was performed to confirm the accuracy of pushover curve of bare frame and frame with the masonry infill. For this purpose, research and analysis work performed by Kareem and Güneyisi (2019) was selected. A 4-storied frame was considered as shown in Figure 5.19. Sizes of column C3 and C4 were 300mm x 550mm and 300mm x 500mm, respectively. Size of beam was considered 250mm x 600mm. Compressive strength of concrete was considered as 30MPa and yield strength of rebar was considered as 365MPa. The dead load was considered as 12.6 kN/m and live load was considered as 8 kN/m.

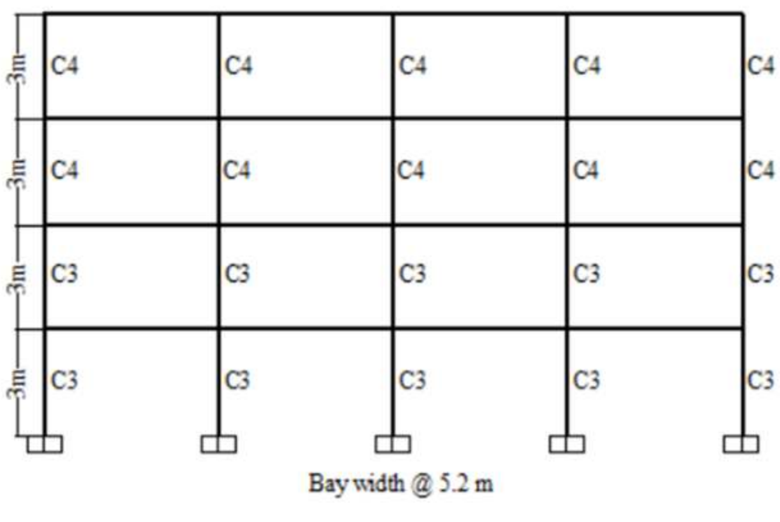

Figure 5.19: 4-storied frame considered by Kareem and Güneyisi (2019)

Figure 5.20 show the comparison between the pushover curves and Table 5.8 show the comparison of maximum roof drift ratio (%) and ratio of bases shear to seismic weight (V/W%) for the present analysis and Kareem and Güneyisi (2019). From these figure and table, it is found that the pushover curves, maximum roof drift ratio (%) and ratio of bases shear to seismic wt. (V/W%) of bare frame and fully infilled frame obtained from present analyses are in a good agreement with those curves and values obtained from Kareem and Güneyisi (2019).

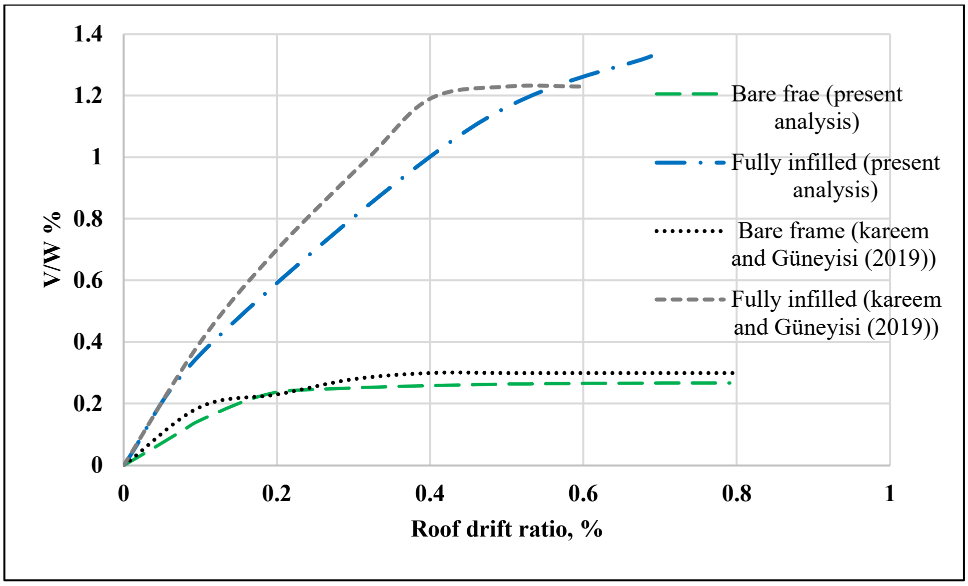

Figure 5.20: Comparison of pushover curves by present analysis and Kareem and Güneyisi (2019)

Table 5.8: Comparison of maximum roof drift ratio (%) and ratio of bases shear to seismic wt. (V/W%) between present analysis and Kareem and Güneyisi (2019)

Frames	**Maximum roof drift ratio, %**			**Ratio of bases shear to seismic wt. (V/W), %**		
	Present analysis, ΔP	**Kareem and Güneyisi (2019), ΔQ**	**ΔP/ΔQ, %**	**Present analysis, Vp**	**Kareem and Güneyisi (2019), Vq**	**Vp/Vq, %**
Bare	0.80	0.80	100%	0.27	0.30	90%
Fully infilled	0.68	0.60	113.33%	1.32	1.23	107%

Chapter 6

RESULTS AND DISCUSSIONS

6.1 General

In this chapter, results of the analyses for different building models are presented and discussed with an aim to assess the seismic response of vertically irregular structures. The obtained results include a comparative study of different methods to estimate lateral storey stiffness, storey drift from equivalent static and dynamic analysis and fundamental periods. The results also include the base shear capacity, ductility factor, overstrength factor and response reduction factor from nonlinear static or pushover analysis. Finally, the results of the study can be utilized to assess the behavior of vertically irregular structures and its design approach.

6.2 Lateral storey stiffness and stiffness ratio

In this section, lateral storey stiffness and stiffness ratio of the bare frame, fully infilled frame and open ground floor (OGF) frames of 4, 6 and 10-storied buildings were estimated using lateral load deflection method. According to draft BNBC 2017, the soft storey condition will be prevail if the stiffness ratio of a particular storey and its adjacent above storey (K_i / K_{i+1}) is less than 0.7. The extreme soft storey condition will prevail if the stiffness ratio is less than 0.6. Tables 6.1 shows the obtained results of storey stiffness by the load deflection method.

Table 6.1: Storey stiffness and stiffness ratio of different stories of 4-storied buildings

Frame	Floor	Lateral Storey stiffness (K), kN/m	Stiffness ratio, (K_i / K_{i+1})	Remarks
Bare Frame	ROOF	52300		
	2nd Floor	67842	1.30	Regular
	1st Floor	73202	1.08	Regular
	Ground Floor	97155	1.33	Regular
Fully Infilled Frame	ROOF	635022		
	2nd Floor	708052	1.12	Regular
	1st Floor	716266	1.01	Regular
	Ground Floor	726228	1.01	Regular

Frame	Floor	Lateral Storey stiffness (K), kN/m	Stiffness ratio, (K_i / K_{i+1})	Remarks
OGF Frame	ROOF	628482		---
	2^{nd} Floor	745908	1.19	Regular
	1^{st} Floor	533253	0.71	Regular
	Ground Floor	162747	0.31	Extreme Soft Storey

A comparison of storey stiffness among bare frame, fully infilled and OGF of has been shown in Figures 6.1. Similar pattern of storey stiffness of bare frame, fully infilled and OGF of 6 and 10-storied buildings were found which have been shown in Appendix A-1. Storey stiffness ratio of different floors of 4 and 6-storied bare, fully infilled and OGF frames were shown in Figure 6.2 to 6.3. In this study, storey stiffness ratio at the ground floors of 4 and 6-storied OGF frames were found as 0.31 and 0.47 which were at extreme soft storey condition and ground floor of 10-storied OGF frames were found as 0.7 which was at regular condition as per draft BNBC 2017. Ground floors of bare and fully infilled frames were found in regular condition. Soft storey condition was not observed at any other storey level in bare frame, fully infilled and OGF frames.

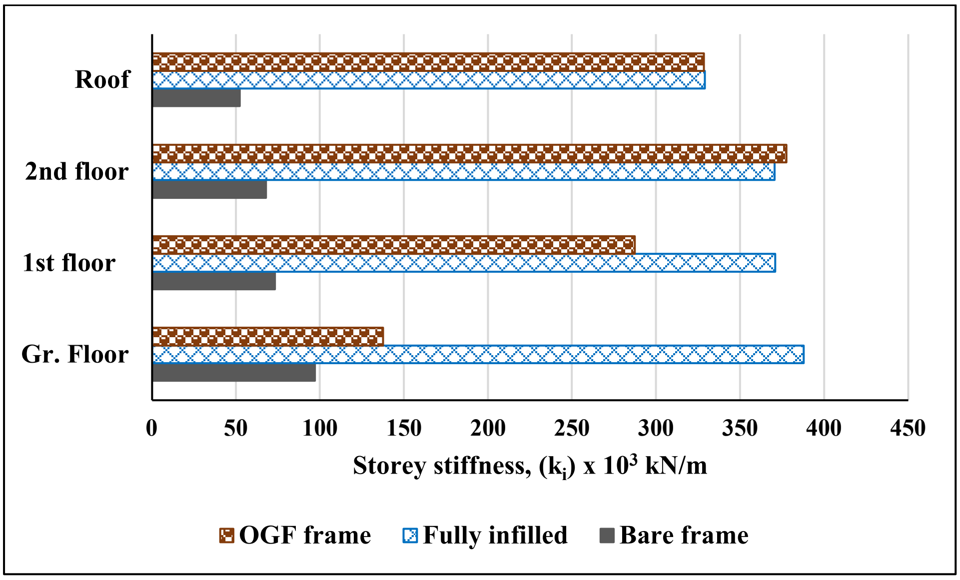

Figure 6.1: Storey stiffness of each floor for different types of 4-storied buildings

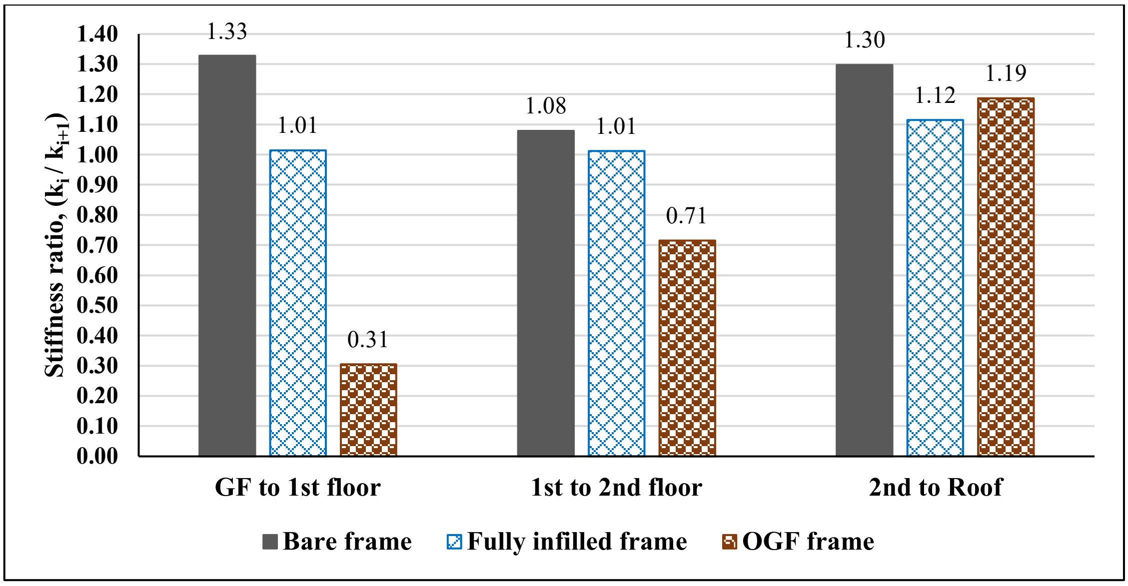

Figure 6.2: Storey stiffness ratio of different floors for 4-storied buildings

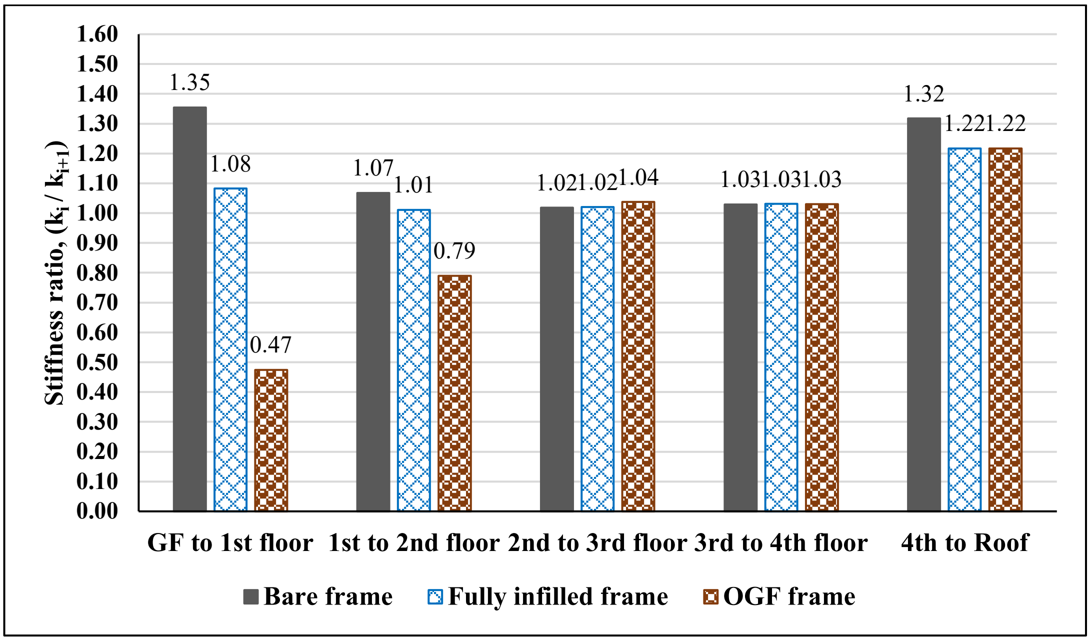

Figure 6.3: Storey stiffness ratio of different floors for 6-storied buildings

6.3 Storey drift (Δ) and allowable storey drift (Δ_a)

In this section, the inelastic deflections of level x were determined in accordance with the following the draft BNBC 2017 provided equation:

$$\delta_x = \frac{C_d \delta_{xe}}{I}$$

where, C_d = Deflection amplification factor

δ_{xe} = Deflection determined by elastic analysis.

I = Importance factor.

In this study, C_d and I were considered as 4.5 and 1.0 respectively as per draft BNBC 2017 considering Intermediate moment resisting frame (IMRF). Value of δ_{xe} was taken from the result of elastic analysis using commercial software ETABS.

The design storey drift at storey x was computed as the difference of the deflections at the top and bottom of the storey under consideration as follows:

$$\Delta = \delta_x - \delta_{x-1}$$

Design storey drift obtained from the above equation were compared with the allowable storey drift limit as per draft BNBC 2017. In this study, allowable drift limit for the 4-storied moment resisting frame structure is $0.025h_{sx}$ and for the 6 and 10-storied moment resisting frame structure is $0.02h_{sx}$. for the considered buildings, typical storey height (h_{sx}) is 3000 mm.

$\Delta_a = 0.025\ h_{sx} = 0.025 * 3000mm = 75$ mm for 4-storied building

$\Delta_a = 0.02\ h_{sx} = 0.02 * 3000mm = 60$ mm for 6- and 10-storied building

Table 6.2 shows the results of the design storey drift for the 4-storied bare frame, fully infilled frame and OGF frame. Similar pattern of storey drift was found for 6 and 10-storied buildings frames which have been shown in Appendix A-2. Then the design storey drift of the respective buildings were compared with the allowable storey drift limits. Figure 6.4 present the storey drift and allowable storey drift of different types of 4-storied buildings in percentage. It was found that, design drift of all of the buildings were within the allowable drift limits as per the code. It was also found that presence of masonry infill walls decreased the deflection and storey drift of the considered buildings.

Table 6.2: Storey drift of 4-storied bare frames, fully infilled frames and OGF frames

Frame	Floor Levels	h_{sx} (mm)	δ_{xe} (mm)	$\delta_x = \frac{C_d \delta_{xe}}{I}$ (mm)	$\Delta = \delta_x - \delta_{x-1}$ (mm)	$\Delta_a = .025h_{sx}$ (mm)	Remarks
Bare Frame	ROOF	3000	44	198	29	75	ok
	2nd Floor	3000	37	169	50	75	ok
	1st Floor	3000	26	119	63	75	ok
	Ground Floor	3000	12	56	52	75	ok
Fully Infilled Frame	ROOF	3000	5	23	2	75	ok
	2nd Floor	3000	5	21	5	75	ok
	1st Floor	3000	3	16	7	75	ok
	Ground Floor	3000	2	9	7	75	ok
OGF Frame	ROOF	3000	11	49	2	75	ok
	2nd Floor	3000	10	47	4	75	ok
	1st Floor	3000	10	43	8	75	ok
	Ground Floor	3000	8	34	31	75	ok

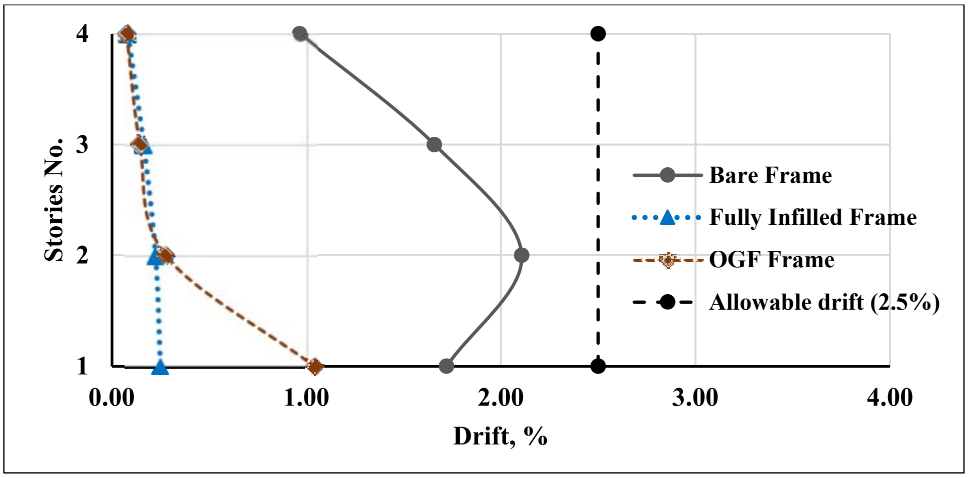

Figure 6.4: Storey drifts of different types of 4-storied buildings

6.4 Modal participating mass factor (%)

In this section, modal participating mass factor of different frame structures have been evaluated. According to draft BNBC 2017, minimum 90% mass should be participated in modal analysis. This requirement was fulfilled satisfactorily as all the frames had more than 90% modal mass participation factor (%). It was also found that about 78% to 90% modal mass was contributed within first three modes of the modal analysis. Therefore, most percentage of the total mass were participated in first three modes.

Table 6.3: Modal participating mass factors (%) of different types of 4-storied buildings

Mode	Bare Frame		Fully Infilled Frame		OGF Frame	
	UX	UY	UX	UY	UX	UY
1	72%	4%	41%	41%	48%	48%
2	77%	77%	83%	83%	95%	95%
3	77%	77%	83%	83%	95%	95%
4	86%	77%	87%	87%	96%	96%
5	86%	86%	90%	90%	96%	96%
6	86%	86%	90%	90%	96%	96%
7	90%	87%	91%	91%	97%	97%
8	90%	90%	92%	92%	97%	97%
9	90%	90%	92%	92%	97%	97%
10	91%	90%	92%	92%	97%	97%

6.5 Fundamental Time (T) by code equation and modal analysis

In this section, fundamental period (T) of the bare frame, fully infilled frame and open ground floor (OGF) frames of 4, 6 and 10-storied buildings were estimated using the both the modal analysis and the code equation. Draft BNBC 2017 recommends both methods to determine the *T*. No different provision is proposed as per the Code to consider any vertical irregularities along height of the building for estimating the fundamental period of the structure.

The fundamental period *T* in seconds can be determined by the following code equation:

$$T = C_t \left(h_n\right)^m$$

For the concrete moment resisting frame structures, the value of C_t and m are 0.0466 and 0.9, respectively. The main parameter in estimation of T as per code equation is the building height. Hence, fundamental period by code equation of bare frame, fully infilled frame and soft storey frame are the same for 4, 6 and 10-storied buildings as shown in Figure 6.5. On the other hand, in case of estimation of the fundamental period by modal analysis procedure in which mass, stiffness and angular frequency of the structure are taken in consideration. The equation of fundamental period of any structure is as follows:

$$T = \frac{2\pi}{\omega_n}$$

where, ω_n is the angular frequency of the structure. In this study values of T by modal analysis were determined directly from ETABS analysis. Fundamental period of bare frame, fully infilled frame and soft storey frame are different for the 4, 6 and 10-storied buildings as shown in Figure 6.6.

It was found that the effect of the presence of infill walls was considered in case of modal analysis whereas in case of code recommended equation it had no effect. It was also found that presence of infill wall decrease the fundamental period of the structure. T of OGF frames were less than that of the bare frames but greater than fully infilled frames as shown in Figure 6.6.

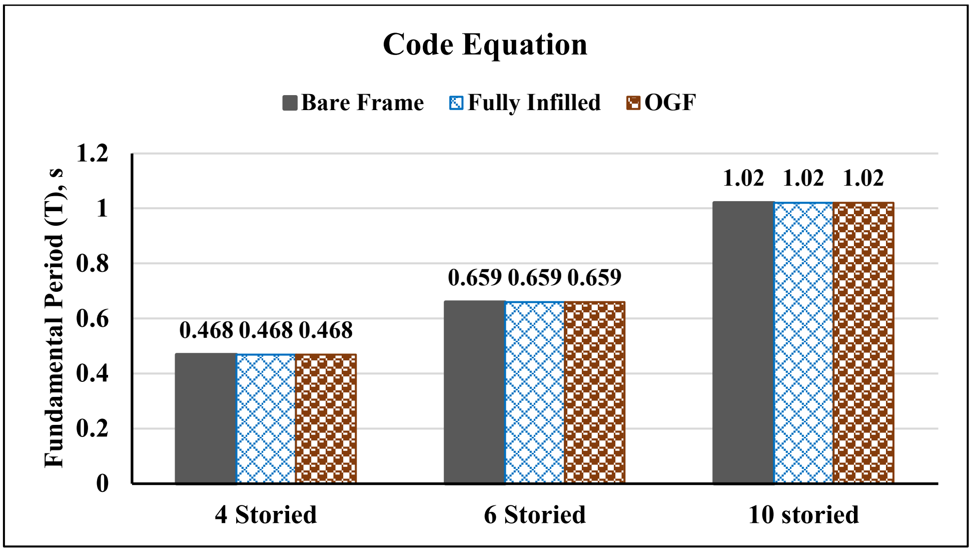

Figure 6.5: T from code equation for different types of 4, 6 and 10-storied buildings

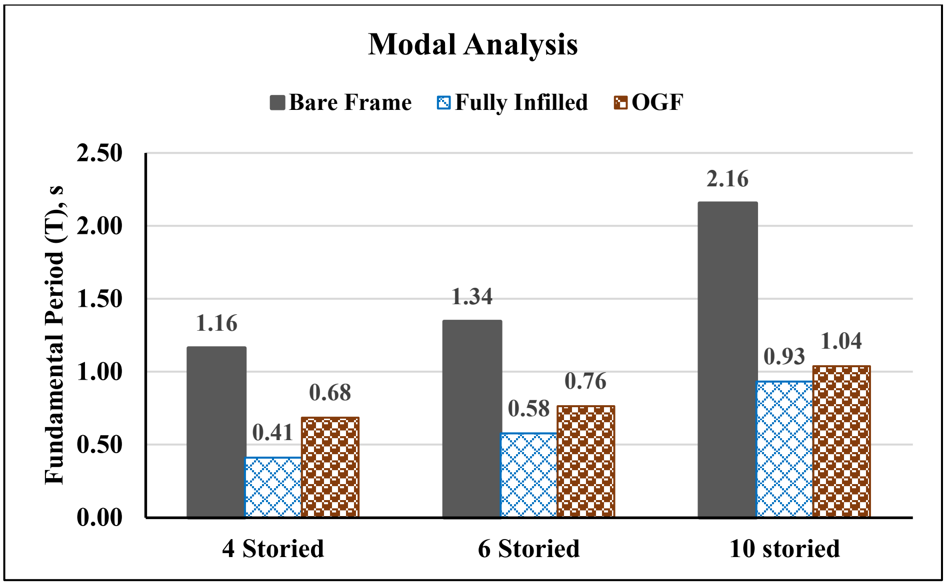

Figure 6.6: *T* from modal analysis for different types of 4, 6 and 10-storied buildings

6.6 Displacement profile for different ground motions by TH analysis

Nonlinear time history analysis was performed using ETABS software. Each ground motion was matched with the target response spectrum provided in draft BNBC 2017. Figure 6.7 to 6.9 shows top displacement for specific ground motions by TH analysis from ETABS. Figures 6.10 to 6.12 presented the comparative displacement profile of different types of 4, 6 and 10-storied buildings under El Centro (1940), Imperial Valley (1979) and Kobe (1995) earthquakes. Similarly, top displacement of other buildings under different earthquakes were shown in Appendix A-4. It was found that bare frame experienced the maximum top displacement for each considered ground motion.

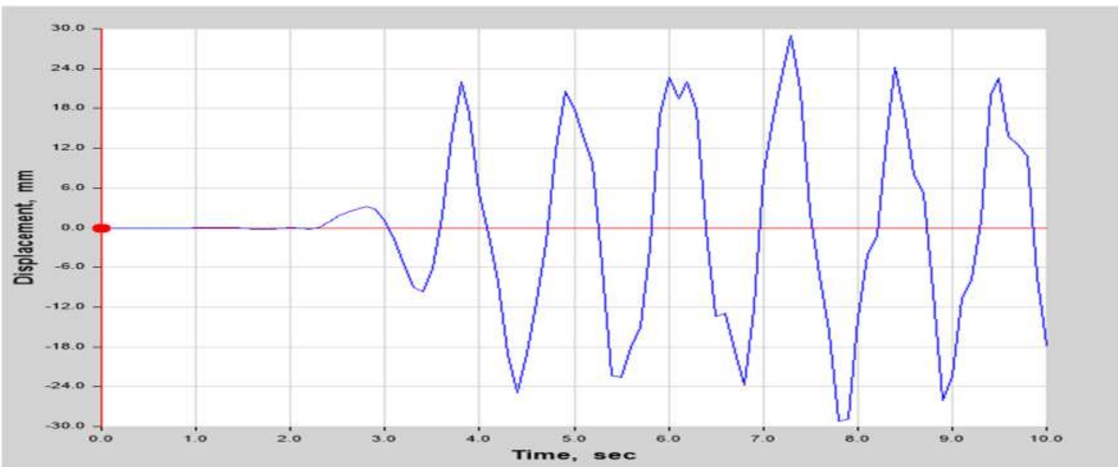

Figure 6.7: Top displacement of 4-storied bare frame under El Centro (1940) earthquake

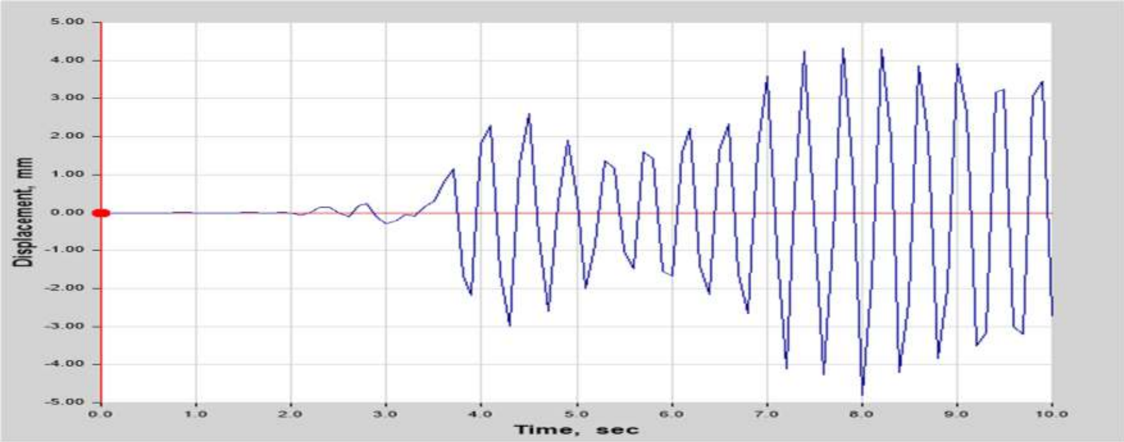

Figure 6.8: Top displacement of 4-storied fully infilled frame under El Centro (1940) earthquake

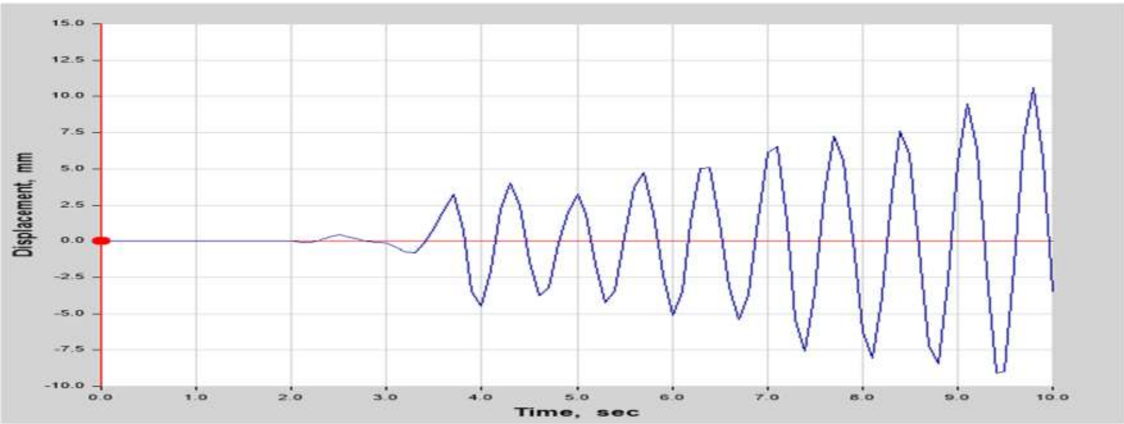

Figure 6.9: Top displacement of 4-storied OGF frame under El Centro (1940) earthquake

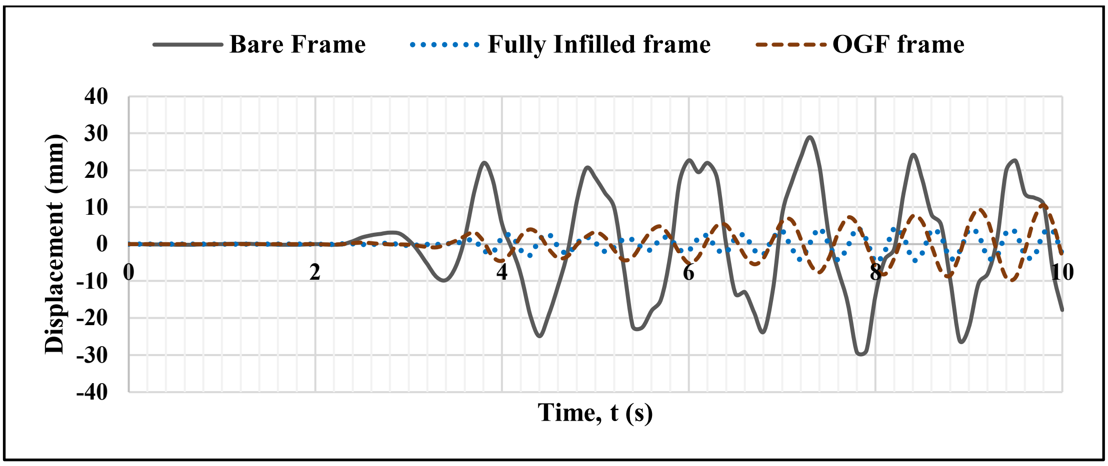

Figure 6.10: Comparison of Top displacement profile of 4-storied buildings under El Centro (1940) earthquake

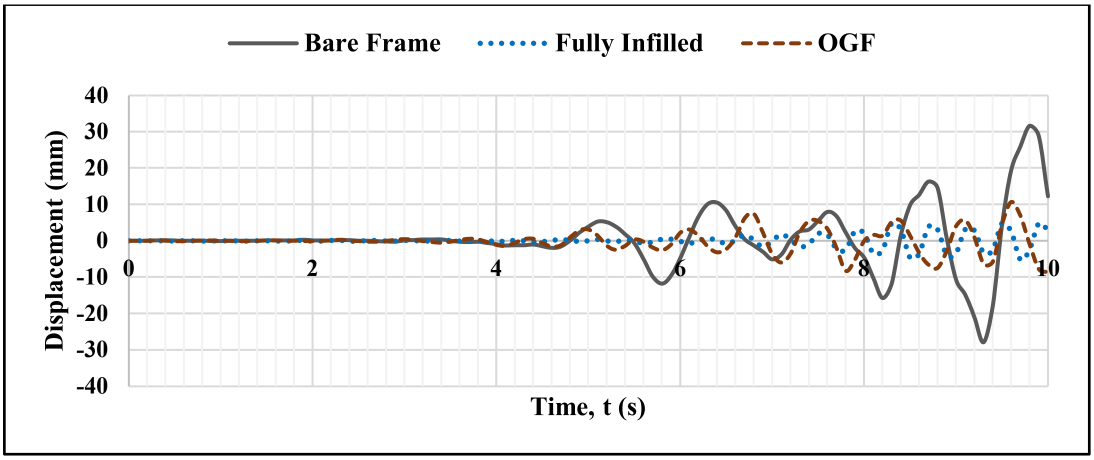

Figure 6.11: Comparison of Top displacement profile of 4-storied buildings under Imperial Valley (1979) earthquake

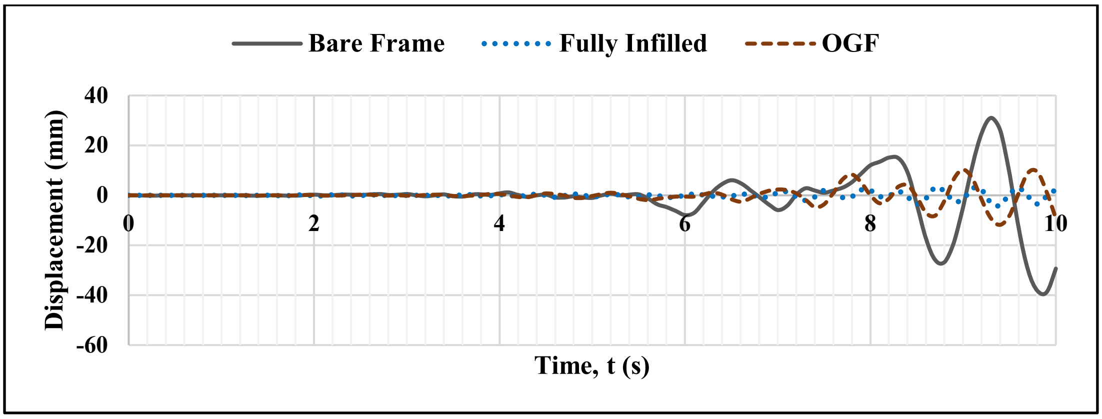

Figure 6.12: Comparison of Top displacement profile of 4-storied buildings under Kobe (1995) earthquake

6.7 Storey Shears by ES, RS and TH analyses

Storey shears from equivalent static analysis, response spectrum analysis and time history analysis (THA) were estimated for 4, 6 and 10- storied bare, fully infilled and OGF frames. It was found that different analysis procedure results in different storey shears at different storey level for each types of frame. Figures 6.13 to 6.15 show the comparison of storey shears of different types of 4-storied buildings by ES, RS and TH analyses. Similarly, comparison of storey shears of different types of 6 and 10-storied buildings by ES, RS and TH analyses were shown in Appendix A-5.

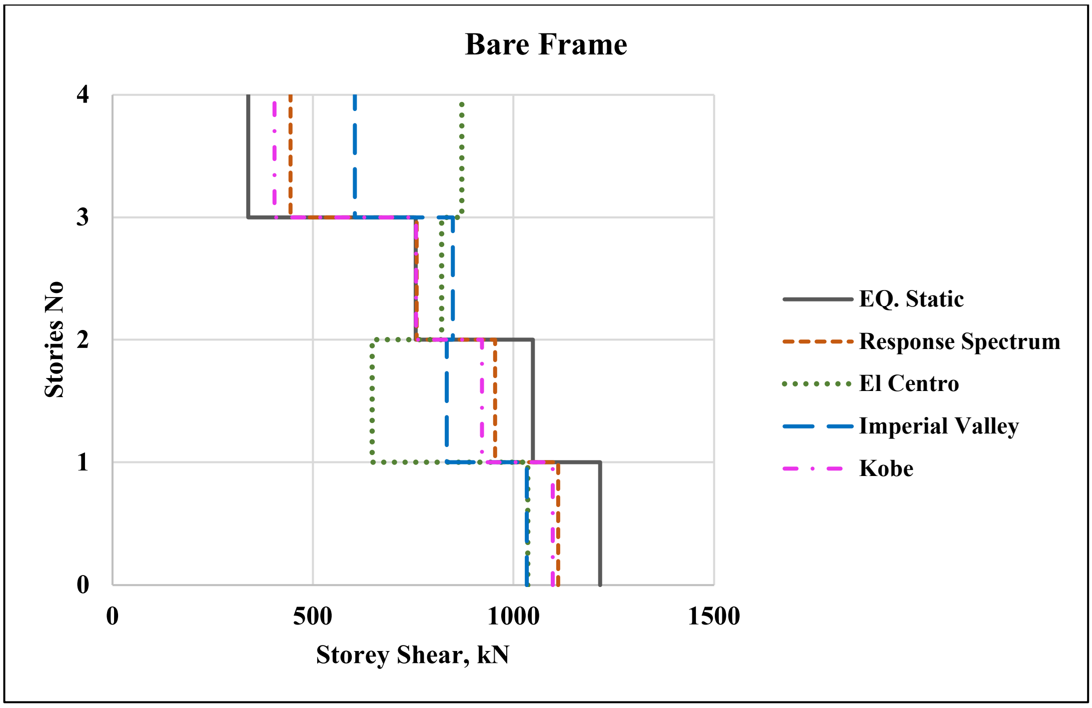

Figure 6.13: Comparison of storey shears for 4-storied bare frames

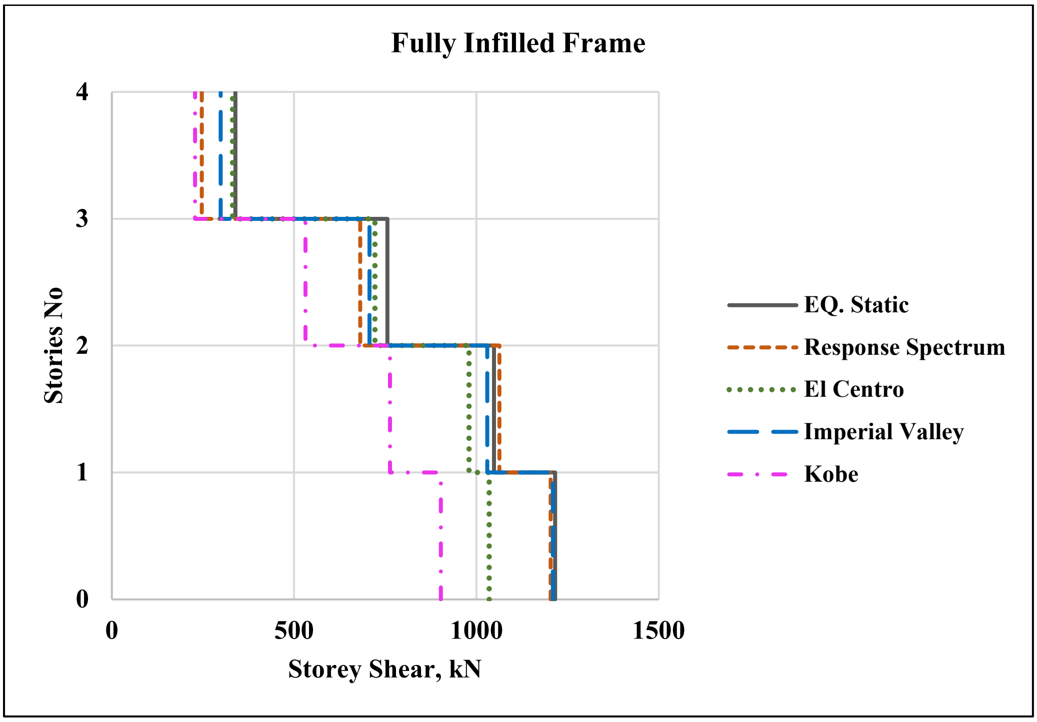

Figure 6.14: Comparison of storey shears of 4-storied fully infilled frames

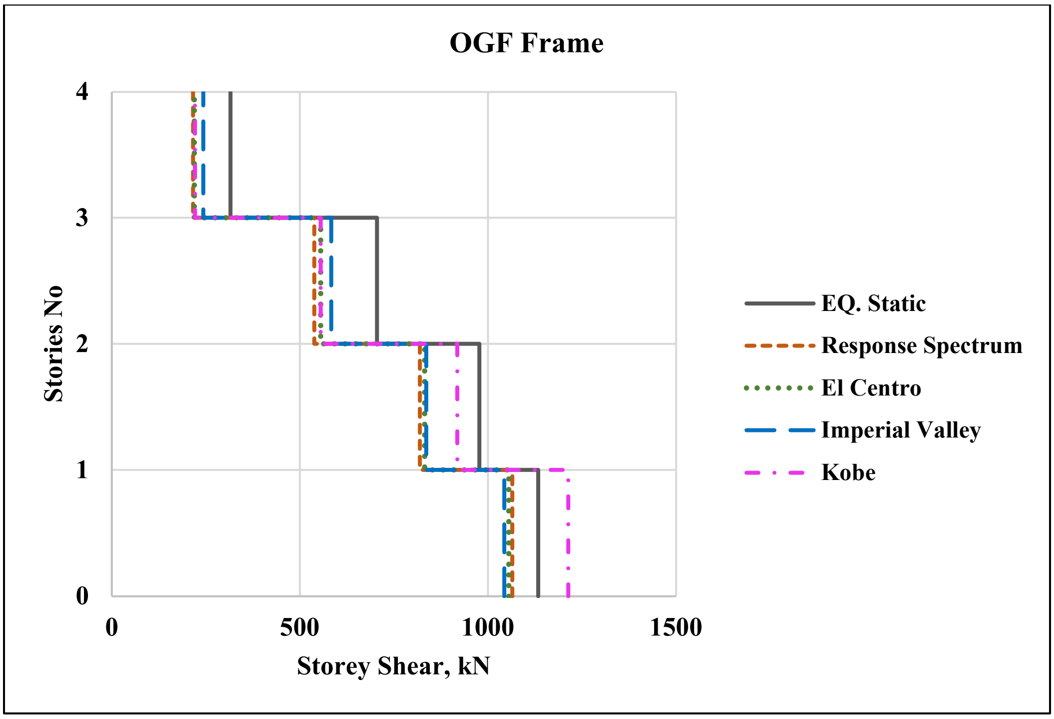

Figure 6.15: Comparison of storey shears for 4-storied OGF frames

6.8 Shear force at GF of bare and OGF frames by ES and TH analyses

To investigate the amplification of shear force at the ground floor of OGF frames than that of the bare frames, a comparative study of design shear forces at the ground floor of bare and OGF frames by ES and dynamic TH analysis respectively was performed. As per draft BNBC 2017, if the number of the ground motion record is less than seven numbers, maximum response should be considered as the design force by dynamic TH analysis.

Comparison of shear force at the ground floor of the bare and OGF frames by equivalent static and time history analysis respectively was shown in Figure 6.16 and Table 6.4. The maximum storey shear force ratio at the ground floor of 4, 6 and 10 storied bare frame by equivalent static and OGF frames by time history analysis was found 1.00. Therefore, there was no the amplification of shear force by dynamic TH analysis at the ground floor of OGF frames than those of bare frames by ES analysis due to absence of infill wall.

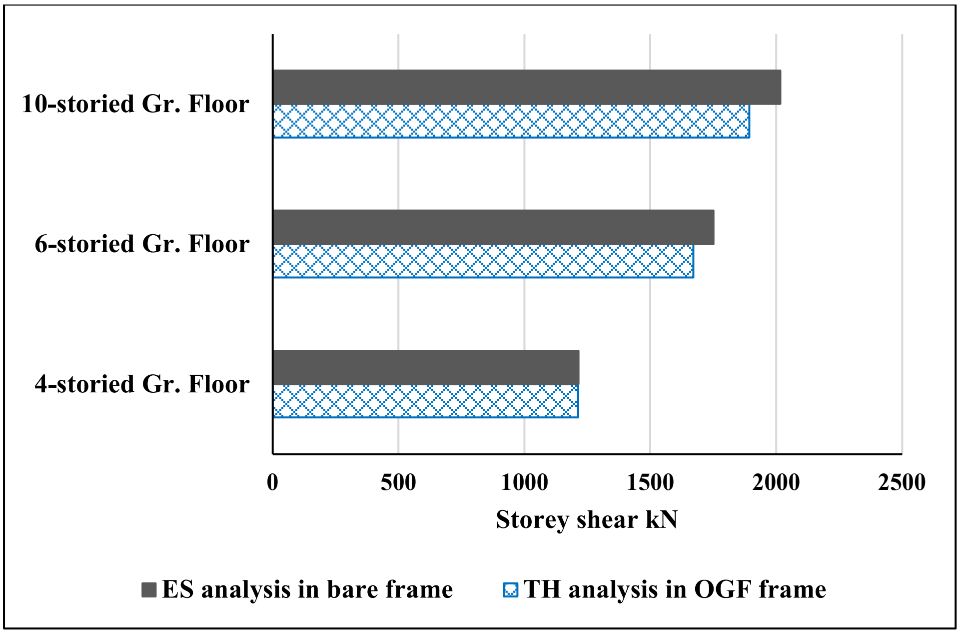

Figure 6.16: Storey shear at the ground floor by ES analysis for bare frame and dynamic TH analysis for OGF frames

Table 6.4: Storey shear at the ground floor by ES analysis for bare frame and dynamic TH analysis for OGF frames

Building	Storey shear by ES analysis (bare frame), kN	Storey shear by TH analysis (OGF frame), kN	Storey shear ratio, (OGF / Bare)
4-storied	1216	1214	1.00
6-storied	1751	1671	0.95
10-Storied	2016	1894	0.94

6.9 Comparison of shear and bending moment by ES and TH analyses

Comparison of shear force and bending moment of a specific column 3C as shown in Figure 6.17 by equivalent static analysis for bare and by dynamic time history for OGF frames has shown in Table 6.5. The maximum ratio of shear force of 3C column at ground floor of OGF frame by dynamic to bare frame by equivalent static analysis was found 1.01 and the maximum ratio of bending moment of OGF frame by dynamic to bare frame by equivalent static analysis was found 0.80. Therefore, there was found no amplification of shear force and bending moment at 3C column of OGF frame compared to bare frame due to absence of infill wall.

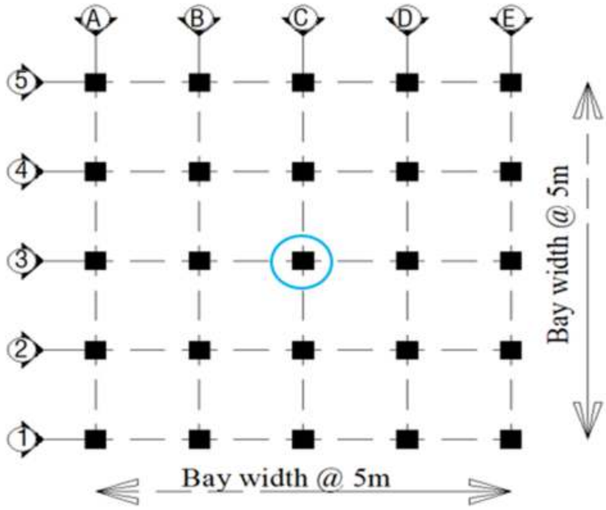

Figure 6.17: Location of 3C column

Table 6.5: Shear force and bending moment of column 3C at the ground floor by ES analysis for bare frame and dynamic TH analysis for OGF frames

Building	Shear force at GF of bare frame by static analysis, kN	Shear force at GF of OGF frame by time history analysis, kN	Ratio of shear force by dynamic to static analysis	Bending moment at bare frame by static analysis, kN-m	Bending moment at OGF frame by time history analysis, kN-m	Ratio of bending moment by dynamic and static analysis
4-storied	54	55	1.01	105	84	0.80
6-storied	78	72	0.92	160	114	0.71
10-storied	89	83	0.93	244	148	0.60

6.10 Pushover curves of different types of 4, 6 and 10-storied buildings

Nonlinear static or pushover analysis were conducted using the ETABS software for all types of models. The pushover analysis consists of the application of the gravity loads and the code recommended lateral load pattern. For simplicity, P-Delta effects were not considered. Figures 6.18 to 6.20 show the pushover curves (base shear vs. top deflection) for all types of considered models. It was found that fully infilled frame has attained the maximum base shear capacity than that of the bare and OGF frames.

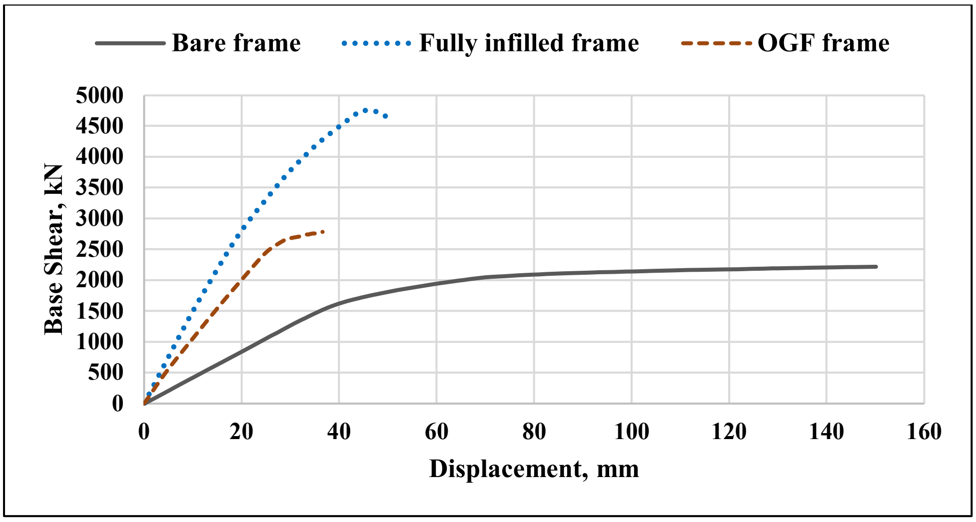

Figure 6.18: Pushover curve for different types of 4-storied buildings

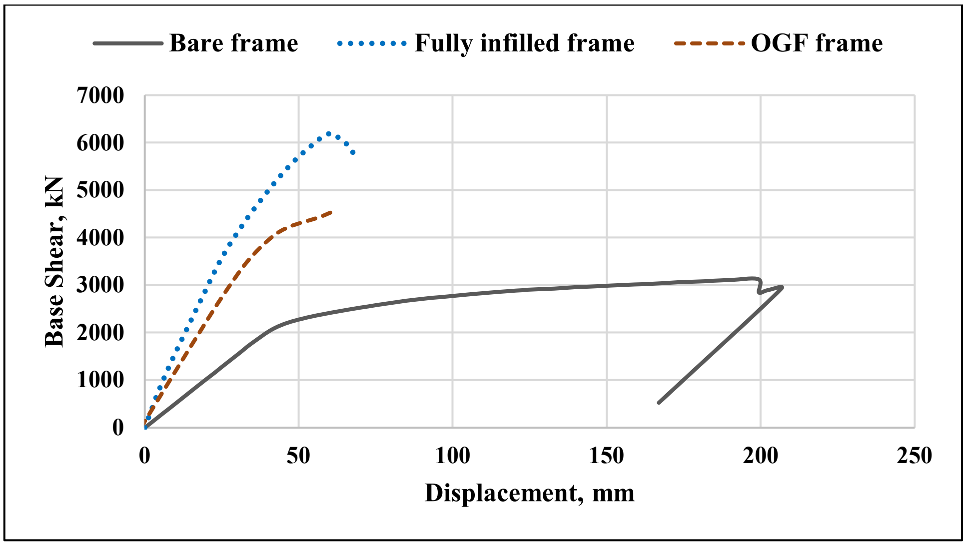

Figure 6.19: Pushover curve for different types of 6-storied buildings

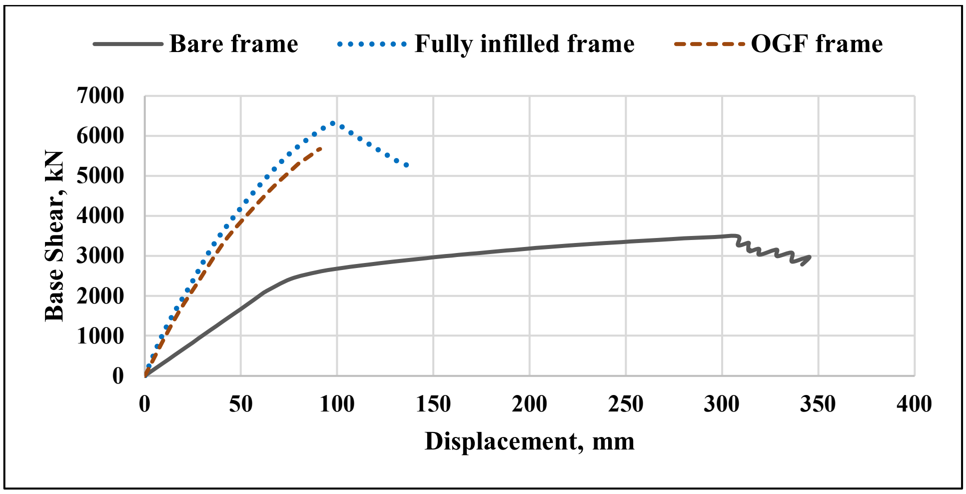

Figure 6.20: Pushover curve for different types of 10-storied buildings

6.11 Response reduction factor (R) of bare, fully infilled and OGF frames

Seismic performance of different types of building models was evaluated in terms overstrength factor (Rs), ductility factor (Rμ) and response reduction factor (R). Overstrength factor (Rs), ductility factor (Rμ) and response reduction factor (R) of different types of structures were shown in Table 6.6.

R value of 4, 6 and 10-storied bare frames were found 5.15, 5.67 and 5.29. These values were 3.1%, 13.5% and 5.85% above than the considered R value 5. R value of 4, 6 and 10 storied fully infilled frames were found 5.44, 5.16 and 5.13. These values were 8.8%, 2.6% and 3.1% above than the considered R value 5. R value of 4, 6 and 10 storied OGF frames were found 3.01, 3.94 and 3.42. These values were 39.8%, 21.1% and 31.5% less than the considered R value 5. Therefore, R values of bare frame and fully infilled frames were always found above than the considered R value whereas in case of OGF frames these values were always found less than the considered value.

Ratios of R values of 4, 6 and 10-storied bares frame and OGF frames were found 1.71, 1.44 and 1.55. Hence, design base shear should be increased when an open ground floor building is designed as bare frame. Draft BNBC 2017 recommends to design the structural elements of open ground floor with storey shear and bending moment magnification factor of 2.5. Therefore, obtained results in this study show the requirement of the special design provision as per draft BNBC 2017 for a building with the open ground floor.

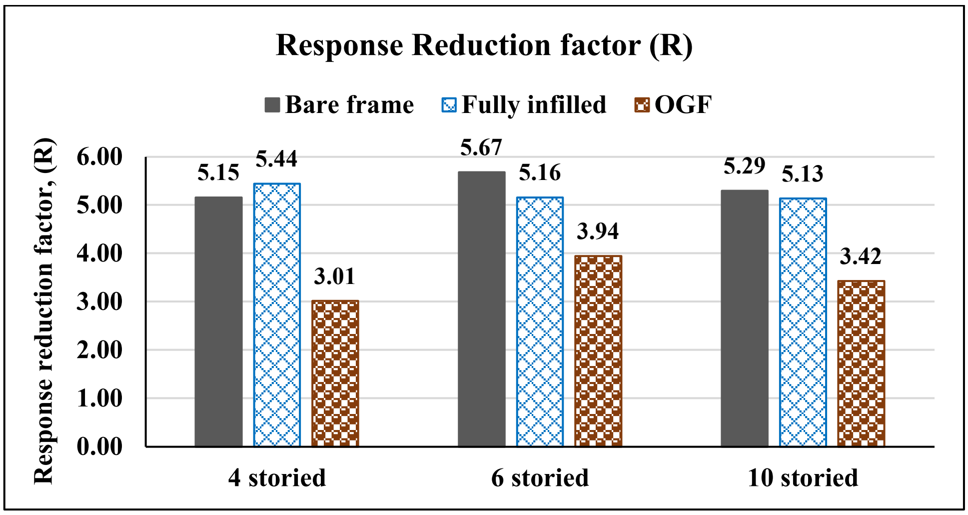

Figure 6.21: R value of different types of 4, 6 and 10-storied buildings

Table 6.6: Rs, Rµ and R factors of different types of 4, 6 and 10-storied buildings

Building	Frame	V_y (kN)	V_d (kN)	Overstrength factor (Rs)	D_{max} (mm)	D_y (mm)	Ductility factor (Rµ)	R
4-storied	Bare Frame	1950	1235	1.58	150	46	3.26	5.15
	Fully Infilled Frame	4200	1235	3.40	48	30	1.60	5.44
	OGF Frame	2500	1139	2.19	33	24	1.37	3.01
6-storied	Bare Frame	2500	1763	1.42	200	50	4.00	5.67
	Fully Infilled Frame	5300	1763	3.01	60	35	1.71	5.16
	OGF Frame	3800	1679	2.26	61	35	1.74	3.94
10-storied	Bare Frame	2600	2019	1.29	308	75	4.11	5.29
	Fully Infilled Frame	5600	2019	2.77	111	60	1.85	5.13
	OGF Frame	4800	1963	2.44	91	65	1.40	3.42

6.12 Mass irregularity

6.12.1 Mass irregularity check

As per draft BNBC 2017, mass irregularity occurs when the masses of any storey is more than twice of that of its adjacent storeys. This irregularity need not be considered in case of roof. In this study, mass irregularity was considered at mid-storey level of 4, 6 and 10-storied frame structures. Storey masses and storey mass ratios of adjacent floors of 4-storied regular and mass irregular frames were shown in Table 6.7. Similarly, storey masses and storey mass ratios of adjacent floors of 6 and 10-storied regular and mass irregular frames were shown in Appendix B-1. In case of regular frames mass ratios were less than 2.00 in all floors. But in case of mass irregular frames, storey mass ratios were found 2.00 and above 2.00 at the certain floors on which special loads were applied. Therefore, mass irregularities were found in the mass irregular frames according to the Code.

Table 6.7: Storey masses of 4-storied regular and mass irregular frames

Floors	Regular frame		Frames with mass irregularity	
	Storey mass, kg	**M_i / M_{i+1}**	**Storey mass, kg**	**M_i / M_{i+1}**
ROOF	249098		249098	
2^{nd} Floor	399665	1.60	399665	1.6
1^{st} Floor	399665	1	807551	2.0
Ground Floor	399665	1	399665	0.5

6.12.2 Storey shear of regular and mass irregular frames

A sudden increase of storey mass due to mass irregularity has effect on storey shear force demand on the structures. Figures 6.22 shows the comparison of storey shear force between 4- storied regular and mass irregular frames. Similar pattern of storey shear force distribution was found in the 6 and 10-storied regular and mass irregular frames which were presented in Appendix B-2.

It was found that at the mass irregular floor and its below floors, storey shear was increased in comparison to that of the regular frames.

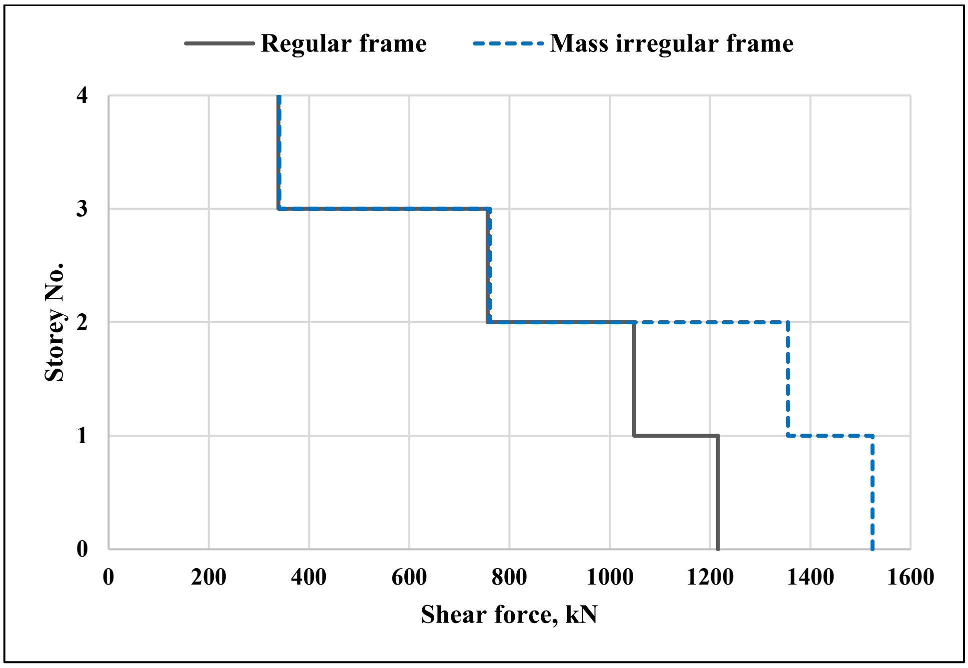

Figure 6.22: Storey shear of 4-storied regular and mass irregular frames

6.12.3 Storey drift of regular and mass irregular frames

Figures 6.23 shows the storey drifts of 4-storied regular and mass irregular frames. Similarly, the comparison of storey drift of 6 and 10-storied regular and mass irregular frames were shown in Appendix B-3. It was observed that, storey drift demand was increased due to the mass irregularity. Storey drift of all mass irregular frames exceeded the allowable drift limit as per draft BNBC 2017. Maximum storey drift (%) of 4-storied mass irregular frame was found as 2.59 which was 3.7% above the allowable limit of 2.5. Maximum storey drift (%) of 6-storied mass irregular frame was found as 2.09 which was 4.4% above the allowable limit 2. Maximum storey drift (%) of 10-storied mass irregular frame was found as 2.16 which was 8.1% higher than the allowable limit 2.

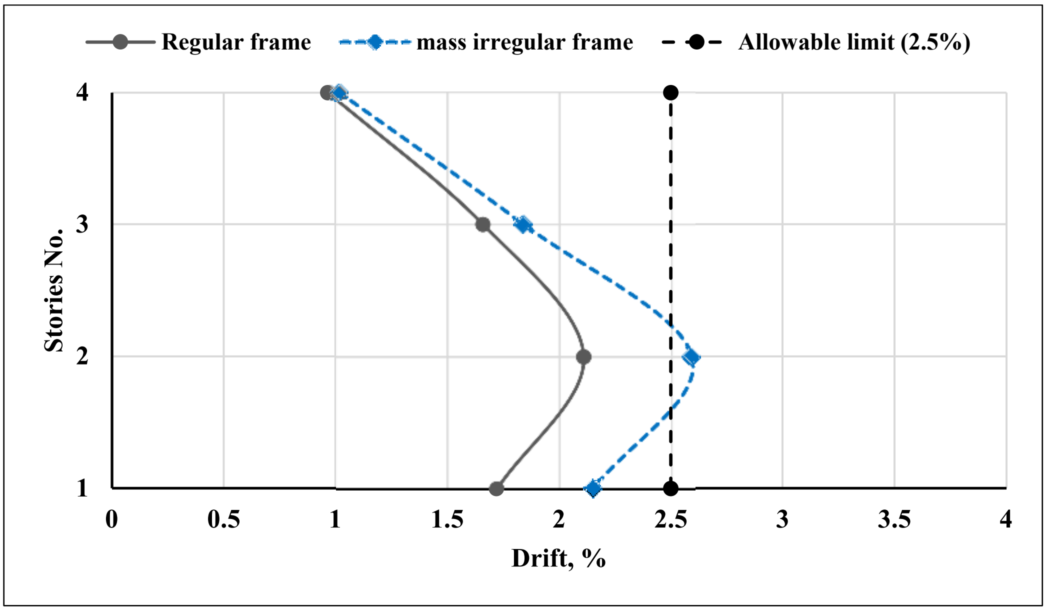

Figure 6.23: Storey drifts of 4-storied regular and mass irregular frames

6.12.4 Modal period of regular and mass irregular frames

Table 6.8 shows the modal period of regular and mass irregular frames. It was observed that, modal period of mass irregular frames were larger than the regular frames. This was because of increased mass in the mass irregular frames.

Table 6.8: Modal period of regular and mass irregular frames

Building	Modal period (T), s	
	Regular frame	Mass irregular frame
4-storied	1.19	1.35
6-storied	1.37	1.46
10-storied	2.20	2.31

6.12.5 Pushover curves of regular and mass irregular frames

Figures 6.24 shows the pushover curves of 6-storied regular and mass irregular frames. Similar pattern of the pushover curves for 4 and 10-storied regular and mass irregular frames were found whose were provided in Appendix B-4.

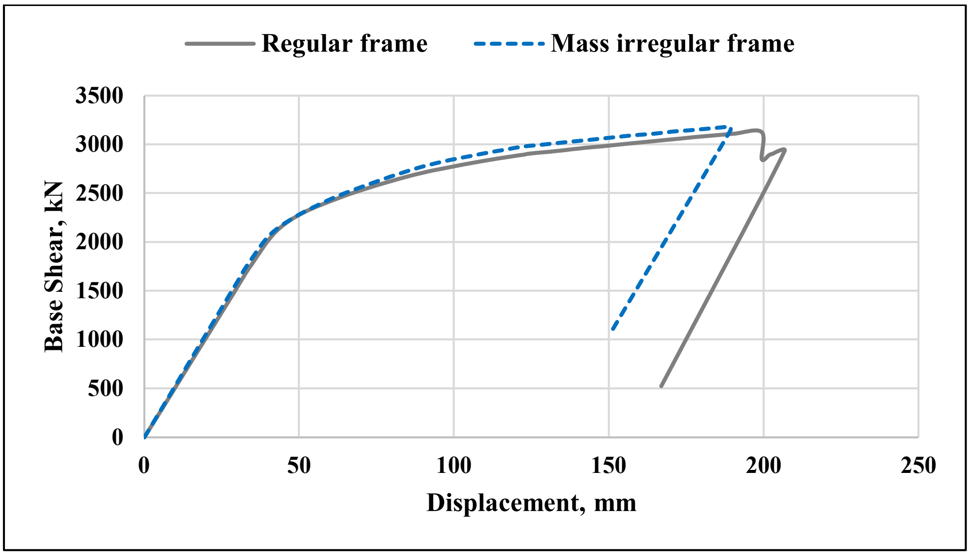

Figure 6.24: Pushover curves of 6-storied regular and mass irregular frames

6.12.6 Response reduction factor (R) of regular and mass irregular frames

A comparative study of overstrength factor (Rs), ductility factor (Rμ) and response reduction factor (R) of 4, 6 and 10 storied regular and mass irregular frames were provided in Table 6.9. R value of 4, 6 and 10- storied mass irregular frames were found 2.31, 4.55 and 4.64, respectively while those of the regular frames were found 5.15, 5.67 and 5.29, respectively. The results show that R values of mass irregular frames were 60%, 25% and 12% less than those of the regular frames. This reduction of R value was due to the presence of mass irregularity in the frame.

Table 6.9: Rs, Rμ and R factors of regular and mass irregular frames

Building	Frame	V_y (kN)	V_d (kN)	Overstrength factor (Rs)	D_{max} (mm)	D_y (mm)	Ductility factor (Rμ)	R
4-storied	Regular	1950	1235	1.58	150	46	3.26	5.15
	Mass irregular	1950	1543	1.26	84	46	1.83	2.31
6-storied	Regular	2500	1763	1.42	200	50	4.00	5.67
	Mass irregular	2450	2039	1.20	189	50	3.79	4.55
10-storied	Regular	2600	2019	1.29	308	75	4.11	5.29
	Mass irregular	2600	2212	1.18	296	75	3.94	4.64

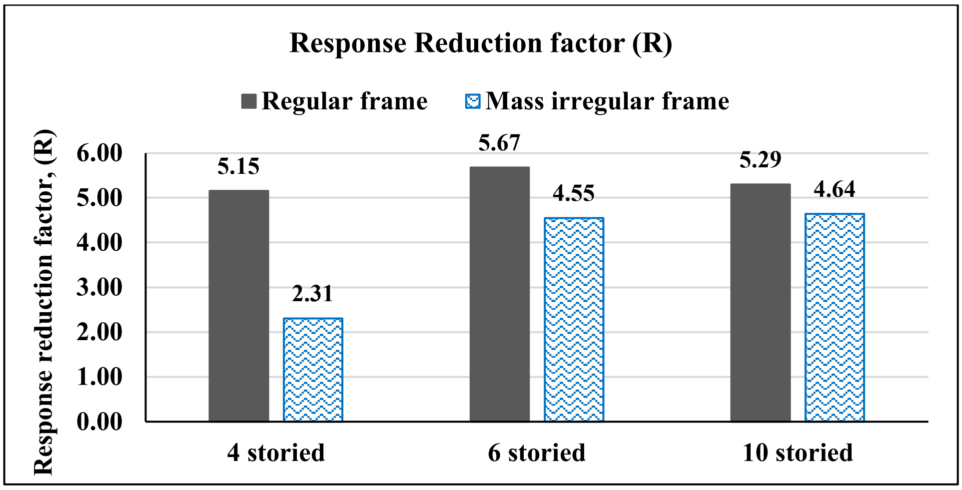

Figure 6.25: R value of 4, 6 and 10-storied regular and mass irregular frames

6.13 Vertical geometric irregularity

6.13.1 Storey shear of regular and geometric irregular frames

Vertical geometric irregularity was considered due to presence of setback in the building. In this study 2 types of setback configurations were considered such as (i) B1-upper and (ii) B1- mid. Figure 6.26 shows the comparison of storey shear between 4-storied regular and different types of geometric irregular frames. Similarly, comparison of storey shear between 6 and 10-storied regular and geometric irregular frames were provided in

Appendix C-1.

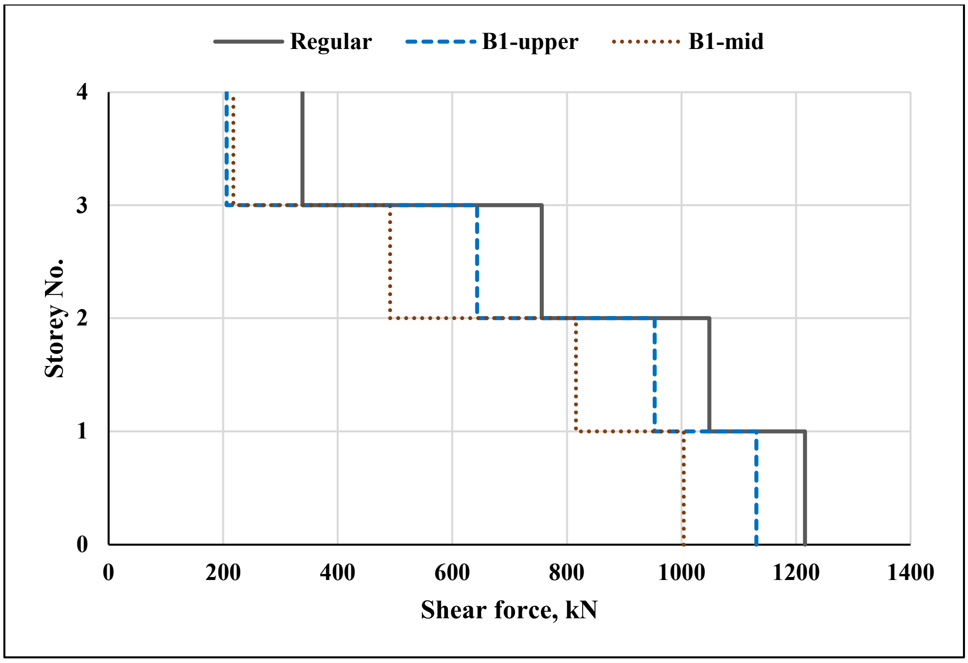

Figure 6.26: Storey shear of 4-storied regular and geometric irregular frames

6.13.2 Storey drifts of regular and geometric irregular frames

Figures 6.27 shows the storey drifts of 4-storied regular and geometric irregular frames. Similarly, the storey drifts of 6 and 10-storied regular and geometric irregular frames were shown in Appendix C-2. Storey drifts of geometric irregular frames were found within allowable drift limit as per the Code.

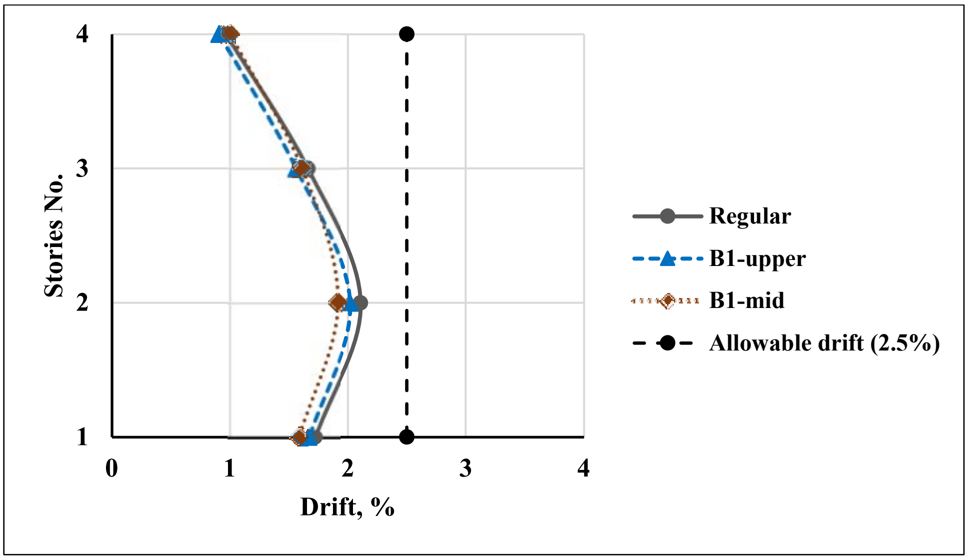

Figure 6.27: Storey drifts of 4-storied regular and geometric irregular frames

6.13.3 Modal period of regular and geometric irregular frames

Table 6.10 shows the modal period (T) of 4, 6 and 10-storied regular and geometric irregular frames. It was observed that, modal period of regular frames were higher than that of the geometric irregular frames.

Table 6.10: Modal period of regular and geometric irregular frames

Building	Modal period (T), s		
	Regular	B1-upper	B1-mid
4-storied	1.19	1.02	1.04
6-storied	1.37	1.28	1.20
10-storied	2.20	2.09	1.92

6.13.4 Pushover curves of regular and geometric irregular frames

Figures 6.28 shows the pushover curves of 6-storied regular and geometric irregular frames. Similar pattern of the pushover curves for 4 and 10-storied regular and geometric irregular frames were found which have been shown in Appendix C-3.

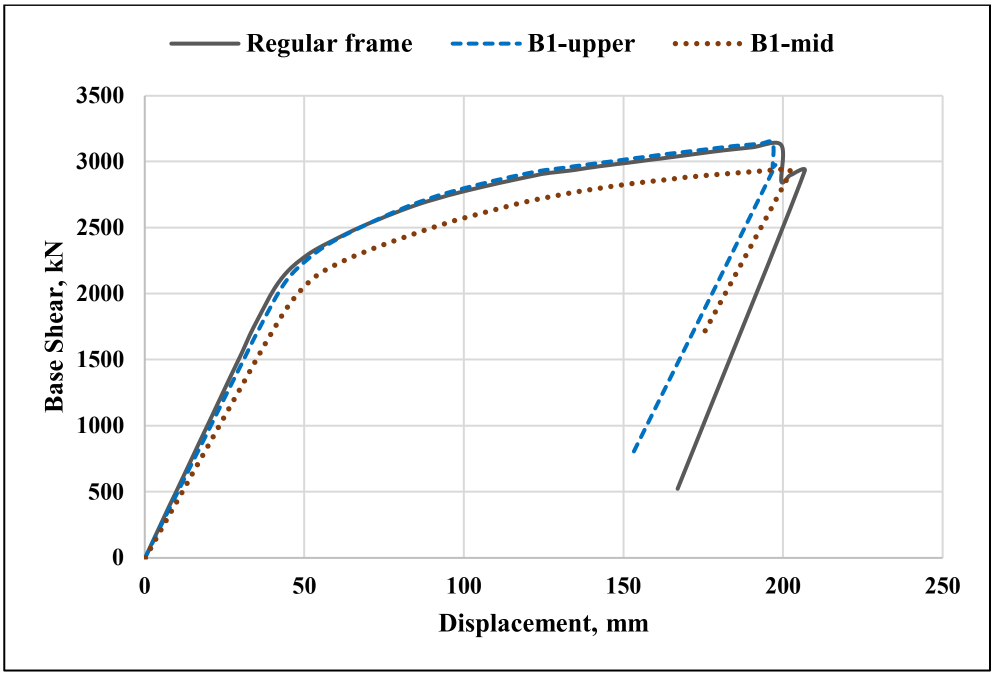

Figure 6.28: Pushover curves of 6-storied regular and geometric irregular frame.

6.13.5 Response reduction factor (R) of regular and geometric irregular frames

Overstrength factor (Rs), ductility factor (Rμ) and response reduction factor (R) values of 4, 6 and 10-storied regular and geometric irregular frames were shown in Table 6.11. R value of 4, 6 and 10-storied buildings with B1-upper type geometric irregular frames were found 39%, 6% and 26% less than the values of regular frames respectively. R value of 4, 6 and 10-storied buildings with B1-mid type geometric irregular frames were found 5%, 2% and 3% less than the values of regular frames respectively Therefore R value of geometric irregular frames were found always less than the regular frames.

Table 6.11: Rs, Rμ and R factors of regular and geometric irregular frames

Building	Frame	V_y (kN)	V_d (kN)	Overstrength factor (Rs)	D_{max} (mm)	D_y (mm)	Ductility factor	R
4-storied	Regular	1950	1235	1.58	150	46	3.26	5.15
	B1-upper	1900	1165	1.63	135	70	1.93	3.14
	B1-mid	1750	1054	1.66	153	52	2.94	4.89
6-storied	Regular	2500	1763	1.42	200	50	4.00	5.67
	B1-upper	2400	1692	1.42	196	52	3.77	5.35
	B1-mid	2250	1480	1.52	202	55	3.67	5.58
10-storied	Regular	2600	2019	1.29	308	75	4.11	5.29
	B1-upper	2600	1970	1.32	223	75	2.97	3.92
	B1-mid	2400	1676	1.43	322	90	3.58	5.12

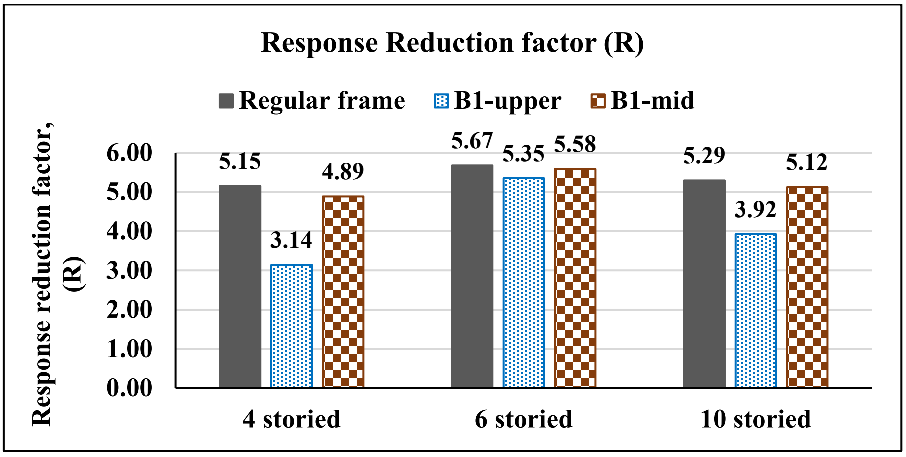

Figure 6.29: R value of 4, 6 and 10-storied regular and geometric irregular frames

Chapter 7

CONCLUSIONS AND RECOMMENDATIONS

7.1 General

Uniformity of structural components along the height of the building is very important as non-uniformity of structural components may weaken the structure in resisting the seismic force during an earthquake. Non-uniformity of structural components along height is known as vertical irregularity of a structure. During an earthquake, damage or failure of a building may be triggered at the point of weakness occurred by vertical irregularities. Many structures are designed with vertical irregularities due to functional, aesthetic or economic reasons. Vertical irregularities are due to sudden changes in stiffness, strength, mass, setbacks and uneven participation of non-structural components along height between adjacent stories. In this thesis, a comprehensive numerical studies have been conducted to assess the seismic behavior of vertically irregular structures. Stiffness irregularity, mass irregularity and geometric – theses three types of vertical irregularity have been considered. Stiffness irregularity cases have been considered due to sudden absence of masonry infill walls at open ground floor for parking facility while mass irregularity by applying a special superimposed dead load at mid storey level. Geometric irregularity have been considered due to presence of setback at upper and mid storey level. Equivalent strut method was used to simulate the infill wall. Three regular buildings having 4, 6 and 10-storied having the same plan layout located at seismic zone 2 according to draft BNBC 2017 were considered. All the frames were designed as reinforced concrete (RC) intermediate moment resisting frame (IMF). Seismic analysis methods such as equivalent static, response spectrum, time history analysis have been considered. To evaluate the seismic performance in terms of global pushover curve, inter-storey drift and response reduction factor have been determined for the considered building models. Nonlinear static or pushover analysis were conducted to assess the seismic behavior of the considered building models.

Equivalent static analysis instead of dynamic analysis is allowed in draft BNBC 2017 for open ground floor/soft storey building. However, for such case a magnification factor of 2.5 is required to determine the design shear and moment of structural elements located in such storey. An evaluation of the applicability of such special provision for the soft storey action provided in draft BNBC 2017 was also performed.

7.2 Conclusions of the study

The main conclusions of the study are summarized as follows:

- Open ground floor buildings were not always soft storey as these depend on limits of storey stiffness ratio recommends by draft BNBC 2017. Only 4 and 6-storied buildings with open ground floor resulted extreme soft storey action while the considered 10-storied were found as the regular one.

- Storey drifts of 4, 6 and 10-storied mass irregular frames were found 3.7%, 4.4% and 8.1%, respectively above the maximum allowable drift limit as per the Code.

- R value of 4, 6 and 10-storied bare frames and fully infilled frames were found 5.15, 5.67, 5.29 and 5.44, 5.16, 5.13, respectively. For the considered 4, 6 and 10-storied buildings with the open ground floor (OGF) frames were found 3.01, 3.94 and 3.42 which were 39.8%, 21.1% and 31.5%, respectively lesser than the considered R value. Hence, a drop of R value from the design value in OGF frames was observed due to the stiffness irregularity caused by the absence of the infill wall at the ground floor.

- Ratio of R values for 4, 6 and 10-storied bare frames to the open ground floor (OGF) frames were found 1.71, 1.44 and 1.55, respectively. Therefore, the obtained results show the requirement for the special design provision as per draft BNBC 2017 for a building with the open ground floor.

- R value of 4, 6 and 10-storied mass irregular frames were found as 2.31, 4.55 and 4.64, respectively while those of the regular frames were 5.15, 5.67 and 5.29, respectively. Therefore, R value in mass irregular frames was decreased in comparison to that of the regular one due to the presence of mass irregularity.

- R value of 4, 6 and 10-storied buildings with B1-upper type geometric irregular frames were found 39%, 6% and 26%, respectively lower than those of the regular frames. R values of 4, 6 and 10-storied buildings with B1-mid type geometric irregular frames were found 5%, 2% and 3% lower than those of the regular frames, respectively Therefore, lower R values in geometric irregular frames were shown due to the presence of vertical geometric irregularity.

7.3 Scope for future study

This work can be extended in future by including the following:

- Seismic response of vertically irregular structures due to stiffness irregularity, mass irregularity and geometric irregularity were assessed in this study. Seismic response of plan irregular RC structures having different types of vertical irregularities can be assessed.
- Dual frame structural system having different types of vertical irregularities can be considered to assess the seismic behavior.
- More acceleration time histories may be considered for dynamic analysis of the buildings with different plan dimensions and vertical irregularities.
- P-delta effect may be included in the building models to assess the seismic response.

REFERENCES

Abdul-Kadir, M. R., *The Structural Behavior of Masonry Infill Panels in Framed Structures,* Ph.D. thesis, University of Edinburgh, Edinburgh, 1974.

Al-Ali, A. A. K. and Krawinkler H., ''Effects of vertical irregularities on seismic behaviour of building structures,'' Report No. 130, The John A. Blume Earthquake Engineering Center, Stanford University, Stanford, California, 1998.

Al-Chaar G. K., Berman, J. B., and Sweeney, S. C., "Investigation of FRP for seismic rehabilitation of RC structural frames with URM infill," Report No. ERDC/CERL TR-03-10, US Army Corps of Engineers, 2003.

AlHamaydeh, M., Abdullah, S., Hamid, A., & Mustapha, A., "Seismic Design Factors for RC Special Moment Resisting Frames in Dubai", *Earthquake Engineering and Engineering Vibration,* UAE, vol. 10(4), pp. 495–506, 2011.

ASCE 41-13 *Seismic rehabilitation of existing buildings.* American Society of Civil Engineers, Reston, VA, USA, 2013.

Athanassiadou C., "Seismic Performance of R/C Plane Fames Irregular in Elevation," *Engineering Structures*, vol. 30(5), pp. 1250-1261, 2008.

ATC-19 (1995) *Structural response modification factors.* Applied Technology Council, Redwood City, California, USA, pp. 5–32.

BNBC 2006: Bangladesh National Building Code- 2006, Housing and Building Research Institute (HBRI), Dhaka, Bangladesh.

BNBC 2017: Bangladesh National Building Code- 2017 (draft), Housing and Building Research Institute (HBRI), Dhaka, Bangladesh.

Buonopane S. G. and White R. N., "Seismic Evaluation of a Masonry Infilled Reinforced Concrete Frame by Pseudo Dynamic Testing," *Journal of Structural Engineering*, vol. 125(6), pp. 578–589, 1999.

Chaulagain, H., Rodrigues, H., Spacone, E., Guragain, R., Mallik, R., and Varun, H. "Response Reduction Factor of Irregular RC Buildings in Kathmandu Valley" *Earthquake Engineering and Engineering Vibration*, vol. 13(3), pp. 455-470, 2014.

Das S. and Nau J.M., "Seismic Design Aspects of Vertically Irregular Reinforced Concrete Buildings", *Earthquake Spectra,* vol. 19(3), pp. 455-477, 2003.

Davis R., Menon D. and Prasad A. M., "Evaluation of magnification factors for open ground storey buildings using nonlinear analyses," *The 14th World Conference on Earthquake Engineering*, Beijing, China, 2008.

Dolsek M. and Fajfar, P., "Simplified Non-linear Seismic Analysis of Infilled Reinforced Concrete Frames", *Earthquake Engineering Structural Dynamics*, vol. 34, pp. 49–66, 2005.

Durrani A.J. and Luo, Y.H., "Seismic retrofit of flat-slab buildings with masonry infills" *Technical Report*, *NCEER workshop on seismic response on masonry infills,* Buffalo, NY, pp. 1–8, 1994.

ETABS 16.2.0 [Computer software]. Computers and Structures, Inc., Berkeley, CA.

Eurocode 8 (2004): Design of structures for earthquake resistance. Part 1: General rules, seismic actions and rules for buildings. Brussels, CEN, EN1998-1.

FEMA 306 (1998): Evaluation of earthquake damaged concrete and masonry wall buildings. Basic Procedures Manual, Federal Emergency Management Agency, Washington, DC, USA.

FEMA 356 (2000): Pre-standard and Commentary for the Seismic Rehabilitation of Buildings", Federal Emergency Management Agency, Washington, D.C. USA. (2000).

Fiorato, A. E., Sözen, M. A., and Gamble, W. L. "An investigation of the interaction of reinforced concrete frames with masonry filler walls," *(UILU-ENG-70-100)* Department of Civil Engineering*,* University of Illinois at Urbana–Champaign, 1970.

Giardini D., Grunthal G., Shedlock K. M. and Zhang P., "The GSHAP Global Seismic Hazard Map," *Annals of Geophysics,* Vol. 42. No. 6, pp. 1225-1230 (1999).

Hashemi A, Mosalam K., "Shake-table Experiment on Reinforced Concrete Structure containing Masonry Infill Wall," *Earthquake Engineering and Structural Dynamics,* vol. 35, pp. 1827–1852, 2006.

Hanafy A.H., Darwish M., Baraka M., "Egyptian code seismic load design provisions for moment resisting frames," *Proceedings of the 1st GeoMEast International Congress and Exhibition on Sustainable Civil Infrastructures,* Egypt, pp. 94–103, 2017.

Kappos A. J., "Evaluation of Behavior Factors on the Basis of Ductility and Overstrength Studies," *Engineering Structures*, vol. 21, pp. 823-835, 1999.

Kappos A. J., Stylianidis K. C. and Michaildis C. N., "Analytical Models for Brick Masonry Infilled R/C Frames Under Lateral Loading," *Journal of Earthquake Engineering*, vol. 2(1), pp. 59-87, 1998.

Kareem K.M. and Güneyisi E.M., "Effect of Masonry Infill Wall Configuration and Modelling Approach on the Behaviour of RC Frame Structures," *Arabian Journal for Science and Engineering,* Vol. 44, pp. 4309–4324, 2019.

Karemore A. and Rayadu S., "Study on Effect of Zone on Magnification Factor for Open Ground Storey Buildings", *International Journal of Innovative and Emerging Research in Engineering,* Vol. 02(5), pp. 58-65, 2015.

Kaushik H.B., Rai D.C. and Jain S.K., "Stress-Strain Characteristics of Clay Brick Masonry under Uniaxial Compression," *Journal of Material Civil Engineering,* ASCE Vol. 19(9), pp. 728–739, 2007.

Kim, J. and Choi, H., "Response Modification Factors of Chevron-Braced Frames," *Journal of Engineering Structures*, vol. 27, pp. 285-300, 2005.

Klingner R. E. and Bertero V. V., "Earthquake Resistance of Infilled Frames," *Journal of the Structural Division*, vol. 104(6), pp. 973–989, 1978.

Lee, D.G., Cho, S.H., and Ko H., "Response Modification Factors For Seismic Design of Building Structures in Low Seismicity Regions," *Korea Earthquake Engineering Research Centre*, 2005.

Landi L., Conti F., Diotallevi P.P., "Effectiveness of Different Distributions of Viscous Damping Coefficients for the Seismic Retrofit of Regular and Irregular RC Frames," *Engineering Structures*, vol. 100, pp. 79–93, 2015.

Lourenço, P.B., *Computational strategies for masonry structures,* Doctoral dissertation, Delft University, Delft, The Netherlands, 1996.

Mainstone, R.J. and Weeks, G.A., “The influence of bounding frame on the racking stiffness and strength of brick walls,” *In: Proceedings of the 2nd International Brick Masonry Conference*, Building Research Establishment, Watford, England, pp. 165–171, 1970.

Massumi A., Tasnimi A.A., Saatcioglu M., “Prediction of seismic overstrength in concrete moment resisting frames using incremental static and dynamic analyses,” *In: 13th world conference on earthquake engineering, conference proceedings*, Vancouver, British Columbia, Canada, pp. 1–6, 2004.

Mitchell, D. and Paultre, P., “Ductility and Overstrength in Seismic Design of Reinforced Concrete Structures,” *Canadian Journal of Civil Engineering*, vol. 21, pp. 1049-1060, 1994.

Miranda E., and Bertero V.V., “Evaluation of Strength Reduction Factors,” *Earthquake Spectra*, Earthquake Engineering Research Institute, vol. 10(2), pp. 357-379, 1994.

Misra P. and Jaisal S.K., “Effect of Magnification Factor in Column and Beam in Open Ground Storey Building”, *International Journal for Scientific Research & Development*, Vol. 5(03), pp. 557-567, 2017.

Moghaddam, H. A., and Dowling, P. J., “The state of the art in infilled frames”, Civil Engineering Department, Imperial College, London. ESEE Research Rep. No 87-2, 1987.

Mosalam, K. M., White, R. N., and Gergely, P., “Static Response of Infilled Frames using Quasi-static Experimentation”, *Journal of Structural Engineering,* ASCE, vol. 123, pp. 1462–1469, 1997.

Murty, C. V. R. and Jain, S. K. “Beneficial influence of masonry infills on seismic performance of RC frame buildings”, *Proceedings, 12th World Conference on Earthquake Engineering,* Auckland, New Zeland, 2000.

Muto K, “A seismic design analysis of buildings”, Maruzen Company, Ltd, Tokyo, pp. 241–260, 1974.

Mwafy, A.M., “Use of Overstrength and Inelastic Response in Seismic Design,” *Structures and Buildings Journal*, the Institution of Civil Engineers, In Press (published online), 2013.

Nassar, A. A. and Krawinkler, H., ‘‘Seismic based design on ductility and cumulative damage demands and capacities.’’ *Workshop on Nonlinear Seismic Analysis of Reinforced Concrete Buildings*, Yugoslavia, 1992.

National Earthquake Hazards Reduction Program (NEHRP): “Recommended Provisions for Seismic Regulations for New Buildings and other Structures”, Building Seismic Safety Council, Washington, D.C. (2000) Edition, Part 2: Commentary,

Newmark N. M., Hall, W. J., “Earthquake spectra and design”, Earthquake Engineering Research Institute, Berkeley, California, 1982.

Osteraas, J. D., and Krawinkler, H. ‘‘Strength and ductility considerations in seismic design,’’ Rep. 90, John A. Blume Earthquake Engineering. Ctr., Stanford University, Stanford, California, 1990.

Panagiotakos, T. B. and Fardis, M. N., “Seismic response of infilled RC frames structures”, *International 11th World Conference on Earthquake Engineering,* Acapulco, Mexico, 1996.

Paulay T. and Priestley M. J. N. (1992) *Seismic design of reinforced concrete and masonry buildings*. Wiley, New York.

Polyakov, S.V. “On the Interaction Between Masonry Filler Walls and Enclosing Frame when Loading in the Plane of the Wall,” Earthquake Engineering Research Institute (EERI), San Francisco, 1960.

Penavaa D., Sarhosisb V., Kožarc I. and Guljaša I., “Contribution of RC Columns and Masonry Wall to the Shear Resistance of Masonry Infilled RC Frames Containing Different in Size Window and Door Openings,” *Engineering Structures,* vol. 172, pp. 105-130, 2018.

Sadashiva V.K., *Quantifying structural irregularity effects for simple seismic design,* PhD thesis, Department of Civil and Natural Resources Engineering, University of Canterbury, New Zealand, 2010.

Sachanski S. K., “Analysis of earthquake resistance of frame buildings taking into consideration the capacity of filling masonry” *Proceeding of II World Conf. on*

Earthquake Engineering, Japan, pp. 2127-2176, 1960.

Sezen H., Whittaker A.S., Elwood K.J., Mosalam K.M., "Performance of Reinforced Concrete Buildings during the August17, 1999 Kocaeli, Turkey Earthquake and Seismic Design and Construction Practice in Turkey," *Engineering Structures*, vol. 25, pp. 103–114, 2003.

Shahrooz, B. M. and Moehle, J. P., "Seismic Response and Design of Setback Buildings," *Journal of Structural Engineering*, vol. 116 (5), pp. 1423-39, 1990.

Sharifi S., and Toopchi-Nezhad H., "Seismic Response Modification Factor of RC-Frame Structures Based on Limit State Design," *International Journal of Civil Engineering*, Vol. 16, pp. 1185-1200, 2018.

Smith, B. S. and Carter, C. "A Method of Analysis for Infilled Frames," *Proceedings of the Institution of Civil Engineers*, vol. 44(1), pp. 31-48, 1969.

Stavridis A., Koutromanos I., and Shing P.B., "Shake-table Tests of a Three-story Reinforced Concrete Frame with Masonry Infill Walls", *Earthquake Engineering & Structural Dynamics,* vol. 41, pp. 1089–1108, 2012.

Uva, G., Porco, F. and Fiore, A., "Appraisal of Masonry Infill Walls Effect in the Seismic Response of RC Framed Buildings: A Case Study," *Engineering Structures*, vol. 34, pp. 514-526, 2012.

Valmundsson, E. V. and Nau, J. M., "Seismic Response of Building Frames with Vertical Structural Irregularities," *Journal of Structural Engineering*, vol. 123(1), pp. 30-41, 1997.

Varadharajan, S., Sehgal, V., and Saini, B., "Seismic Behavior of Multistory RC Building Frames with Vertical Setback Irregularity", *The Structural Design of Tall and Special Buildings*, vol. 23 (18), pp. 1345-1380, 2013.

Vijayanarayanan, A. R., Goswami, R, and Murty, C. V. R., "Estimation of storey stiffness in multi-storey buildings," *16th World Conference on Earthquake*, Santiago, Chile, 2017.

Wong, C. M. and Tso, W. K., "Seismic Loading for Buildings with Setbacks," *Canadian Journal of Civil Engineering*, vol. 21(5), pp. 863-871, 1994.

Yadab A. and Mishra A. K., "Earthquake Resistant Design of Open Ground Storey Low Rise Building," *International Journal of Science Technology and Management*, Vol. 6, No. 5, pp. 557-567, 2017.

APPENDICES

Appendix A-1: Lateral storey stiffness and stiffness ratio

Table A.1.1: Storey stiffness and stiffness ratio of different types of 6-storied buildings

Frame	Floor	Lateral Storey stiffness (K), kN/m	Stiffness ratio, (K_i / K_{i+1})	Remarks
Bare Frame	ROOF	91806		
	4th Floor	120934	1.32	Regular
	3rd Floor	124481	1.03	Regular
	2nd Floor	126806	1.02	Regular
	1st Floor	135427	1.07	Regular
	Ground Floor	183429	1.35	Regular
Fully Infilled Frame	ROOF	620163		
	4th Floor	754960	1.22	Regular
	3rd Floor	778258	1.03	Regular
	2nd Floor	793825	1.02	Regular
	1st Floor	802442	1.01	Regular
	Ground Floor	868623	1.08	Regular
OGF frame	ROOF	620092		
	4th Floor	754785	1.22	Regular
	3rd Floor	777464	1.03	Regular
	2nd Floor	806465	1.04	Regular
	1st Floor	636818	0.79	Regular
	Ground Floor	302156	0.47	Extreme soft storey

Table A.1.2: Storey stiffness and stiffness ratio of different types of 10-storied buildings

Frame	Floor	Lateral Storey stiffness (K), kN/m	Stiffness ratio, (K_i / K_{i+1})	Remarks
Bare Frame	ROOF	78340		
	8th Floor	121725	1.55	Regular
	7th Floor	131570	1.08	Regular
	6th Floor	133978	1.02	Regular
	5th Floor	134787	1.01	Regular
	4th Floor	135615	1.01	Regular
	3rd Floor	137496	1.01	Regular
	2nd Floor	142426	1.04	Regular
	1st Floor	155737	1.09	Regular
	Ground Floor	229735	1.48	Regular
Fully Infilled Frame	ROOF	465767		
	8th Floor	687494	1.48	Regular
	7th Floor	746608	1.09	Regular
	6th Floor	777444	1.04	Regular
	5th Floor	798117	1.03	Regular
	4th Floor	813801	1.02	Regular
	3rd Floor	828353	1.02	Regular
	2nd Floor	842680	1.02	Regular
	1st Floor	860965	1.02	Regular
	Ground Floor	1033386	1.20	Regular
OGF frame	ROOF	465231		
	8th Floor	687266	1.48	Regular
	7th Floor	746587	1.09	Regular
	6th Floor	777326	1.04	Regular
	5th Floor	797727	1.03	Regular
	4th Floor	813776	1.02	Regular
	3rd Floor	828069	1.02	Regular
	2nd Floor	837007	1.01	Regular
	1st Floor	699199	0.84	Regular
	Ground Floor	491998	0.70	Regular

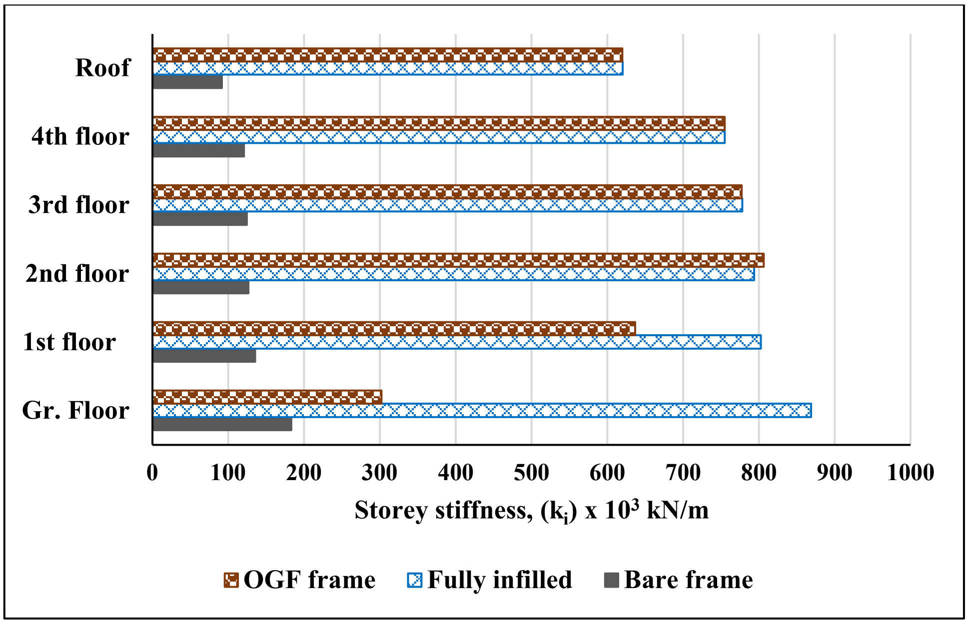

Figure A.1.1: Storey stiffness of each floor for different types of 6-storied buildings

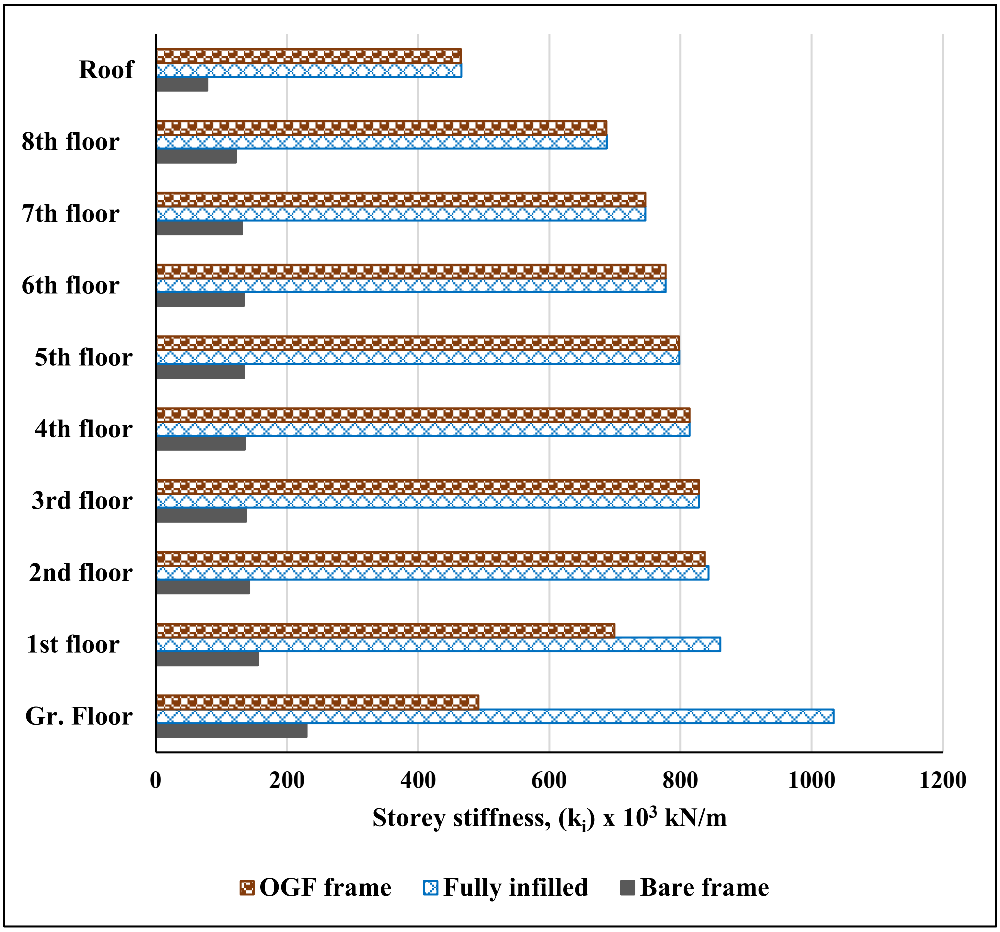

Figure A.1.2: Storey stiffness of each floor for different types of 10-storied buildings

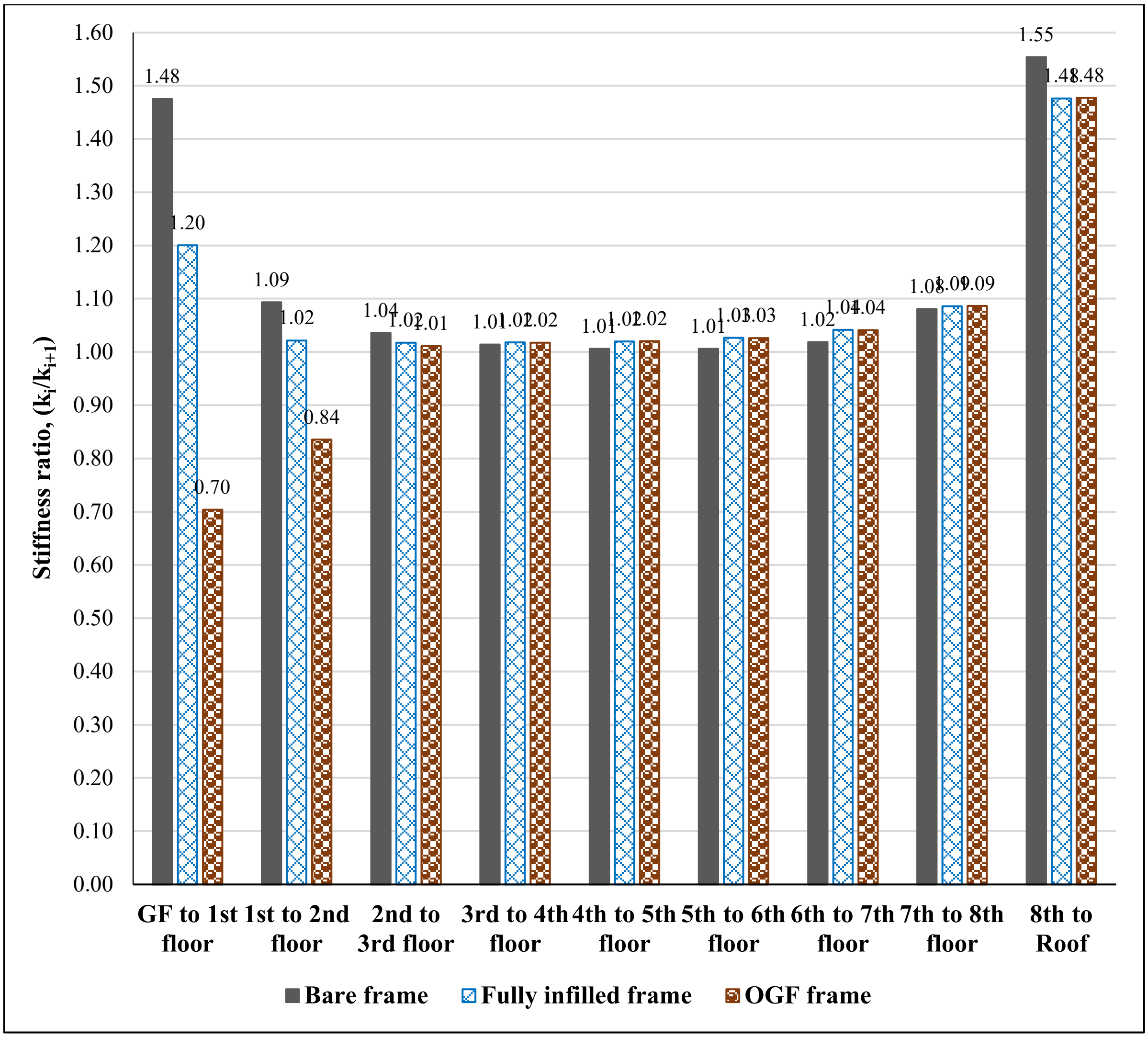

Figure A.1.3: Storey stiffness ratio of different floors for 10-storied buildings

Appendix A-2: Storey drifts of different frames

Table A.2.1 and A.2.2 and Figure A.2.1 and A.2.2 show storey drift 6 and 10-storied bare frames, fully infilled frames and OGF frames.

Table A.2.1: Storey drift 6-storied bare frames, fully infilled frames and OGF frames

Frame	Floor Level	h_{sx} (mm)	δ_{xe} (mm)	$\delta_x = \frac{C_d \delta_{xe}}{I}$ (mm)	$\Delta = \delta_x - \delta_{x-1}$ (mm)	$\Delta_a = .02h_{sx}$ (mm)	Remarks
Bare Frame	ROOF	3000	53.1	238.8	17.30	60	ok
	4th Floor	3000	49.2	221.5	30.25	60	ok
	3rd Floor	3000	42.5	191.3	42.63	60	ok
	2nd Floor	3000	33.0	148.6	51.53	60	ok
	1st Floor	3000	21.6	97.1	53.95	60	ok
	Ground	3000	9.6	43.2	40.01	60	ok
Fully Infilled Frame	ROOF	3000	9.4	42.4	2.6	60	ok
	4th Floor	3000	8.8	39.8	4.9	60	ok
	3rd Floor	3000	7.8	34.9	6.9	60	ok
	2nd Floor	3000	6.2	28.1	8.3	60	ok
	1st Floor	3000	4.4	19.7	9.3	60	ok
	Ground	3000	2.3	10.4	9.0	60	ok
OGF Frame	ROOF	3000	14.0	62.9	2.6	60	ok
	4th Floor	3000	13.4	60.4	4.9	60	ok
	3rd Floor	3000	12.3	55.5	6.9	60	ok
	2nd Floor	3000	10.8	48.6	8.2	60	ok
	1st Floor	3000	9.0	40.4	11.7	60	ok
	Ground	3000	6.4	28.7	26.1	60	ok

Table A.2.2: Storey drift of 10-storied bare, fully infilled frames and OGF frames

Frame	Floor Level	h_{sx} (mm)	δ_{xe} (mm)	$\delta_x = \frac{C_d \delta_{xe}}{I}$ (mm)	$\Delta = \delta_x - \delta_{x-1}$ (mm)	$\Delta_a = .02h_{sx}$ (mm)	Remarks
Bare Frame	ROOF	3000	94.8	426.6	15.5	60	ok
	8th Floor	3000	91.4	411.1	23.9	60	ok
	7th Floor	3000	86.1	387.2	33.2	60	ok
	6th Floor	3000	78.7	354.0	41.9	60	ok
	5th Floor	3000	69.3	312.1	49.3	60	ok
	4th Floor	3000	58.4	262.7	55.1	60	ok
	3rd Floor	3000	46.1	207.6	58.7	60	ok
	2nd Floor	3000	33.1	148.9	59.1	60	ok
	1st Floor	3000	20.0	89.8	53.4	60	ok
	Ground	3000	8.1	36.5	33.9	60	ok
Fully Infilled Frame	ROOF	3000	17.5	78.6	2.6	60	ok
	8th Floor	3000	16.9	75.9	4.3	60	ok
	7th Floor	3000	15.9	71.7	5.9	60	ok
	6th Floor	3000	14.6	65.8	7.3	60	ok
	5th Floor	3000	13.0	58.5	8.4	60	ok
	4th Floor	3000	11.1	50.0	9.3	60	ok
	3rd Floor	3000	9.1	40.7	10.0	60	ok
	2nd Floor	3000	6.8	30.8	10.4	60	ok
	1st Floor	3000	4.5	20.4	10.5	60	ok
	Ground	3000	2.2	9.9	8.8	60	ok
OGF Frame	ROOF	3000	20.3	91.4	2.6	60	ok
	8th Floor	3000	19.7	88.8	4.3	60	ok
	7th Floor	3000	18.8	84.5	5.9	60	ok
	6th Floor	3000	17.5	78.6	7.3	60	ok
	5th Floor	3000	15.9	71.3	8.4	60	ok
	4th Floor	3000	14.0	62.9	9.3	60	ok
	3rd Floor	3000	11.9	53.6	10.0	60	ok
	2nd Floor	3000	9.7	43.6	10.4	60	ok
	1st Floor	3000	7.4	33.2	12.9	60	ok
	Ground	3000	4.5	20.3	18.5	60	ok

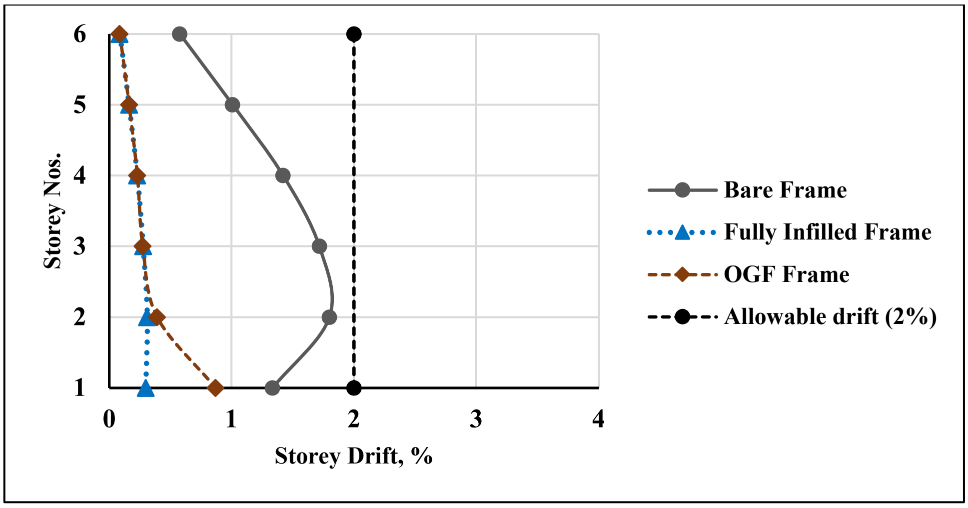

Figure A.2.1: Storey drifts of different types of 6-storied buildings

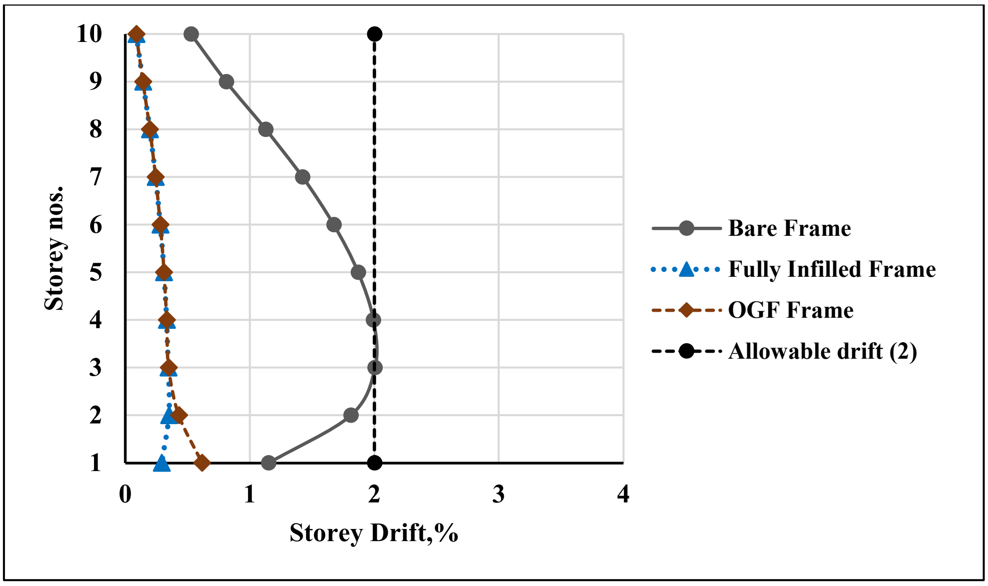

Figure A.2.2: Storey drifts of different types of 10-storied buildings

Appendix A-3: Modal participating mass factors (%) of different frames

Table A.3.1 and A.3.2 show modal participating mass factors (%) of 6 and 10-storied bare frames, fully infilled frames and OGF frames.

Table A.3.1: Modal participating mass factors (%) of different types of 6-storied buildings

Mode	Bare Frame		Fully Infilled Frame		OGF Frame	
	UX	UY	UX	UY	UX	UY
1	75%	2%	40%	40%	46%	46%
2	77%	77%	81%	81%	92%	92%
3	77%	77%	81%	81%	92%	92%
4	87%	77%	85%	85%	94%	94%
5	87%	87%	90%	90%	96%	96%
6	87%	87%	90%	90%	96%	96%
7	91%	87%	91%	91%	97%	97%
8	91%	91%	93%	93%	97%	97%
9	91%	91%	93%	93%	97%	97%
10	92%	92%	93%	93%	97%	97%

Table A.3.2: Modal participating mass factors (%) of different types of 10-storied buildings

Mode	Bare Frame		Fully Infilled Frame		OGF Frame	
	UX	UY	UX	UY	UX	UY
1	76%	1%	40%	40%	44%	44%
2	77%	77%	79%	79%	87%	87%
3	77%	77%	79%	79%	87%	87%
4	86%	77%	84%	84%	91%	91%
5	86%	86%	89%	89%	95%	95%
6	86%	86%	89%	89%	95%	95%
7	90%	86%	91%	91%	96%	96%
8	91%	91%	93%	93%	97%	97%
9	91%	91%	93%	93%	97%	97%
10	93%	91%	93%	93%	97%	97%

Appendix A.4: Top displacement for 4, 6 and 10-storied buildings by TH analysis

Figure A.4.1 to A.4.3 show top displacement of different 6-storied buildings for Kobe (1995) earthquake by TH analysis. Figure A.4.4 to A.4.9 shows the comparison of top displacement among different types of 6 and 10- storied buildings.

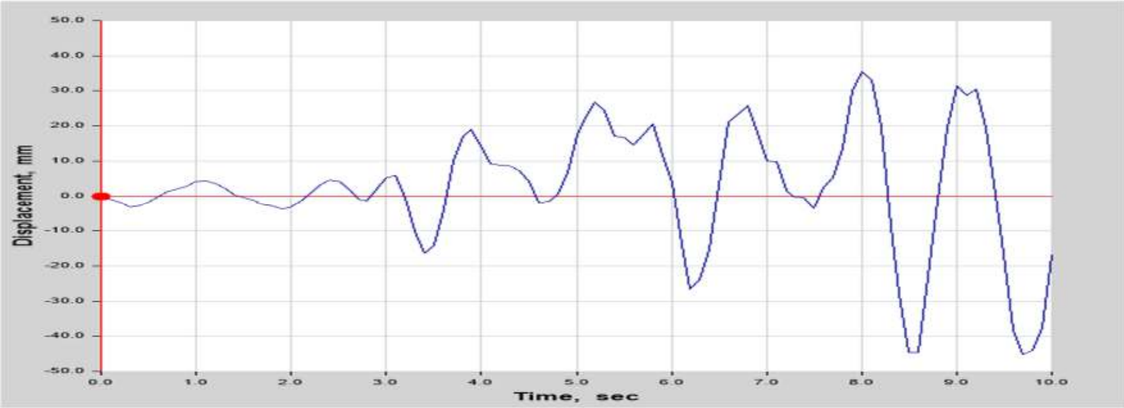

Figure A.4.1: Top displacement for Kobe (1995) earthquake of 6- storied bare frame

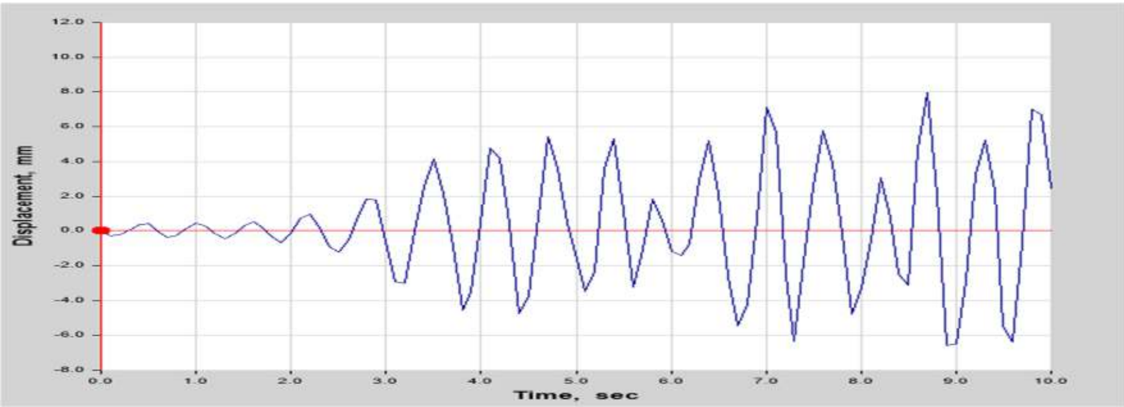

Figure A.4.2: Top displacement for Kobe (1995) earthquake of 6-storied fully infilled frame

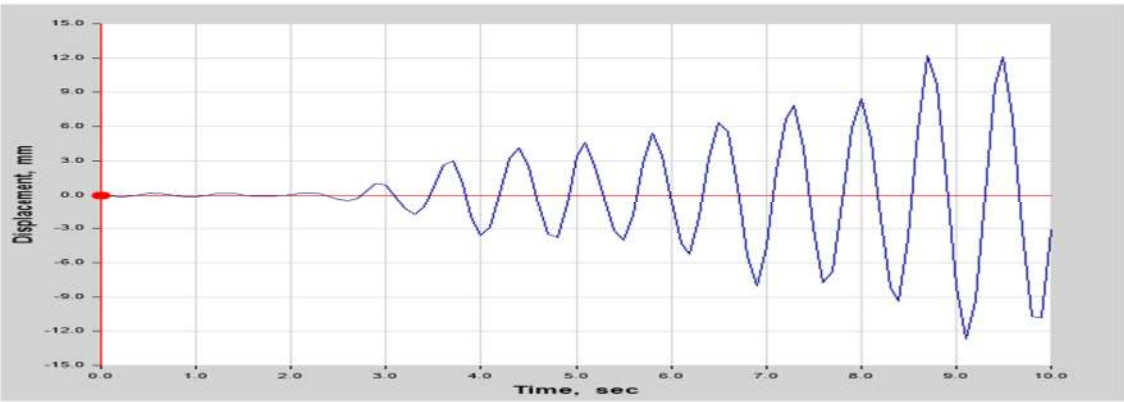

Figure A.4.3: Top displacement for Kobe (1995) earthquake of 6 storied OGF frame

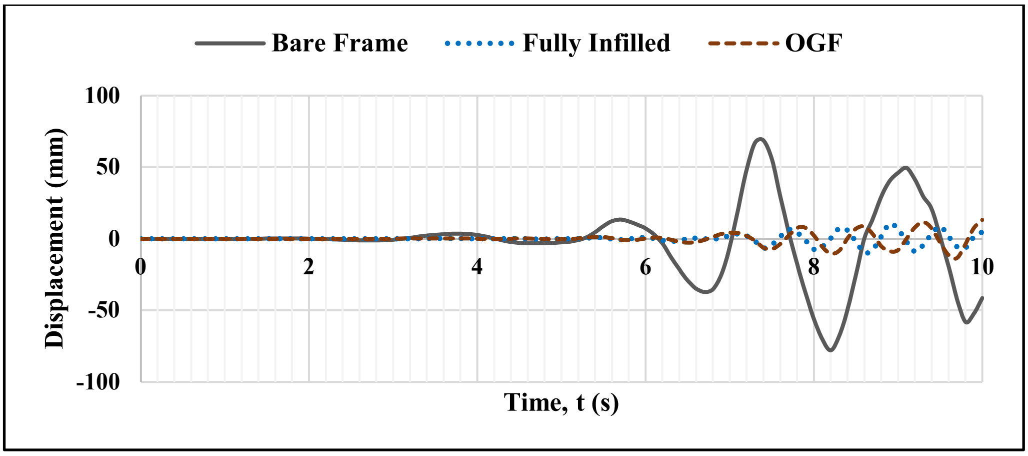

Figure A.4.4: Comparison of Top displacement profile of 6-storied buildings under El Centro (1940) earthquake

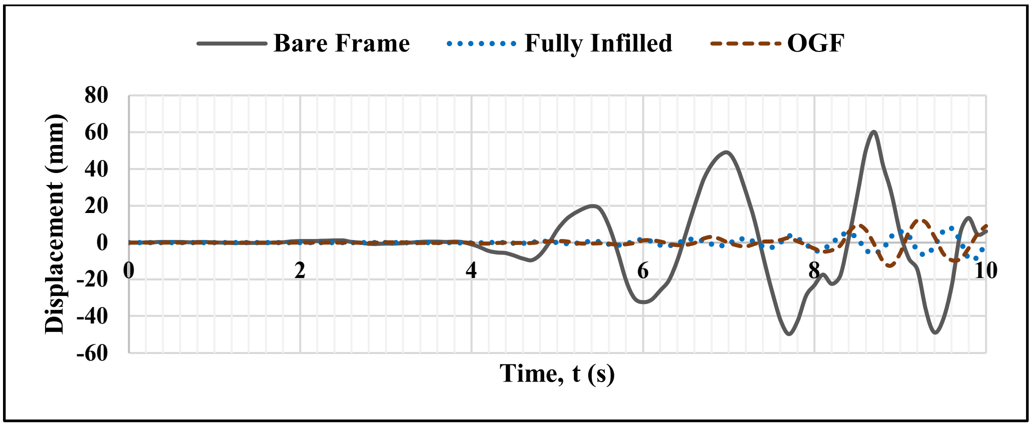

Figure A.4.5: Comparison of Top displacement profile of 6-storied buildings under Imperial Valley (1979) earthquake

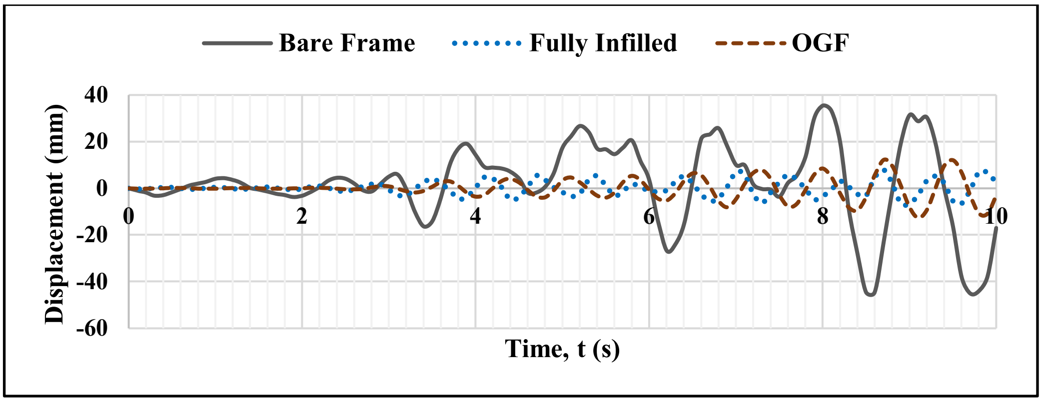

Figure A.4.6: Comparison of Top displacement profile of 6-storied buildings under Kobe (1995) earthquake

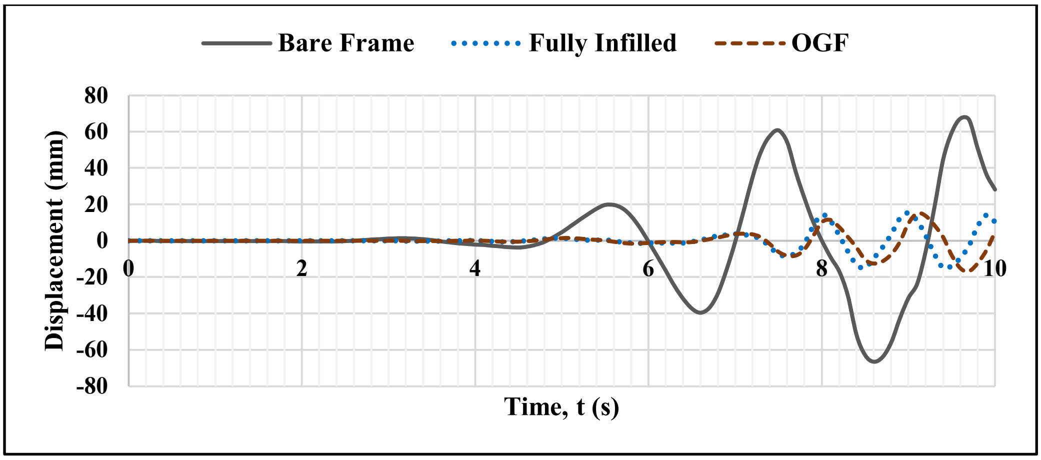

Figure A.4.7: Comparison of Top displacement profile of 10-storied buildings under El Centro (1940) earthquake

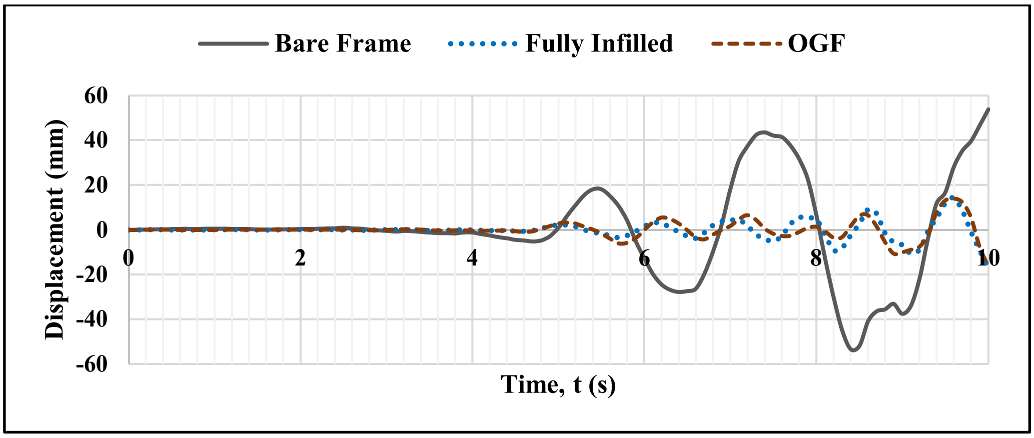

Figure A.4.8: Comparison of Top displacement profile of 10-storied buildings under Imperial Valley (1979) earthquake

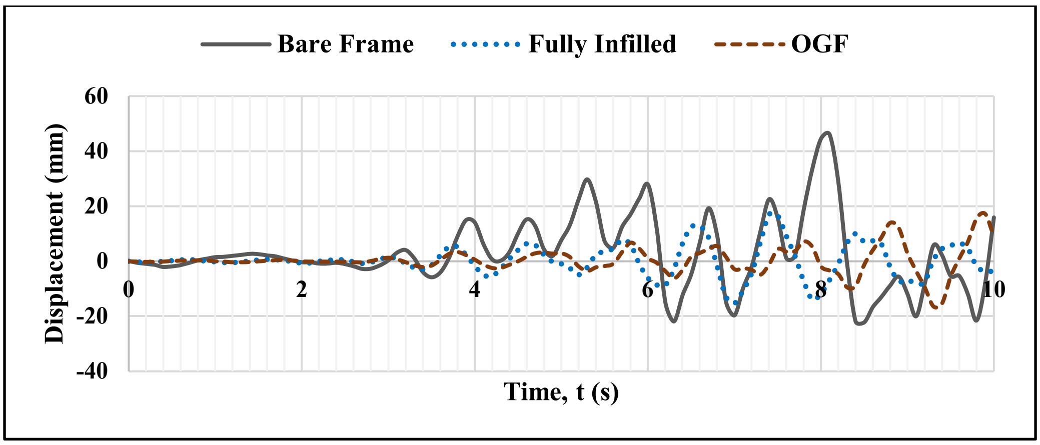

Figure A.4.9: Comparison of Top displacement profile of 10-storied buildings under Kobe (1995) earthquake

Appendix A-5: Storey shear of different frames

Figure A.5.1 and A.5.2 show storey shear of 6 and 10-storied bare frames, fully infilled frames and OGF frames by different seismic analyses methods.

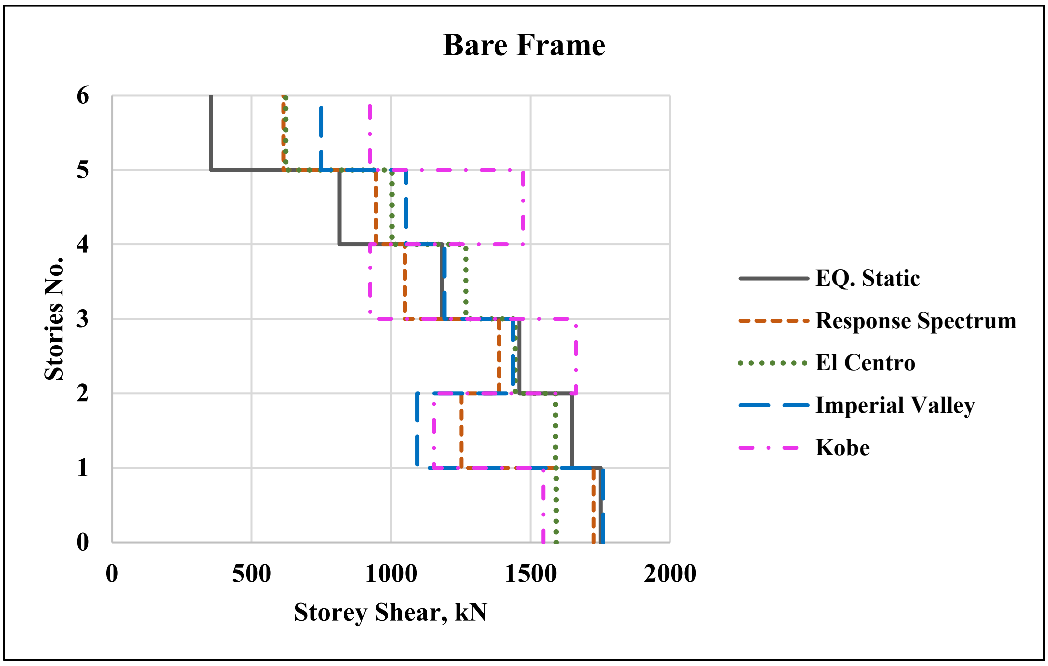

Figure A.5.1: Comparison of storey shears for 6-storied bare frames

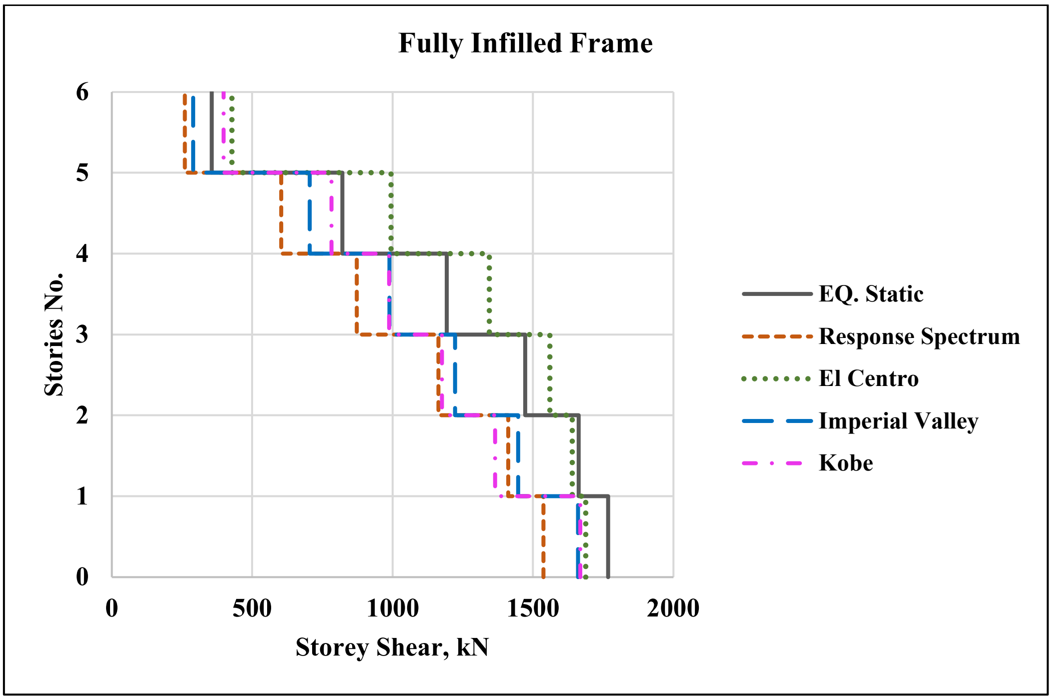

Figure A.5.2: Comparison of storey shears for 6-storied fully infilled frames

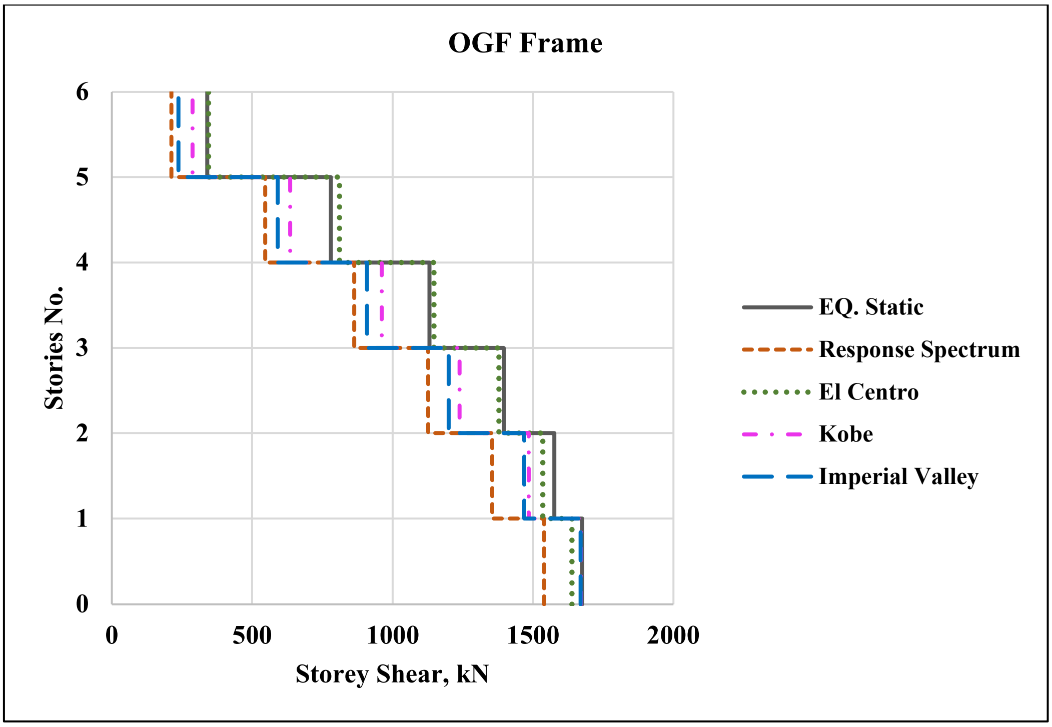

Figure A.5.3: Comparison of storey shears of 6-storied OGF frames

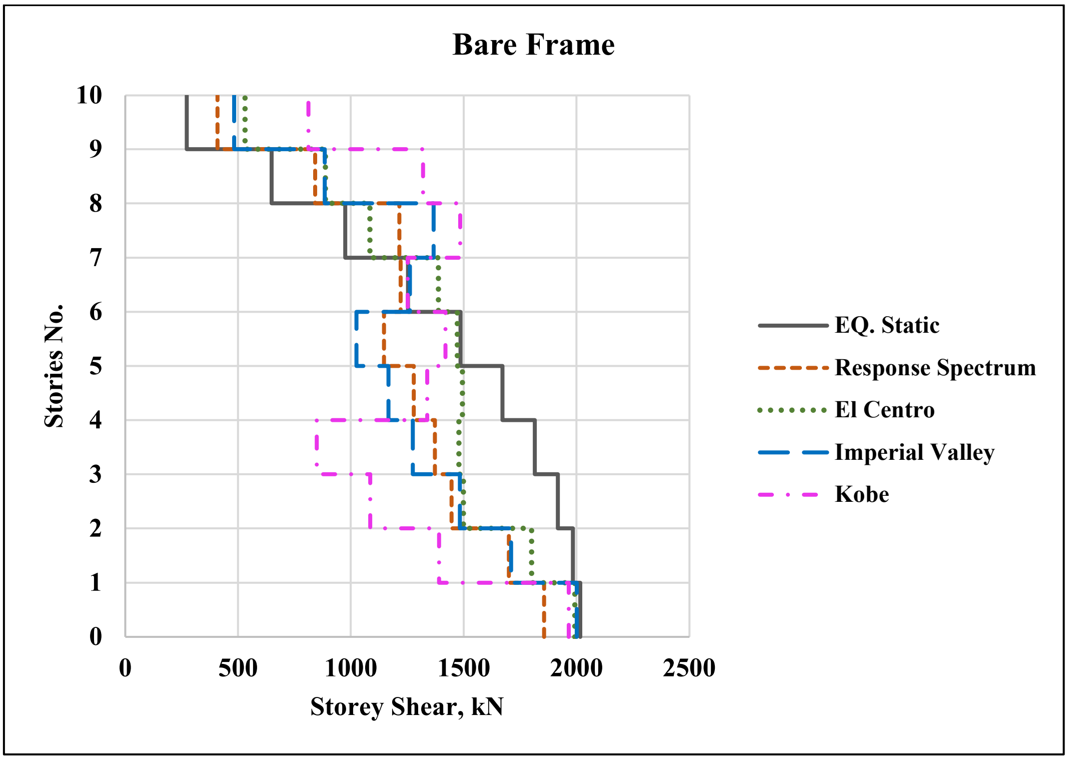

Figure A.5.4: Comparison of storey shears of 10-storied bare frames

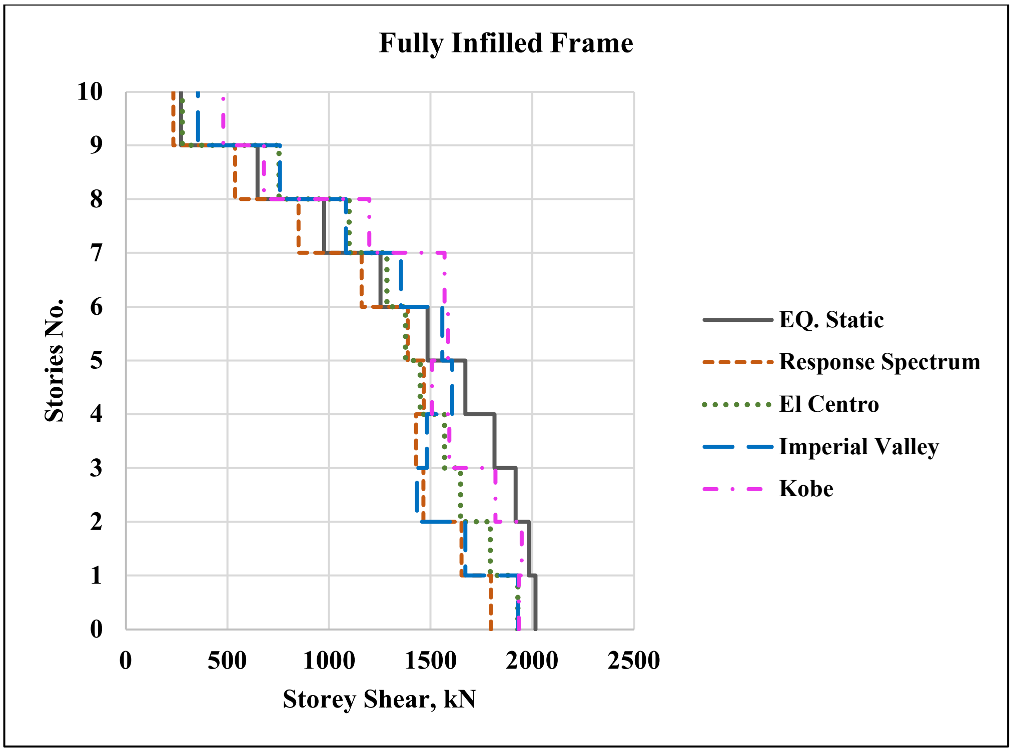

Figure A.5.5: Comparison of storey shears of 10-storied fully infilled frames

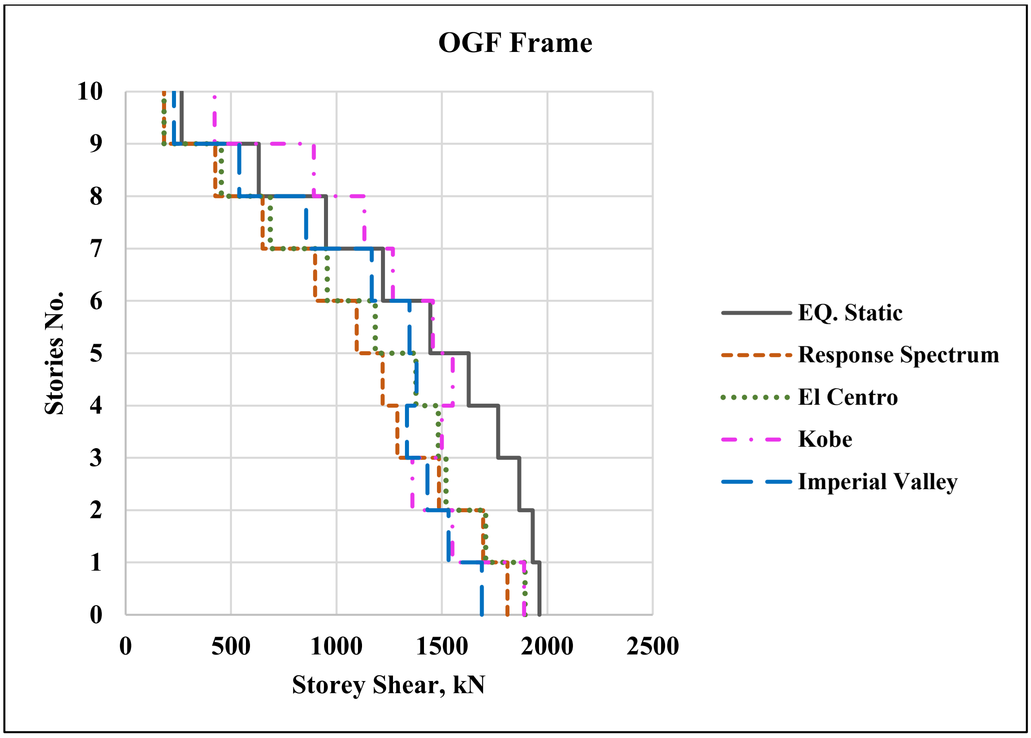

Figure A.5.6: Comparison of storey shears for 10-storied OGF frames

Appendix B-1: Storey masses and mass ratios of regular and mass irregular frames.

Table B.1.1 and B.1.2 show storey masses and mass ratios of 6 and 10-storied regular and mass irregular frames.

Table B.1.1: Storey masses of 6-storied regular and mass irregular frames

Floors	Regular frame		Frames with mass irregularity	
	Storey mass, kg	M_i / M_{i+1}	Storey mass, kg	M_i / M_{i+1}
ROOF	272461		272461	
4th Floor	424628	1.56	424628	1.6
3rd Floor	424628	1	424628	1.0
2nd Floor	424628	1	832515	2.0
1st Floor	424628	1	424628	0.5
Ground Floor	424628	1	424628	1.0

Table B.1.2: Storey masses of 10-storied regular and mass irregular frames.

Floors	Regular frame		Frames with mass irregularity	
	Storey mass, kg	M_i / M_{i+1}	Storey mass, kg	M_i / M_{i+1}
ROOF	280317		280317	
8th Floor	441662	1.58	441662	1.6
7th Floor	441662	1.00	441662	1.0
6th Floor	441662	1.00	441662	1.0
5th Floor	441662	1.00	441662	1.0
4th Floor	441662	1.00	869942	2.0
3rd Floor	441662	1.00	441662	0.5
2nd Floor	441662	1.00	441662	1.0
1st Floor	441662	1.00	441662	1.0
Ground Floor	441662	1.00	441662	1.0

Appendix B-2: Storey shear of regular and mass irregular frames.

Figure B.2.1 and B.2.2 show storey shear of 6 and 10-storied regular and mass irregular frames.

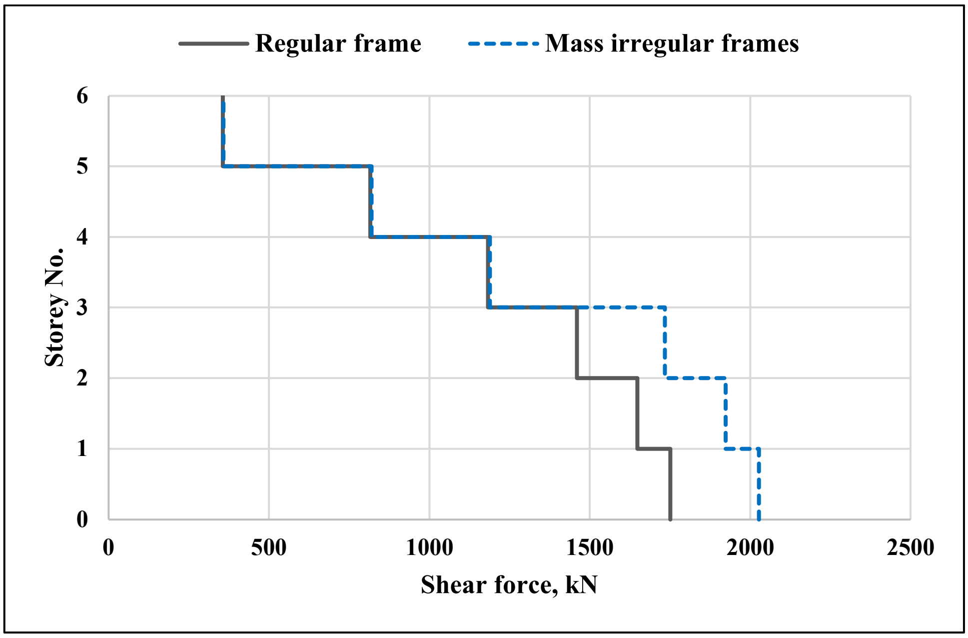

Figure B.2.1: Storey shear force of 6-storied regular and mass irregular frames

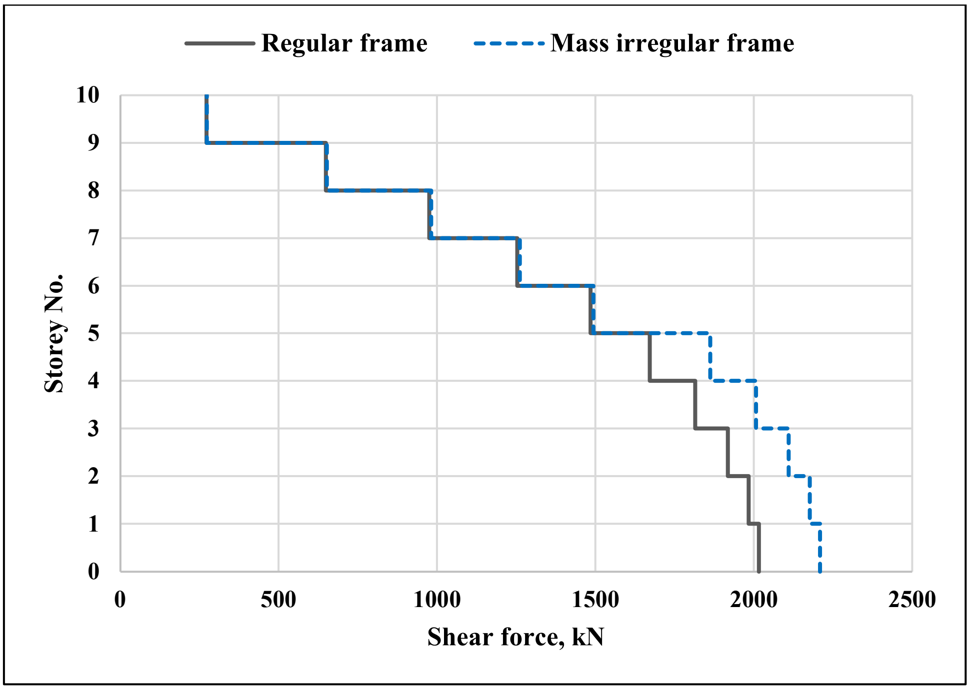

Figure B.2.2: Storey shear force of 10-storied regular and mass irregular frames

Appendix B-3: Storey drifts of regular and mass irregular frames

Figure B.3.1 and B.3.2 show storey drifts of different floors of 6 and 10-storied regular and mass irregular frames.

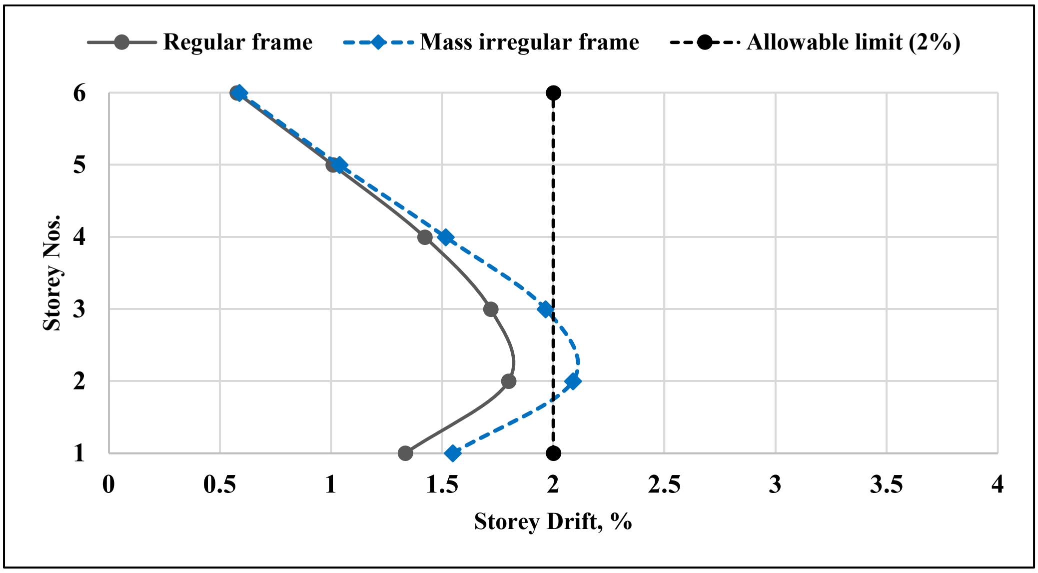

Figure B.3.1: Storey drifts of 6-storied regular and mass irregular frame.

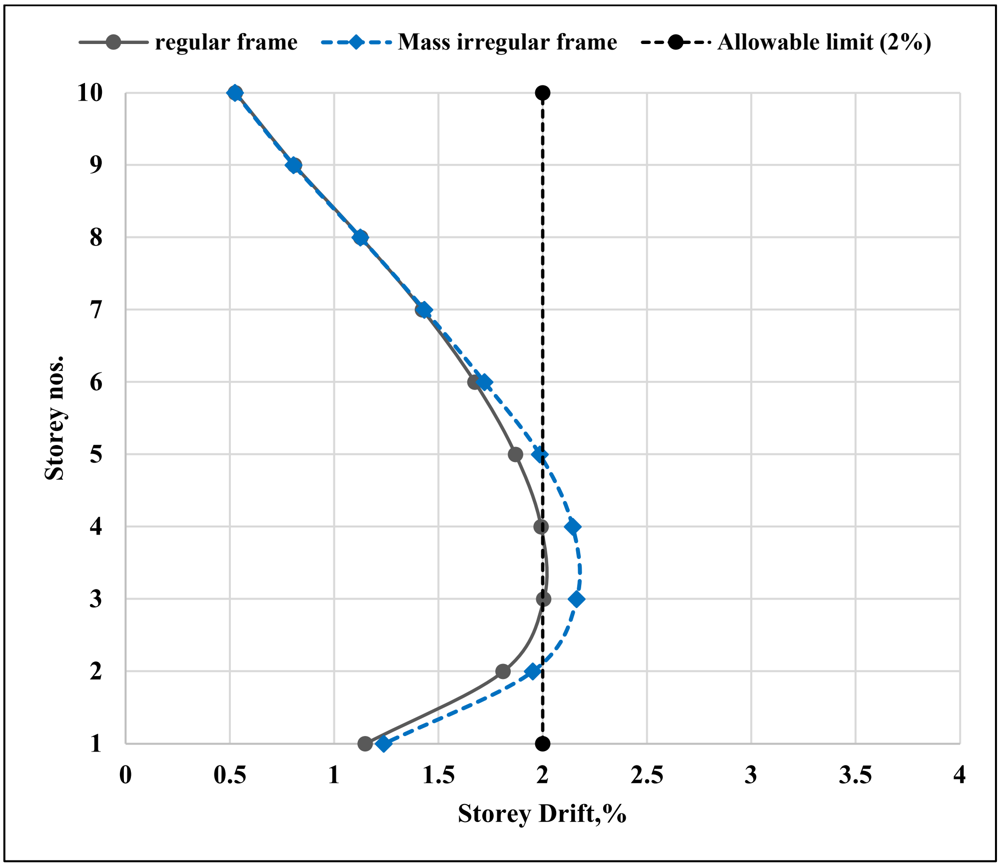

Figure B.3.2: Storey drifts of 10-storied regular and mass irregular frame.

Appendix B-4: Pushover curves of regular and mass irregular frames

Figure B.4.1 and B.4.2 show pushover curves of 4 and 10-storied regular and mass irregular frames.

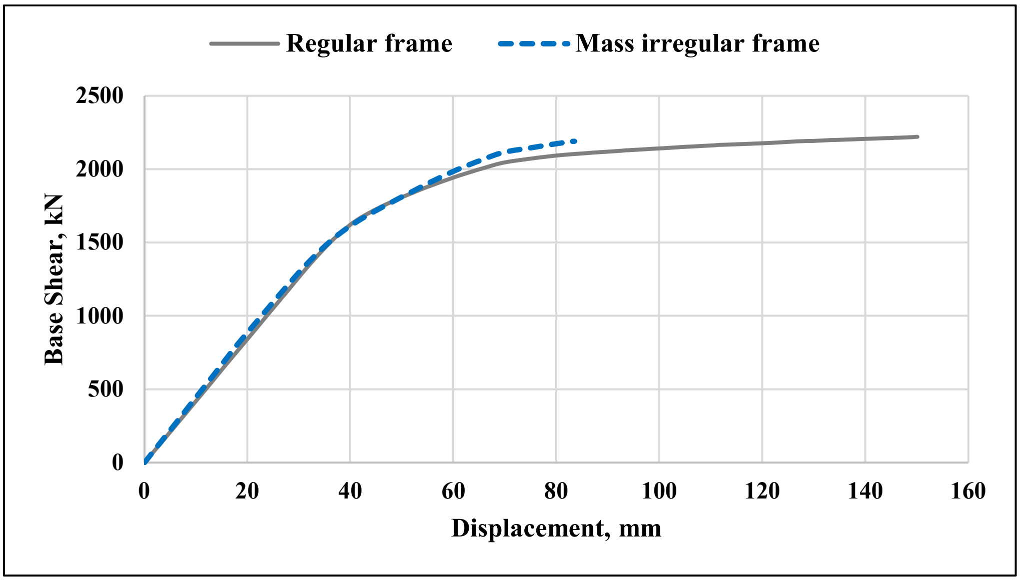

Figure B.4.1: Pushover curves of 4-storied regular and mass irregular frames

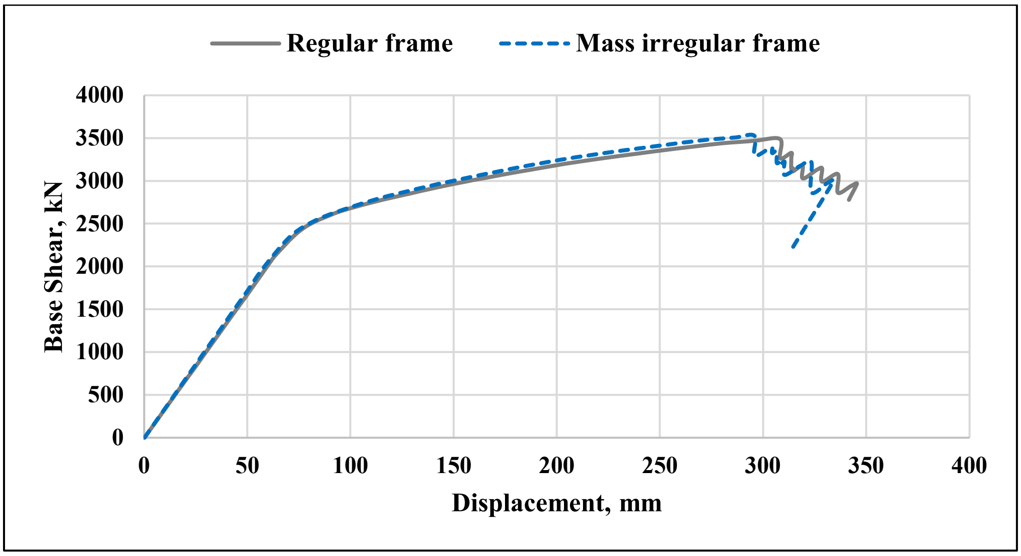

Figure B.4.2: Pushover curves of 10-storied regular and mass irregular frames

Appendix C-1: Storey shear of regular and geometric irregular frames

Figure C.1.1 and C.1.2 show storey shear of 6 and 10-storied regular and geometric irregular frames.

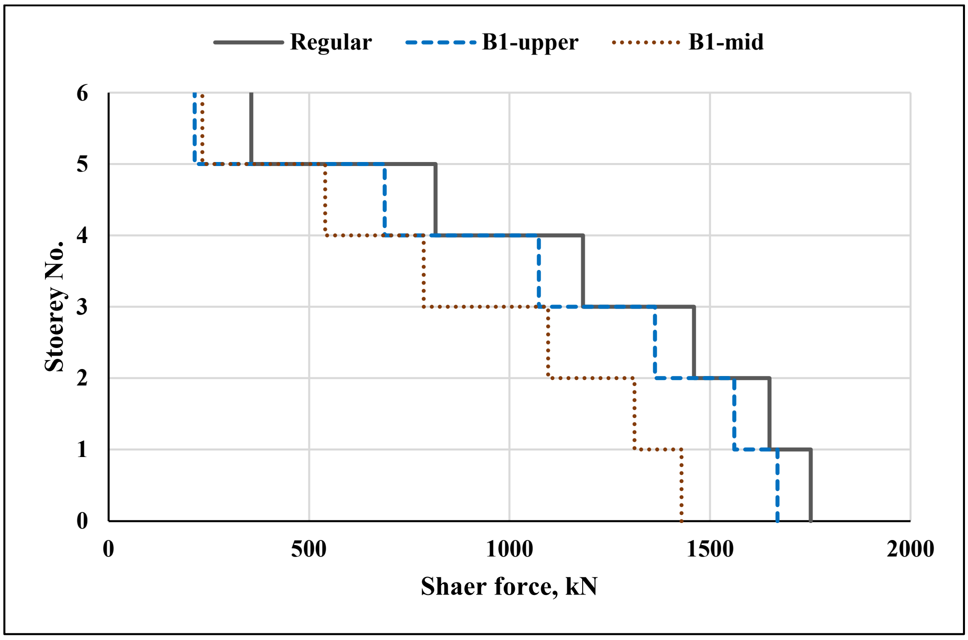

Figure C.1.1: Storey shear force of 6-storied regular and geometric irregular frames

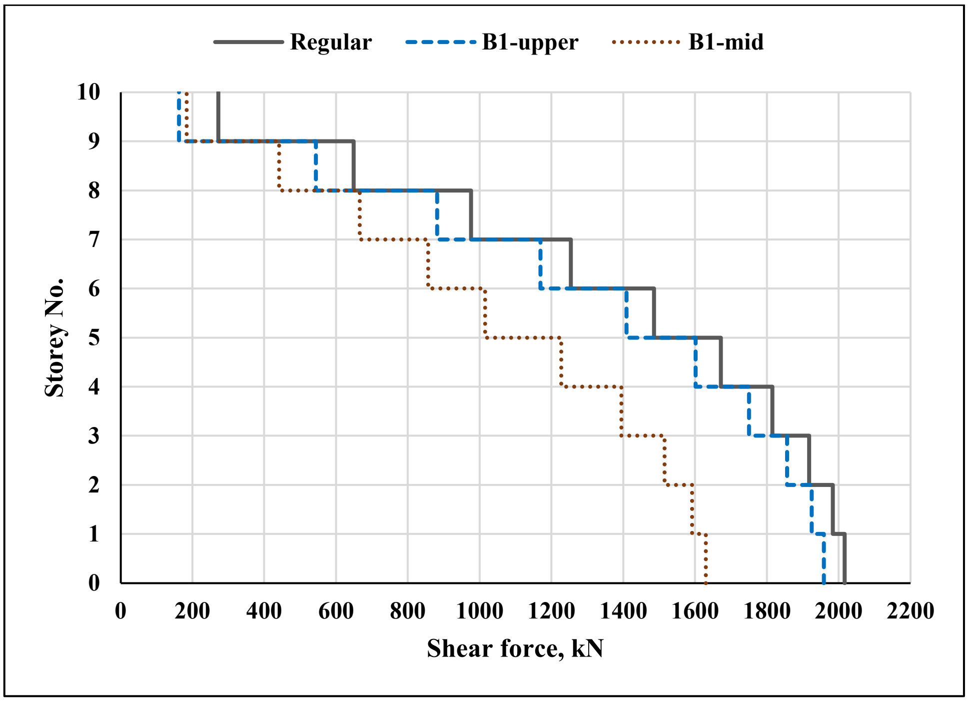

Figure C.1.2: Storey shear force of 10-storied regular and geometric irregular frames

Appendix C-2: Storey drift of regular and geometric irregular frames

Figure C.2.1 and C.2.2 show storey drifts of different floors of 6 and 10-storied regular and geometric irregular frames.

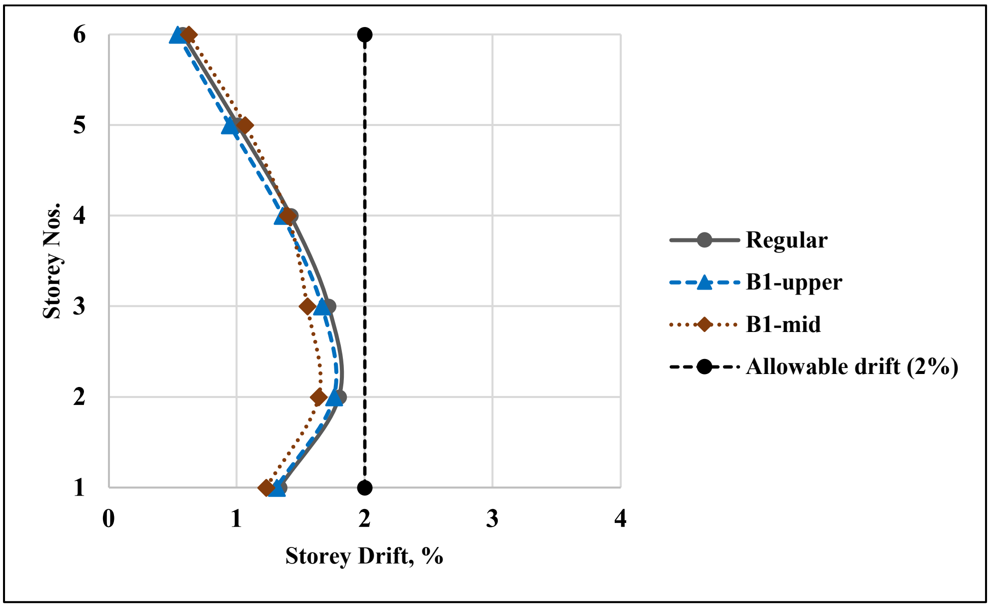

Figure C.2.1: Storey drifts of 6-storied regular and geometric irregular frames

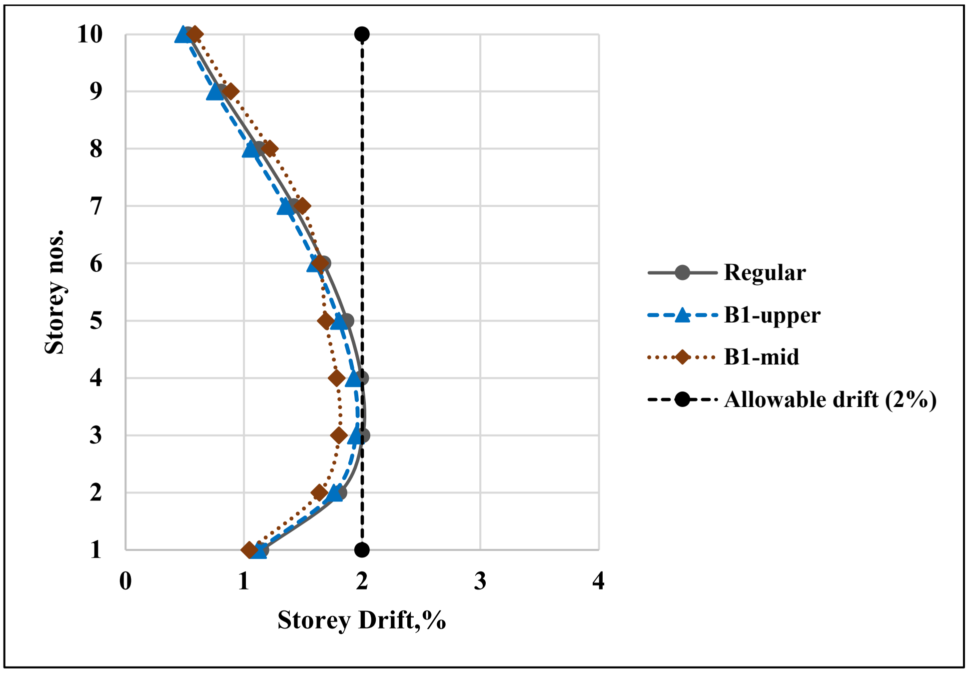

Figure C.2.2: Storey drifts of 10-storied regular and geometric irregular frames

Appendix C.3: Pushover curves of regular and geometric irregular frames

Figure C.3.1 and C.3.2 show pushover curves of 4 and 10-storied regular and geometric irregular frames.

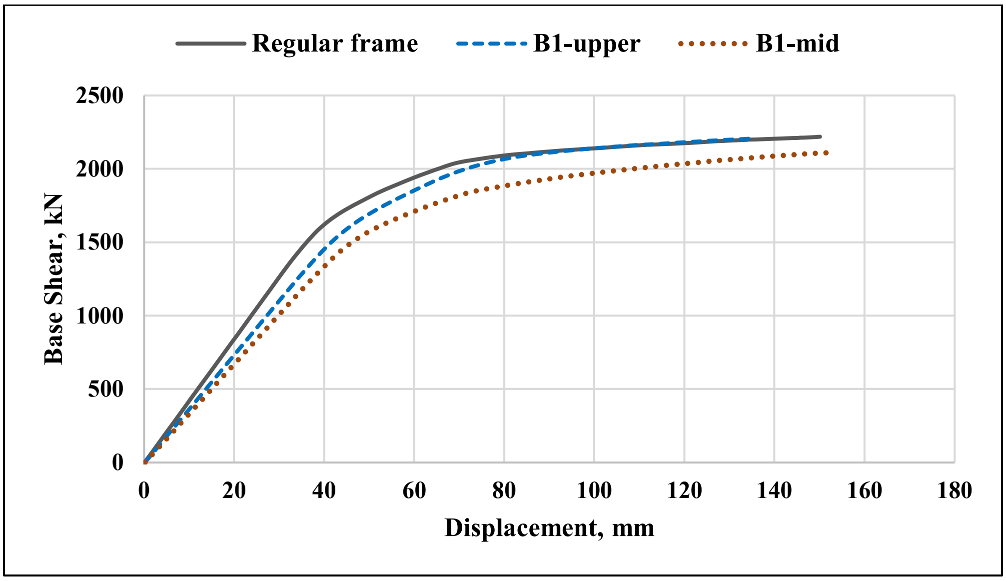

Figure C.3.1: Pushover curves of 4-storied regular and geometric irregular frames

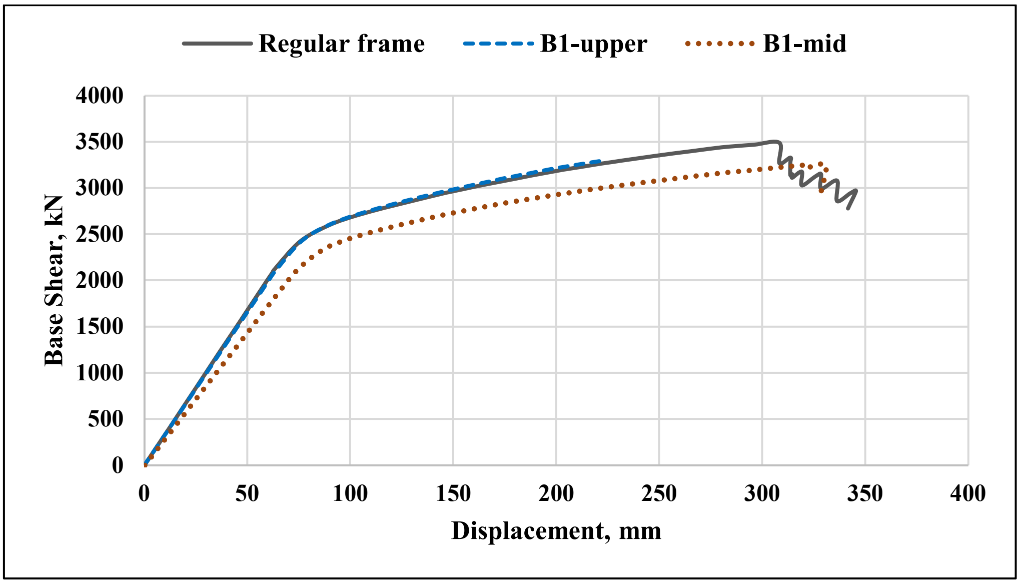

Figure C.3.2: Pushover curves of 10-storied regular and geometric irregular frames